Design of Supramolecular Complexes for Stability Enhancement of Membrane Protein-Based Biomaterials

by

Manoj K. Sharma

Design of Supramolecular Complexes for Stability Enhancement of Membrane Protein-Based Biomaterials

by

Manoj K. Sharma

A Dissertation Submitted to the Graduate Faculty in Engineering in Partial Fulfillment of the Requirements for the Degree of Doctor of Philosophy

The City University of New York

2005

UMI Number: 3187458

ProQuest Information and Learning Company
300 North Zeeb Road
P.O. Box 1346
Ann Arbor, MI 48106-1346

This manuscript has been read and accepted for the Graduate Faculty in Engineering in satisfaction of the dissertation requirement for the degree of Doctor of Philosophy.

Date	Prof. M. Lane Gilchrist Chairman of Examining Committee
Date	Prof. Mumtaz Kassir Executive Officer

Prof. M. Lane Gilchrist (Mentor)

Prof. Alexander Couzis

Prof. Charles Maldarelli

Prof. John Tarbell

Prof. David H. Calhoun

Supervisory Committee

THE CITY UNIVERSITY OF NEW YORK

Abstract

Design of Supramolecular Complexes for Stability Enhancement of Membrane Protein-Based Biomaterials

by

Manoj K. Sharma

Advisor: Prof. M. Lane Gilchrist

Membrane proteins are some of the most sophisticated molecules found in nature. Due to their extraordinary molecular recognition capabilities they represent a vast source of functional building blocks for potential use in sensing and drug screening applications. However, the strict requirement of the native lipid environment to preserve their structure and functionality presents an impediment in building biologically-based materials from these molecules. In general, the purification protocols remove the stabilizing native lipid structures found in the cellular environment. Our research is focused on a biomimetic approach to reintroduce the supporting structures of membrane proteins. The goal is to fabricate robust assemblies for membrane proteins that can withstand analyte flows and processing conditions (e.g., temperature, high ionic strength, organic solvents etc.) while retaining their functionality.

Reconstitution of membrane proteins into the bilayer of lipid vesicles is a standard approach to recreate their microenvironment after isolation from a native cel-

lular source. However, the inherent delicate nature of the lipid membrane limits the applicability of the liposomes. In the current study we have designed lipid bilayers internally anchored to a solid microparticle interface through integral tethering molecules. In earlier designs of tether-supported membranes, primarily single lipid moieties at the end of the tethers have been used to anchor the membranes to solid supports. We utilized bacteriorhodopsin (bR), a transmembrane protein, as a tethering molecule as it is expected to impart more stability to the tethered bilayer compared to a lipid tether. We conjugated bR with biotin-PEG_{3400} through amine-based coupling to use it as a tether. The conjugate was further labeled with Texas Red to facilitate localization via fluorescence imaging. The conjugates were characterized using SDS-PAGE and MALDI-MS.

A bottom-up, silane-based method was used to functionalize the surface of silica microspheres (5-μm) with streptavidin in order to provide bR-PEG_{3400}-biotin tether anchoring sites for the supported membrane. Tether-supported lipid-bilayer membranes with native-like fluidity were assembled successfully on the functionalized silica microspheres, verified using confocal microscopy. This method is a new platform for the immobilization of active membrane proteins in native lipids, and a gateway to new materials and diagnostics based on membrane protein molecular recognition.

Preface

This thesis describes an experimental study on the fabrication of solid-supported lipid bilayer membranes on silica microparticles. We have used bacteriorhodopsin (bR) based conjugates to anchor the lipid bilayer to the supporting silica particles. This work can be divided into three major parts: synthesis and characterization of bR conjugates, modification of silica surface to make it suitable for use as a supporting surface, and fabrication of lipid bilayers on silica surface using bR conjugates as integrated anchors.

In chapter 1, we have provided the basic motivation for our work. We have discussed the various issues related to the use of membrane proteins for a range of potential applications. These include the stability related questions, which are directly linked to the functionality of these molecules. Our strategy to stabilize these assemblies based on the biomimetic approach of the cytoskeleton structure of the cell has been described. The overall objectives of the project have been discussed. Background information on the lipids and the lipid bilayer assemblies has been provided. Also, the basic information on fluorescence and confocal microscopy has been discussed. Fluorescence recovery after photobleaching (FRAP) technique has also been introduced.

Chapter 2 describes the construction of biotin-PEG_{3400}-bR conjugates. We have used amine-based coupling to conjugate biotin-PEG_{3400} to bR. The conjugates were further labeled with Texas Red to facilitate their localization via fluorescence imaging. The protocols to characterize these conjugates using sodium dodecyl sulfate polyacrylamide gel electrophoresis (SDS-PAGE) and Matrix-Assisted Laser Desorption Ionization Mass Spectrometry (MALDI-MS) have been described. The experimental analysis to identify the Lys conjugation site in bR using the trypsin digestion

method followed by MALDI-MS analysis has been explained.

Chapter 3 deals with the details of the surface modification of silica microspheres. We have discussed the requirement to modify the silica bead surface. A brief literature review for silica surface modification using the silanization technique has been provided. Various experimental steps resulting in the immobilization of streptavidin on the bead surface have been described. Analysis of the modified beads at various steps using confocal microscopy has been discussed. Also, the discussion of the tests for non-specific adsorption of the lipids on the modified bead surface has been included.

Fabrication of the biotin-PEG_{3400}-bR tether supported lipid bilayer assemblies on streptavidin modified silica bead surface has been described in chapter 4. Various trials and tribulations of the method have been discussed. Characterization of the lipid assemblies on the bead surface using confocal microscopy has been described. Lateral fluidity of the fluorescently tagged lipids was analyzed using FRAP technique and was compared with the case of untethered lipid bilayer on plain silica bead surface.

Finally, chapter 5 gives an overview of the results achieved in the current thesis and relates them to the overall objectives of the project. This motivates the future work that needs to be done. Preliminary data obtained for the incorporation of the photosynthetic reaction center into these lipid assemblies has also been discussed.

Acknowledgments

I sincerely thank my advisor, Prof. M. Lane Gilchrist for being a wonderful mentor. I learned a lot from him over the course of past five years. More than an advisor, he has been a very good friend to me, providing the extra freedom and independence that nurtures the original thinking and creativity in a student. He has always tried to keep my morale high through the highs and the lows of my graduate study period. I thank Prof. Alexander Couzis and Prof. Charles Maldarelli for helping me from time to time in my academic as well as professional matters. I also thank Prof. David Calhoun and Prof. John Tarbel for providing valuable feedback and comments.

I thank my colleagues who I worked with at the City College: Janet, Hongjie, Harsha, Xinyu, Nikhil and Bin. Also, thanks to Mary Ann Gawinowicz of Columbia University for her support with the tryptic digestion and Maldi-MS analysis. Thanks to Prof. Marilyn Gunner (CCNY, Physics Dept) for providing the Photosynthetic Reaction Center. I also thank my classmate, Bo Jin, for his help in thesis formatting.

My stay in New York during graduate studies gave me a chance to make some wonderful friends. The complete list is very long but I would like to mention few of them — Pradeep, most wonderful person to have as a friend; Ravi and Chandra, the nicest people; Jeevan, ever cheerful person; Anil, the only one of his kind; Shyam and Rohit, the duo; John, always ready to help; and Ashish, the unpredictable.

I dedicate this thesis to my parents, Mr. O. P. Sharma and Mrs. Sushma Sharma. It is the result of their enduring efforts, love and support that I have been able to undertake this task and do justice to it. I also thank my sister and brother-in-law for their love and affection. Also, special thanks to my brother and sister-in-law for their encouragement and support. Finally, my niece Vasudha deserves a big thank you for making my days by her baby talks over the phone conversations.

Contents

List of Tables

List of Figures

Chapter 1

Introduction

1.1 Motivation

Biological systems are the most elaborate and intricate systems. These systems can perform the most complicated tasks accurately down to the molecular level. Cells, even as they are the basic building blocks of living organisms, can serve as an example of an extremely sophisticated biological system. A cell envelops an array of complex components performing highly specialized tasks essential for life. There has been an ever-increasing drive to learn from biological systems and utilize the highly elaborative biomolecules for designing novel materials. Membrane proteins, in this regard present a rich source of biomolecules, which have not yet been explored to a great extent.

Membrane proteins are one of the highly sophisticated molecules designed by nature. These molecules have extraordinary recognition properties; hence they represent a vast source of specialized materials with potential uses in sensing and screening applications. However, the strict requirement of the native lipid environment presents an impediment in building biomaterials from these molecules.

In general the purification of membrane proteins from the cellular source utilizes some sort of detergent and the purified membrane protein is present in detergent-solubilized, mixed micellar form. In this form, many integral membrane proteins are unstable and some are inactive or not folded into the active conformation. The viability of membrane proteins can be recovered in certain cases when these are reconstituted into lipid bilayers, provided that the lipid composition is similar to the native environment. Lipid bilayers are self-assembled colloidal structures composed of lipid molecules. Lipid monomer's structure consists of a polar head group and a hydrophobic part consisting of two fatty acid chains. In water these bilayers form higher order assembled structures, giving rise to spherical vesicles called liposomes (Figure 1.1). A liposome with a membrane protein incorporated into its

bilayer is called a proteoliposome (Figure 1.2A). On a supporting surface membrane proteins can be reconstituted in a two-dimensional array of lipid molecules called the supported membrane (Figure 1.2B). In both the cases, the membrane protein is embedded in the lipid bilayer, which provides it with the native membrane-like environment, retaining its structural and functional features. Protein stability in both cases is directly related to the stability of the lipid bilayer.

Interfacing of biological molecules with surfaces of interest to build biomaterials is becoming an attractive area to researchers worldwide. In this context, these membrane protein based biomaterials have potential applications in various areas, viz. a viz. biosensors, biocatalysts, receptor-targeted drug delivery systems and novel biomaterials for tissue engineering. The major issue regarding the development of membrane protein-based materials is the inherent instability of the lipid bilayer membranes hosting the proteins. Various conditions encountered in potential applications can destabilize the bilayer assemblies. These include shear stress, osmotic shocks, dissolution by surfactants or organic solvents, and disruption by divalent cations such as calcium.

Our aim is to redesign these supramolecular complexes to enhance their stability. This is to be accomplished by designing spherically-supported membranes such that the bilayer carrying the membrane protein is supported internally by a solid interface (of a microparticle or a nanoparticle). The motivation for our approach comes from the cytoskeleton structure of the cell. This natural supramolecular structure consists of arrays of protein filaments forming an internal network, providing the cell with the shape, strength, and locomotive abilities. In our strategy, lipid bilayer will be anchored to the solid surface through polymer tethers. We chose to fabricate supported bilayer on spherical geometry instead of a flat interface, as there are certain advantages to this approach. It allows much more surface area to work with compared with flat geometry. Second, in spherical geometry there is a possibility

of achieving the compartmentalization of an aqueous space between the bilayer and the supporting surface. This is a very crucial aspect as it can allow us to encapsulate a number of molecules in the enveloped volume. These molecules could vary from simple tracer molecules to the highly complicated signaling proteins essential in the downstream signaling pathway of the transmembrane receptor proteins, e.g., G. Protein Coupled Receptors (GPCR).

1.2 Research Outline

The overall objectives of current research in the light of above discussion are the following. We needed to identify suitable microparticles with desired properties. These properties include, surface smoothness, amenability for surface modification, ease of handling, solution stability, minimal background UV/Vis or fluorescence properties etc. We also needed to identify a suitable molecule to be used as a tether. Desired properties of the tether are, suitable terminal functionality to be used to link it to the surface, a long chain spacer, which will keep the bilayer at a distance from the surface, and a molecule at the far end, which will interact and integrate itself with the bilayer. Figure 1.3 shows a schematic representation of such a tethering molecule. This required synthesis of the tethering molecule of desired properties by bioconjugation techniques as will be discussed in details in further chapters. Silica microspheres were chosen to internally support the bilayers. Silica surface is highly hydrophilic and is expected to be resistant to variety of hydrophobic molecules ranging from fluorescent tracers to membrane proteins that we needed to utilize in the project. In order to modify the silica surface, silane chemistry was utilized. This was done to functionalize the surface for attaching the tether. Once this was accomplished we had to figure out the best way to fabricate supported bilayers around the tether-linked particles.

1.3 Why Study Supported Membranes

It is imperative to mention why supported lipid membranes have become a subject of great interest. There are a few important properties/characteristics of these assemblies, which make them highly desirable for the development of biomaterials based on membrane proteins. These are as follows:

- Supported membranes present stable, native-like microenvironments for membrane proteins. In vivo membrane proteins are found in cellular membrane which is a hydrophobic and a fluidic environment necessary for maintaining the structure and preserve the functionality of these biomolecules. Supported membranes can recreate this native like environment.

- Supported lipid membranes can preserve the lateral diffusivity of membrane protein. Some membrane proteins form multimeric complexes in their functionally active form (e.g., Epidermal Growth Factor Receptors). This requires the lateral movement that enables interactions with other molecules. If the lateral diffusivity is absent, this type of membrane protein will be functionally inactive. Supported lipid membranes can preserve the mobility of the reconstituted protein, hence retaining its activity.

- In certain cases, the membrane proteins act as the transducers (e.g. G-protein coupled receptors, GPCRs) of the information from extracellular side to the cytoplasmic side. This is an allosteric process, where the binding of the stimuli (a hormone, peptide, or a ligand) to extracellular part of the protein leads to rearrangement of the protein structure resulting in the activation of G-proteins bound it on the intracellular side. From this point of view, interactions of the lateral surface of the membrane protein with neighboring lipid molecules of the bilayer can play a crucial role. [1, 2, 3, 4]

1.4 Potential applications

There are a number of potential applications of supported lipid membranes. One that is directly relevant to the current study is the design of flow based sensing devices (Figure 1.4). Such a device consists of arrays of microparticles on a functionalized surface. Individual particle could have supramolecular assemblies of membrane proteins in tether supported lipid bilayer. Such a system could have an applicability as a sensing and or screening device for molecules of interest in the flow, e.g. biohazardous chemicals, potential drug molecules etc. The tether-supported membranes described here could be used as a robust counterpart of supported membranes previously designed by a number of researchers. In addition, supported membranes can be used to biofunctionalize a given surface for making novel biomaterials. Supported membranes are a model for biological membranes; so we can use them to study various processes occurring at cell surface, e.g. receptor-ligand interactions, cell adhesion etc. Moreover, as lipid bilayers provide the membrane proteins with a stable, native-like microenvironment, these can be used to design new biocatalysts based on membrane protein enzymes.

1.5 Background

1.5.1 Lipids, lipid bilayers and liposomes

Lipid molecules are the major constituents of biological membranes. The most abundant membrane lipids are the glycerophospholipids. The structure of glycerophospholipids (also called phosphoglycerides) can be divided into two parts, a polar head group and two hydrocarbon chains, which are hydrophobic. This provides these molecules with an amphipathic nature. The tails are usually fatty acids containing 16 to 18 carbon atoms (with some exceptions). In the case of two end chains, one of the tails is generally saturated while the other one is unsaturated

with a double bond in the middle of the chain. Presence of unsaturation in the hydrocarbon tail affects the packing efficiency of the lipids and hence the phase transition temperature (T_g) of the assembled lipid bilayers. Amphipathic nature of the lipid molecules causes them to self-assemble in aqueous environments in such a way that the hydrophobic tails are hidden from water. Due to their cylindrical shape, lipid monomers self assemble in a bilayer structure with the hydrophobic tails sandwiched between the polar head groups, which interact favorably with water molecules. However, even this bilayered structure leaves the lipid tails exposed to water at the edges of the leaflet. This leads to spontaneous closure of phospholipids bilayer to form sealed compartments (Figure 1.1). These structures are called lipid vesicles or liposomes.

It has been well established that lipid bilayer membranes are fluidic in nature where the individual lipid molecules are constantly in motion. The degree of fluidity depends on the lipid composition and the temperature. At temperatures below the phase transition temperature of the bilayer exists in the ordered gel phase where the lipid molecules are closely packed against each other in a perfect crystalline structure and show minimal mobility. Above the phase transition temperature, bilayer exists as the liquid crystalline phase where the lipid molecules are randomly packed in the bilayer and are constantly diffusing around. Phase transition temperature depends on a number of factors including the chain length, presence of unsaturation in the hydrophobic tails, head group species etc. It increases with the chain length as interaction energy of the hydrocarbon tails increases with the chain length. Presence of a double bond produces a kink in the hydrophobic tail and interferes with efficient packing of the hydrophobic tails, thus reducing the transition temperature. Diffusion coefficient (D) of the lipid molecule for lateral movement is of the order of 10^{-8} cm^2/sec, which means that an individual lipid molecule can travel a distance of 2 μm in 1 second.

Lipid vesicles or liposomes are colloidal particles with the capability of encapsulating an aqueous space. They consist of one or more concentric lipid bilayers that self assemble due to their amphipathic nature. Bangham and Horne [5] were the first people to see phospholipid dispersions in water using electron microscopy technique and established that they self assemble to form 'bag-like' structures. These self-assembling vesicles were named liposomes. Since then the field of liposomes has become a major area of research and significant progress has been made [5, 6, 7, 8, 9, 10, 11].

Liposomes have been the focus of attention for researchers worldwide because they present a working model for biological cell membranes. They provide membrane proteins with native-like environment and so they can retain their activity. In this manner liposomes can be utilized to study and understand the signaling processes and the communication of the cell with its exterior. Moreover the encapsulated aqueous space and biocompatibility makes them good candidates for encapsulating drugs for specific targeting applications. Sato et al. [12] and Gregoriadis et al. [6] have recently reviewed biotechnological and medical relevance of liposomes.

1.5.2 Classification of liposomes

There are three categories in which liposomes have been divided based on size as follows: multilamellar vesicles (MLV, size 10,000 nm), large unilamellar vesicles (LUV, size 50–10,000 nm) and small unilamellar vesicles (SUV, size 20–50 nm). In addition there are a number of terms given to liposomes produced by different techniques. Unilamellar liposomes obtained from aqueous-organic emulsion by evaporation of organic phase are called reverse phase evaporation vesicles (REV, size 150–450 nm)[13]. Unilamellar vesicles produced by extrusion of large vesicles are called vesicles by the extrusion techniques (VETs) [14, 15].

Others classification of liposomes are based on the type of lipids forming the

liposome vesicles. They could be formed by lipids, which are stabilized natural lecithin (Phosphatidylcholine, PC) mixtures, synthetic identical-chain phospholipids or glycolipid containing liposomes. All membrane lipids are amphipathic in nature; which is the main factor governing their self-assembly into vesicular structures. These lipids can be further categorized based on their structures: lipids containing fatty acid chains (glycerolipids, phospholipids and sphingolipids) and lipids which do not contain fatty acids e.g. cholesterol.

The latter type cannot form bilayers by itself but serves to facilitate the close packing of lipids forming bilayer [16]. The head group of the lipids forming the bilayer could be non-ionic or zwitterionic (phosphatidyl -choline, -ethanolamine etc.) presenting no net charge on the surface, or, ionic (phosphatidylserine, phosphatidic acid), depending on the pH of the medium. The presence of a net charge on the surface of liposome leads to electrostatic repulsion between the vesicles and reduces the aggregation and thus enhances the stability. A small percentage of ionic lipids ($5-10\%$) is sufficient to reduce the aggregation phenomena [17].

1.5.3 Methods of preparation of liposomes

Classical methods of liposome preparation have been reviewed in detail by Szoka and Papahadjopoulos [10]. In general, liposomes or lipid vesicles are formed upon hydration of lyophilized lipid films. It is very important to dissolve the lipid constituents using some organic solvent in order to get a homogeneous film upon solvent evaporation. Generally chloroform or chloroform:ethanol mixture is used to dissolve lipids at $10-20$ mg/ml or higher if possible. After complete solubilization of the lipids the organic solvent is evaporated completely using a vacuum pump. The lipid film thus obtained is stored at –20°C under argon until it is required for hydration. Storage at low temperature under oxygen and moisture free environment minimizes the degradation of the lipid molecules by oxidation or hydrolysis mechanisms. Hy-

dration of lipid film followed by agitation leads to formation of large multilamellar vesicles (MLV). The main concern at this point is that the hydration temperature should be above the phase transition temperature, T_g of the lipid mixture. Bilayer thus formed above T_g is in liquid crystalline phase, while below T_g it changes into a gel phase. Another implication of this is that the hydration buffer must have boiling point above T_g. Hydration buffers differ according to the application but in general de-ionized water buffered in the biological pH range is used. Care should be taken that it is free of divalent cations e.g. Ca^{2+}, which lead to aggregation and fusion of liposomes [18] and lateral phase separation of lipids [19]. This is taken care of by adding small amounts (usually 1 mM) of the chelating agent EDTA.

Multilamellar vesicles obtained by above procedure can be reduced in size to obtain the desired sized vesicles by input of mechanical energy. Sonication of the suspension above T_g gives rise to small unilamellar vesicles (SUVs) in the range of 20 nm$-$50 nm depending on the lipid composition and time of sonication ([10] and references therein). It should be noted that due to high degree of curvature, the SUVs are inherently unstable and thus gradually fuse together to give larger vesicles when stored for longer times (Avanti Polar Lipids). Extrusion of MLVs, originally introduced by Olsen et al. [20] and Mayer et al. [21] is another technique to get SUVs of a defined size range. The multilamellar vesicle suspension is forced multiple times through a polycarbonate membrane of known pore size and this leads to formation of unilamellar vesicles with a size distribution monodispersed near the pore size of the polycarbonate membrane used [15]. It is important to keep the entire system above T_g, which in the case of high melting lipids is usually achieved by mounting the whole extrusion assembly on a heating plate.

Among other methods is the use of detergent containing buffers to hydrate the lipid films. Subsequent removal of the detergent leads to lipid assembly and results in vesicle formation. Ollivon et al [8] have recently reviewed this technique. Hy-

dration of the lipid films with detergent containing buffer leads to the formation of lipid-detergent mixed micelles. A lipid-detergent mixed micelle consists of a lipid monomer surrounded by the detergent molecules. Upon removal of the detergent by a suitable technique these micelles transform to give unilamellar lipid vesicles. A number of techniques can be utilized to remove detergent, e.g. dialysis, gel chromatography, bio-beads, successive dilution, enzymatic reactions, temperature and pressure jumps etc. The useful feature that allows removal of detergent molecules selectively from detergent-lipid mixed micelles is that the detergent molecules have much larger solubility in the aqueous phase compared to lipid molecules of about similar size and similar amphipathic properties ([8] and references therein).

The technique based on use of detergents is the most efficient technique for the preparation of protein reconstituted liposomes or proteoliposomes. Proteoliposomes as defined earlier are lipid vesicles containing membrane proteins inserted in the lipid bilayer. The effectiveness of this technique can be attributed to the fact that proteins need to be purified from the natural membranes before they can be reconstituted into the artificial lipid bilayer, which is easily achieved by solubilizing them using a suitable detergent. The protein solubilized in a suitable detergent can then be added into the lipid-detergent mixed system such that the lipid to protein ratio is roughly 80–150 (w/w) or 3000–5000 mol/mol [8, 22, 23, 24]. This ratio is required in order to have the protein in very dilute amount compared to the lipids so that it does not interfere with the detergent-lipid mixed-micelle to lipid vesicle transformation upon removal of the detergent [25]. Moreover, because the relative proportion of the protein is very small there is flexibility to utilize a different detergent to solubilize a given protein and it does not interfere with the interaction of other detergent with the lipids.

1.5.4 Liposome stability issues

Liposomes are nanoparticles containing a lipid bilayer shell encapsulating an aqueous space. Many of the bilayer forming lipids have their phase transition temperatures below room temperature, hence the lipid bilayer normally exists in liquid crystalline form at room temperature. Hence the liposomes are not very stable systems and are prone to all kinds of destabilization mechanisms, e.g. coagulation, shear stress, dissolution by surfactants/organic solvents, disruption by divalent cations e.g. Ca^{2+} or sucrose solution, etc. Difference in the ionic concentration between encapsulated phase and bulk media leads to osmotic pressure differences causing the vesicles to become unstable. These issues have been discussed earlier by Lasic et al. [7] and Ringsdorf et al. [26]. A number of solutions have been proposed to tackle these issues. Polymerization of lipid chains inserted in the bilayer [27] can give robust vesicles but that destroys the lateral mobility of the lipids − a crucial dynamic property of the biological membranes for their proper functioning [28]. Another solution is to formulate vesicles using synthetic block copolymers laterally cross linked to each other to form tight bilayer like network [29]. However, these systems have eliminated lipids altogether; which could make these vesicles less biocompatible. Moreover these systems can no longer provide natural membrane like environment for membrane spanning proteins from cellular sources. Hence it is necessary to enhance the stability of the vesicles based on lipids, i.e. liposomes. Sterical stabilization of liposomes based on hydrophilic polymer Polyethylene Glycol (PEG) on the surface has been widely used. Long polymer chains on the surface of liposomes present a steric barrier to any foreign objects and also avoid aggregation of liposomes. PEG is a biocompatible polymer and hence PEGylated liposomes are suitable for in vivo applications. Different groups have reviewed stabilizing liposomes using PEG [11, 30]. There are different ways to chemically link PEG to the

surface of the liposomes [11]. PEG linked to Phosphatidylethanolamine (PE) can be added to the lipid formulation. Upon self-assembly PE gets inserted into the bilayer along with other lipids and the PEG portion is displayed on the surface of liposomes. It has been established that optimum steric stabilization in vivo can be achieved with 5–10 mol % of PEG-PE with PEG of molecular mass ranging from 1000−2000 [30].

1.6 Techniques

1.6.1 Fluorescence and confocal microscopy

Fluorescence is the phenomenon of emission of electromagnetic radiations of visible light by certain molecules when they are excited by the absorption of incident radiation of suitable wavelength. Fluorescence is originated by the electronic transitions in a molecule due to its interaction with the excitation radiation. The emitted light is generally of higher wavelength compared to the absorbed light. Due to a large number of molecules in the sample and the degeneracy of the electronic energy states, a fluorescent molecule has a characteristic excitation and emission spectrum instead of unique spectral lines. These spectra depict the probability distribution for the wavelength dependent excitation, or emission of light, by the molecule. Figure 1.5 shows a crude representation of the phenomena of fluorescence and Figure 1.6 shows representative excitation and emission spectra for a fluorescent molecule Texas Red-X. The first step in the fluorescence is the absorption of incident radiation, which takes the molecule to an excited electronic energy state; a transition governed by the overlap between the probability distribution functions of the ground and excited state vibrational levels. This is an instantaneous process (10^{-15} sec) and involves no movement of the nuclei as dictated by Franck-Condon Principle. In the second stage, the molecule relaxes down to lowermost vibrational energy level of the first excited electronic energy state (S_1); a phenomenon which is called Internal

Conversion and takes about an order of picoseconds (10^{-12} sec). Finally, the loss of electronic energy stored in the molecule can occur in a number of ways (radiative and nonradiative) which take the molecule to ground electronic energy state. Fluorescence is one such radiative process, which occurs when the molecule directly relaxes down to the ground electronic energy state. Lifetimes associated with the fluorescence phenomenon are order of nanoseconds (10^{-9} sec). Other radiative process (Phosphorescence) which leads to delayed emission of light is through crossing of the molecule to the triplet state and subsequent relaxation to ground electronic state.

Molecules, which are capable of undergoing the electronic transitions resulting in fluorescence, are termed as fluorescent probes or dyes. Each fluorescent probe has a characteristic excitation and emission spectrum, which is affect by a number of parameters including solvent composition, pH, solvent polarity etc. A fluorescent dye can be tagged to a larger macromolecule (e.g., a protein, lipid or nucleic acid) in order to trace these molecules in a structural assembly such a macromolecule is called a fluorophore [Olympus microscopy resources http://www.olympusmicro.com/]. Fluorophores can be divided into two categories, intrinsic and extrinsic. Intrinsic fluorophores occur naturally. Examples include aromatic amino acids (Tyr, Trp, Phe), porphyrins, and green-fluorescent proteins. Extrinsic fluorophores are synthetic molecules tagged on to a macromolecule to impart it with specific spectral properties.

Main usage of a fluorescent molecule can be as a reporter or tracer group in a structural assembly. Present project entails building molecular self-assembled structures around microspheres and hence fluorescence microscopy fits in as the ideal technique of analysis. Various fluorescent molecules can be used at different stages to verify the structural assembly. Use of a fluorescent marker, which can stain the modified silica surface at various stages of surface modification, can facilitate the

analysis of surface homogeneity of the added functionality. Fluorescent tagging of the tethering molecule can assist in establishing if the tether is successfully immobilized on the bead surface. It can also assist in studying the distribution of the tether on the surface. Finally, as our aim is to build supported lipid bilayer; use of fluorescently tagged lipid molecules can aid in visualizing the lipid bilayer assembly on modified silica particles.

Besides localization studies of a single fluorophore, we have advanced capabilities to get further insight into the fabricated assemblies. These include, colocalization studies, fluorescence resonance energy transfer (FRET) and fluorescence recovery after photobleaching (FRAP). In our assemblies, we have the option of using one fluorophore for tethering molecule and another fluorophore for the lipid. Selection of more than one fluorophores requires a careful analysis of the excitation-emission properties. If the aim is to detect them individually and avoid any cross talk, one needs to make sure that there is minimal overlap between the respective excitation (and emission) characteristics of the two probes. Moreover, in order to minimize any possibility of energy exchange, the emission spectrum of the low wavelength emitting fluorophore should be sufficiently far from the excitation spectrum of high wavelength emitting probe. Analysis of the fluorophores in the final structure, chosen according to the above-mentioned criteria, will reveal information about colocalization of the tether with lipid bilayer. A much more accurate way to analyze this would be to use fluorescence recovery after photobleaching (FRET). FRET is defined as the transfer of excited-state energy from one molecule (Donor) to another (Acceptor) through dipole-dipole interactions between the two molecules. The rate of energy transfer depends on a number of parameters − spectral overlap of the emission spectrum of the donor with the absorption spectrum of the acceptor, the quantum yield of the donor, relative orientation of the two donor and acceptor dipoles, and the physical distance between the two molecules. A very strong de-

pendence on the intermolecular distance (r^{-6}) makes this technique highly suitable for the analysis of proximity of different reporter molecules down to the accuracy of few nanometers. Another important criterion that can be used to establish the structure of a supported lipid bilayer is the essential fluidity of the bilayer. This can be analyzed by a technique call fluorescence recovery after photobleaching (FRAP). This technique will be discussed in details in later section.

1.6.2 Confocal Microscopy

Fluorescence based techniques have gained numerous importance in the field of optical imaging. These techniques find applications in different disciplines, which include biological systems, medical sciences, engineering applications and physics community. Laser scanning confocal microscopy is the latest revolutionary advancement in the field of fluorescence based microscopy technique. This technique enables control over the depth of field for imaging thick specimens and an ability to reject out of focus light to get sharply defined images. A number of slices can be taken for a thick sample and can be combined to render a three-dimensional reconstruction of the sample. Key features of a laser scanning confocal microscope are the use of point-by-point scanning of the sample with an attenuated laser bead and the rejection of out of focus light through spatial filtering of the emitted light beam.

Basics of a confocal microscope

Main hardware parts of a confocal laser scanning microscope (CLSM) are: illumination laser sources, a scan head with necessary optics and electronics including the photomultiplier tube detectors, a microscope, and a computer interface. Schematic representation of the beam path for a confocal microscope has been shown in Figure 1.7. Incident light beam from the laser source is first attenuated through a narrow aperture called the source pinhole, which reduces the beam size to few microns.

The beam is subsequently reflected through a dichromatic mirror, passes through the objective and illuminates a point on the focal plane on the sample. Part of fluorescence generated from this illuminated spot which travels backward through the objective can pass through the dichroic mirror and is subsequently focused onto the detector pinhole.

It is the combination of source and detector pinholes which makes laser confocal scanning much more prominent compared to traditional widefield fluorescence microscopy. In a widefield microscope incident light from a mercury or xenon light source is focused down to the sample using an objective, thus illuminating a large spot on the sample. This leads to fluorescence generation from the entire depth of the illuminated spot and results in poor resolution along the depth of the sample. In laser scanning confocal, the source pinhole attenuates the incident beam size down to a few microns, which subsequently gets focused down to a small spot on the sample (≈ 1 μm diameter). The sample is then scanned point-by-point with a fine illuminated spot on the sample plane and fluorescence signal is accumulated on the PMT detector through the detector pinhole. 3-D intensity variation of a focused laser beam in CLSM, called the point-spread function (PSF) is assumed to be radially and axially Gaussian [31]. This implies that there will be minimal excitation of the sample above and below the focal plane. Furthermore, any fluorescence signal generated from Out-of-Focus excitation gets further attenuated at the detector pinhole. Hence the combination of source and detector pinhole improves the vertical resolution significantly. In traditional widefield epi-fluorescence microscopy the fluorescence from the illuminated region can be viewed directly through the eyepiece or recorded onto a detector. In the case of confocal laser scanning microscope, fluorescence image is generated through point-by-point scanning of a defined region of the sample. The scan head controls the movement of the illuminated fine spot through galvanometer-based raster scanning mirror system.

Major advantages of laser confocal scanning system are as follows: first major advantage is the improvement in the vertical resolution and contrast as discussed above. In addition, one can image multiple focal planes of a thick sample and reconstruct a three-dimensional image from it. Also, scanning confocal microscopes have the ability to excite and detect multiple fluorescent probes simultaneously. This opens the opportunity for studying the structures based on distribution of specific labeling of a complex structure. This also gives the ability to study structures based on co-localization of the fluorescent probes of interest. Another major advantage of the confocal systems is the inherent improvement in the speed of the image acquisition. This leads to the possibility of dynamic studies on the structures of interest. One such technique that is relevant to current study is FRAP and is discussed in details below.

Fluorescence recovery after photobleaching

Fluorescence recovery after photobleaching (FRAP) is a method for characterization of the molecular mobility of fluorescent molecules in a sample. This technique was originally developed by Axelrod et al. [32, 33] for quantifying two dimensional diffusion characteristics of cell membrane bound florescent probes. This technique works on the basis of two physical phenomena: (i) photobleaching, and (ii) diffusion of fluorescent probes. Photobleaching is the permanent loss of the fluorescence properties of a probe due to light induced irreversible changes in the molecule. In the relatively long-lived excited triplet state, the fluorescent molecule can interact with other molecules to result into a non-fluorescent entity. The photobleaching rate of a population of fluorescent molecules is linearly dependent on the illuminating laser intensity for one-photon excitation [34, 35, 36]. In every excitation-emission cycle a fraction of the population is rendered inactive, and the average number of cycles that a molecule is fluorescent depends on the molecular structure and local

microenvironment. In a typical FRAP experiment a selected region of a fluorescent sample ($\approx 1\ \mu$m) is subjected to an intense laser beam, which leads to photobleaching of the molecules in that region. If the molecules in the sample are in mobile form, fluorescent molecules from other regions gradually replenish the bleached molecules in the selected region. This would lead to a gradual buildup of the fluorescence signal in the photobleached region. Analysis of the average florescence intensity of the selected region before and after the bleach event can provide the details about the mobility characteristics, e.g. diffusion coefficient, mobile fraction etc.

Confocal laser scanning microscopes (CLSM) have made the FRAP experiments highly convenient to perform. Major advantages offered by CLSM based system are the following: (i) ability to rapidly switch laser power (micro to milliseconds) using acousto-optical tuneable filter (AOTF) between bleach and acquisition sequence; (ii) high speed acquisition for fast diffusing components; (iii) ability to bleach a wide variety of geometries and ability to individually monitor the fluorescence changes in different regions of interest (ROIs). Detailed discussion of various aspects of mobility measurements using confocal laser scanning microscope can be found in literature. (See [31, 37, 38] and references therein).

In general there are three stages in a FRAP experiment as shown schematically in Figure 1.8. In step 1 called the prebleach series the sample is imaged at a low intensity illumination. This provides a reference level for fluorescence recovery and also indicates any fluorescence loss during acquisition. Second step is the bleach event where one or more region(s) of interest is/are subjected to high laser illumination. In general the bleach event should be instantaneous in order to minimize any recovery during the bleach event itself. The last step of a FRAP experiment is the acquisition of a series of images after the bleach event at attenuated laser illumination. Analysis of the fluorescence intensity recovery of the bleached areas can give the parameters related to mobility of the fluorescent molecules of interest.

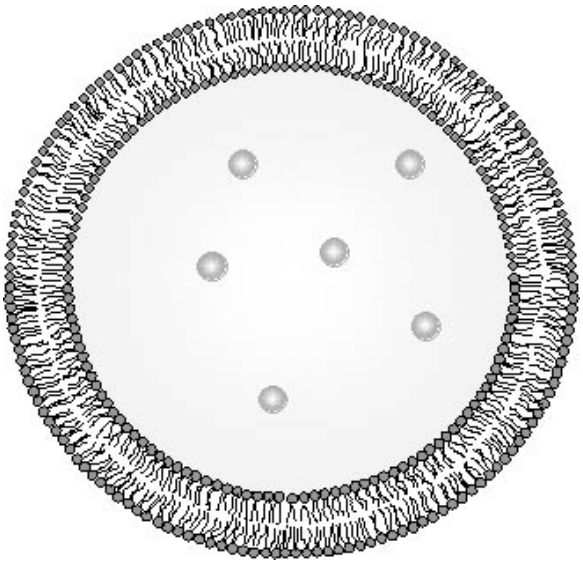

Figure 1.1: Schematic representation of a lipid vesicle or liposome showing the encapsulated contents separated from outside by a membrane barrier.

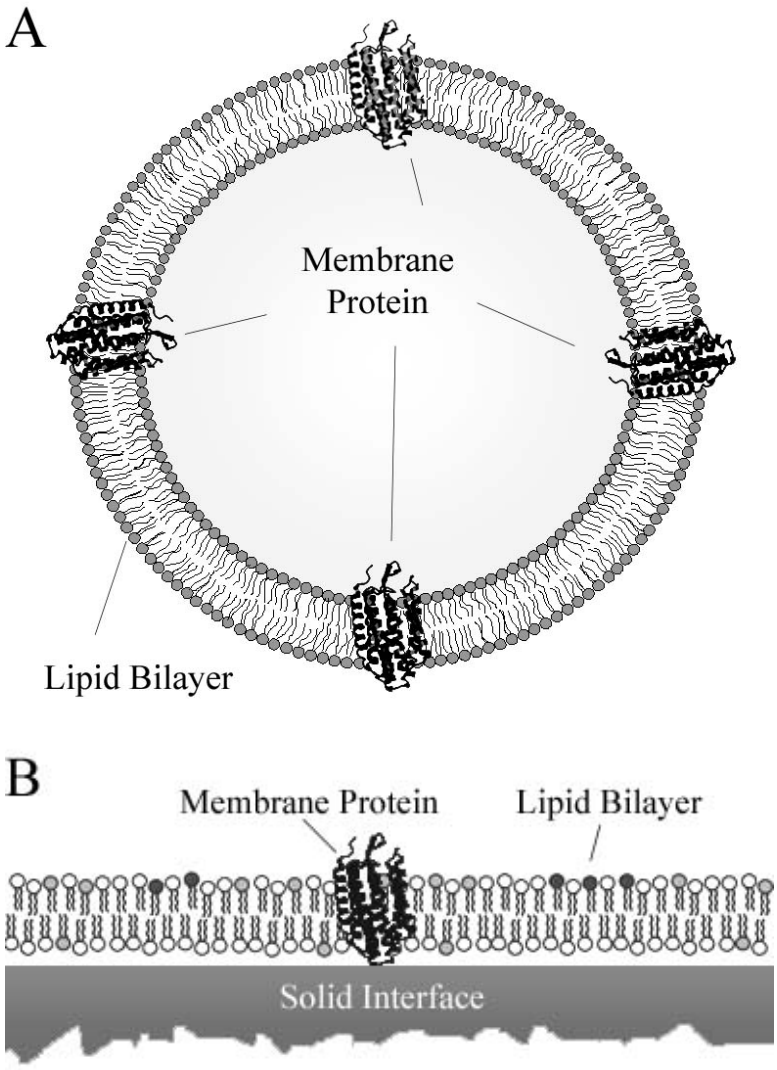

Figure 1.2: Reconstitution of a membrane protein in native, functionally active form in lipid bilayer assemblies, (A) In aqueous phase these assemblies are called proteoliposomes, (B) On a solid interface they are termed as supported membranes.

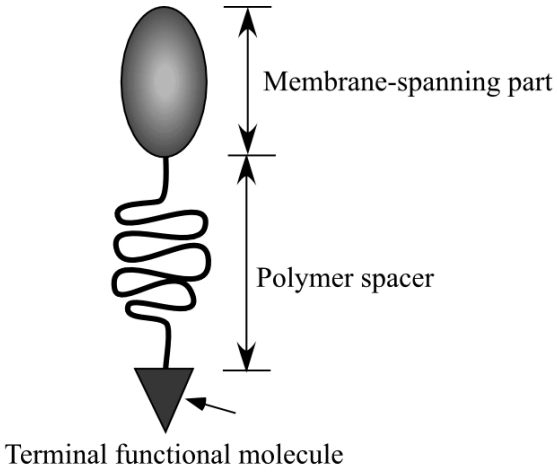

Figure 1.3: Schematic representation of a molecule suitable for use as a membrane tether. Membrane-spanning part interacts with lipid molecules through hydrophobic interactions and the terminal functional molecule can be attached to a suitable supporting surface.

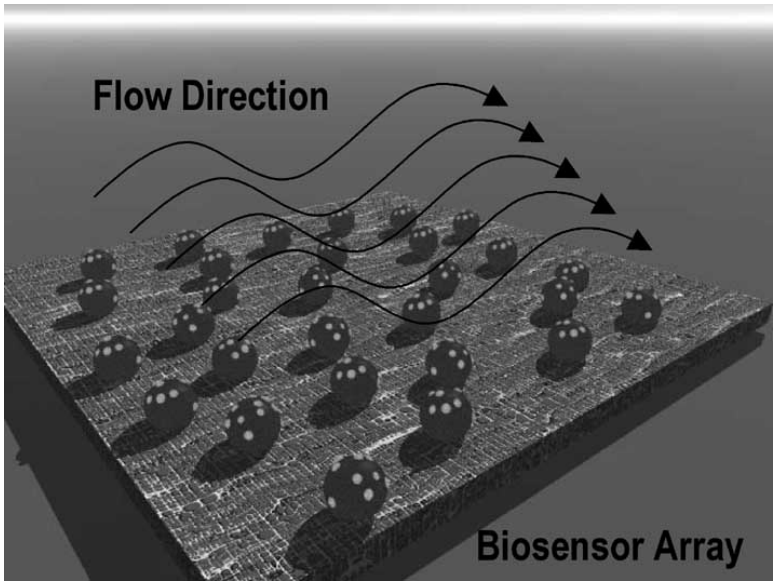

Figure 1.4: Schematic representation of a flow-cell based biosensor device. Surface can be modified with a suitable functionality such that it can be used to immobilize microparticles in a specific array. Membrane protein of interest is displayed in its functionally active form on the microparticle surface. This can be achieved by forming supported lipid membrane around individual particle. This sort of a device can be used to detect the presence of target molecules in the flow-system and/or to screen potential drug candidates against the target protein of interest.

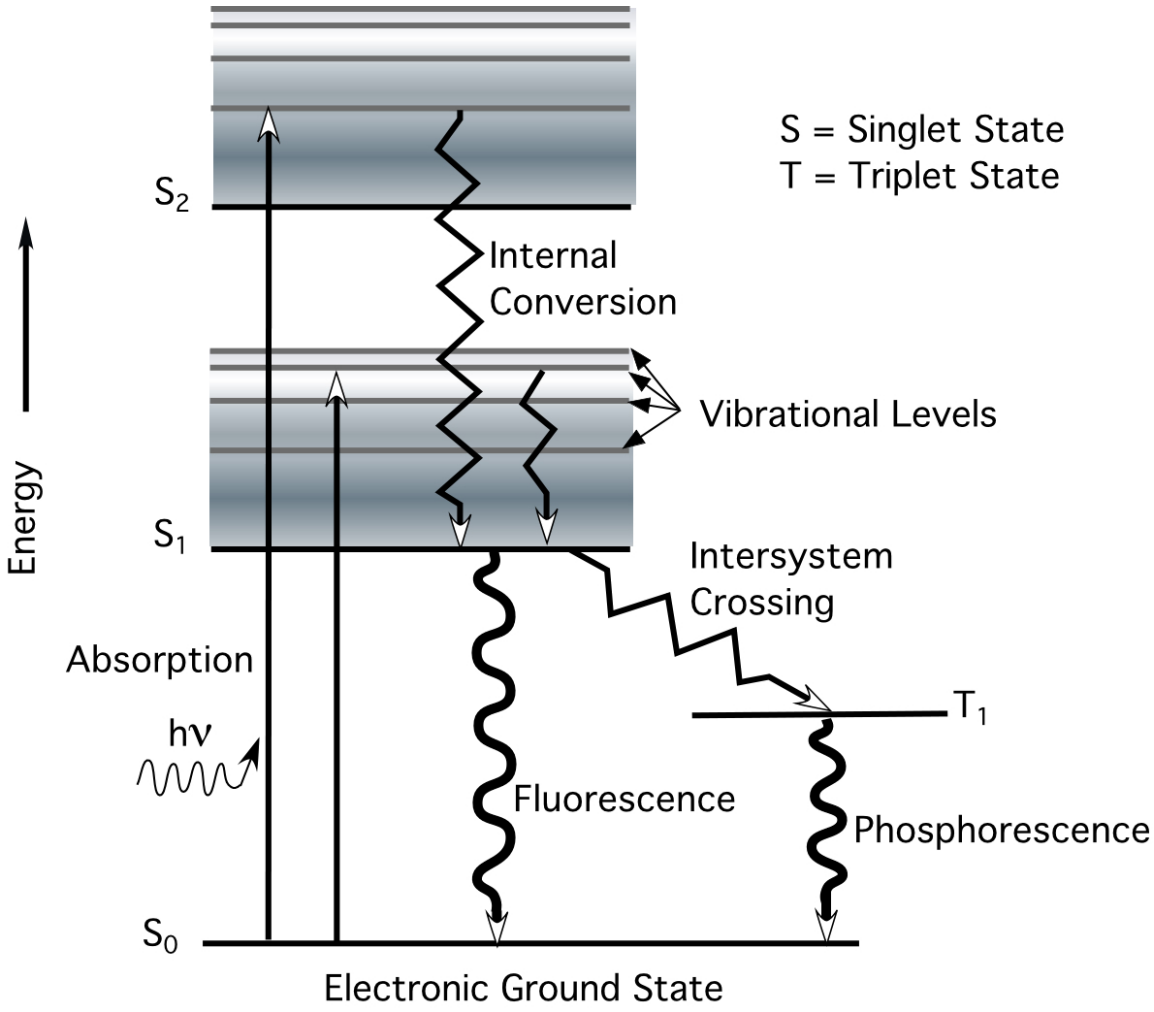

Figure 1.5: Simplified Jablonski diagram representation of the electronic transitions occurring in fluorescence. S_0 represents the ground electronic energy state while S_1 and S_2 represent first and second excite singlet states. Horizontal gray lines represent the vibrational energy levels corresponding to a particular electronic energy state. Vibrational levels corresponding to the ground electronic energy state (S_0) are not shown for simplicity. Three main transitions (absorption, internal conversion and fluorescence) have been shown using vertical lines with arrows. Fluorescence signal is generated when the molecule relaxes from the lowermost vibrational level of the first singlet state down to the ground electronic state. Also shown is the other relaxation mechanism (intersystem crossing), which involves spin conversion and takes the molecule to the prohibited triplet state. From the triplet state the molecule can relax down to the ground electronic energy state with the emission of light. This process (termed Phosphorescence) has much longer time scales associated with it (10^{-3}–100 sec.)

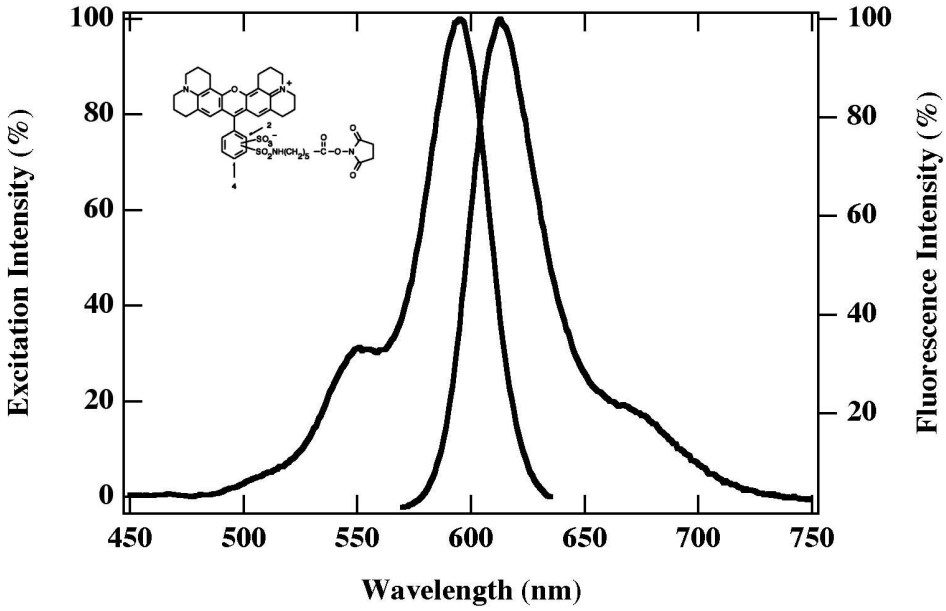

Figure 1.6: Representative excitation and emission spectrum of a fluorescent molecule Texas Red-X (Molecular Probes) in aqueous phase (pH 7.2) are shown. Molecular structure of the compound is shown in the insert. It can be noticed that the emission peak is red shifted compared to the excitation peak. This is the apparent Stokes shift, which results from the fact that energy associated with an excitation event is always higher than the corresponding fluorescence event. Another important aspect of excitation-emission spectra of some dyes is that they are mirror images of each other. This can be clearly seen for the case of Texas Red-X probe.

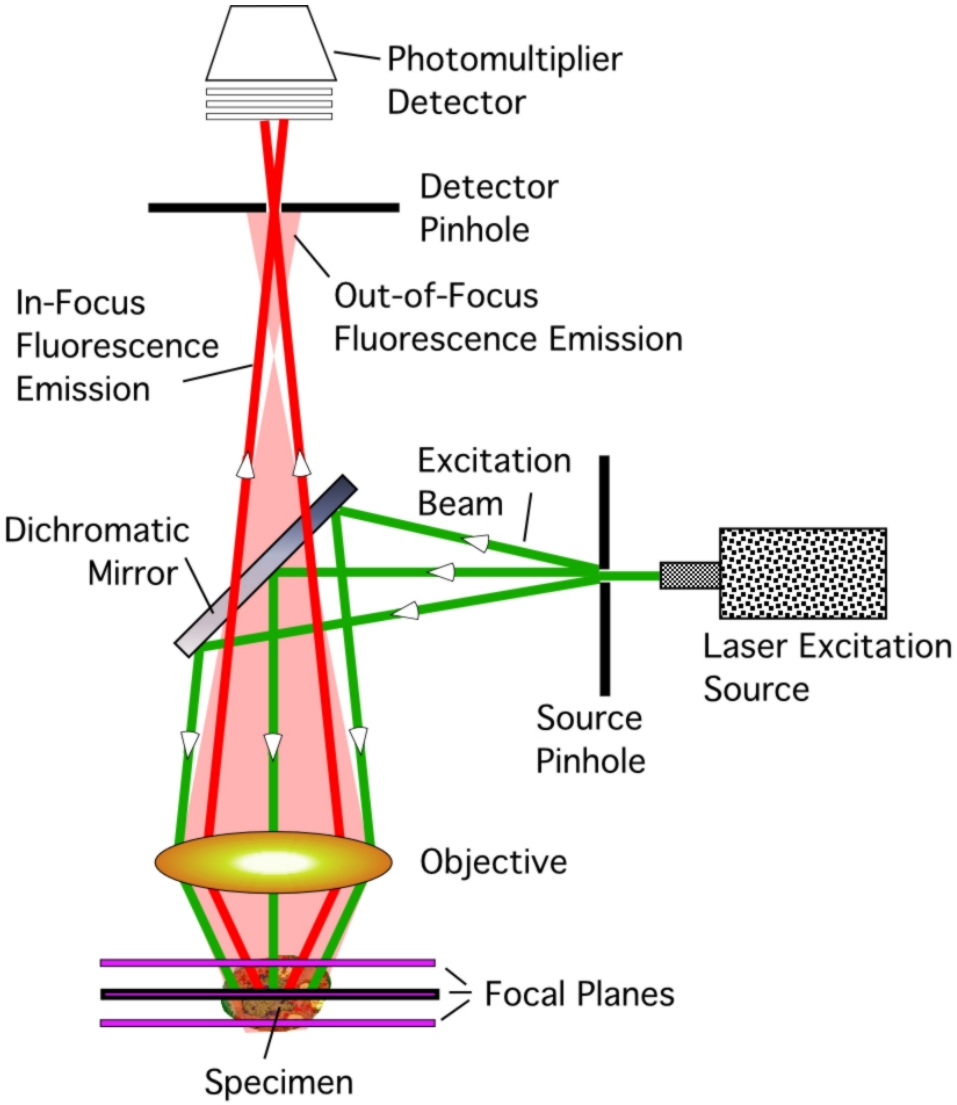

Figure 1.7: Schematic representation of the beam path in a confocal laser scanning microscope (CLSM). Excitation beam is attenuated by source pinhole, reflected by the dichroic mirror and is focused onto a small spot by the objective. Fluorescence generated from the excitation plane makes its way through the objective, dichroic mirror and detector pinhole into the photomultiplier detector. Fluorescence signal generated from the Out-of-Focus plane is rejected by the detector pinhole.

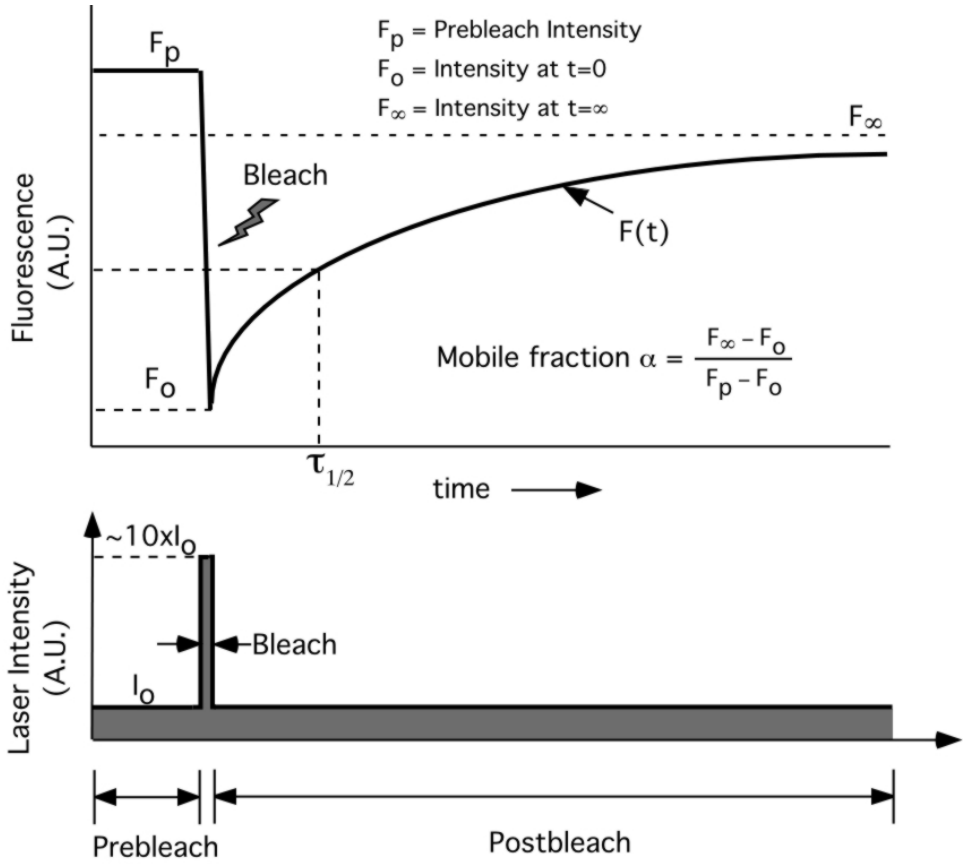

Figure 1.8: Schematic representation of a FRAP experiment showing the variation of fluorescence intensity of a region of interest (ROI) with time. Relevant parameters of the experiment have been shown. Also shown is the pulse sequence for the laser illumination intensity. A burst of laser intensity ($\approx$ 10X) for a short period of time leads to the bleach event. Postbleach detection is again done at attenuated laser power. Due to the mobility in the sample, fluorescence in the bleached region recovers back to a certain level F_∞, which is generally lower than the prebleach intensity F_p. The difference of the two quantities can be used to calculate the mobile fraction of the molecules. Transient behavior of fluorescence recovery F(t) can be used to predict the diffusion coefficient of the molecules. Also, $\tau_{1/2}$ denotes the half time of fluorescence recovery and is related to the characteristic time period τ_D ($\tau_D = \frac{\tau_{1/2}}{\beta}$ and $D = f(\tau_D)$, where β is a function of the degree of bleaching).

Chapter 2

Synthesis of Membrane Tethers from Bacteriorhodopsin

2.1 Introduction

The means of constructing supported membranes for the immobilization of membrane proteins has progressed rapidly from simple physical adsorption of lipid bilayers to more sophisticated approaches involving polymer tethering [39, 40, 41, 42, 43, 44]. In the case of a lipid bilayer supported on a solid surface without any tethers, the membrane is separated from the interface by a thin, lubricating layer of water ($\approx$ 1–3 nm) [45, 46]. This thin water layer is sufficient to provide the lateral mobility to the lipids in the supported bilayer. However, it presents various issues when integral membrane protein is reconstituted into the supported membrane, as the extraneous portions of the protein facing the support tend to interact with the surface. This can lead to immobilization of these molecules and can completely remove their ability to diffuse laterally in the membrane. To address this issue, a number of attempts have been made in recent years with an overall goal of separating the membrane from the surface with a polymeric cushion [43]. Bilayers fabricated in this manner are either supported on the polymer layer or are tethered to the polymer through various approaches. In the cases involving tether-supported membranes, a wide variety of tethering molecules have been employed ranging from polymers to peptides [39, 43]. Thus far, primarily single lipid moieties connected at the end of tethers have been used to anchor membranes to solid supports [47, 48, 49, 50].

In the present research, our aim was to construct biotin-PEG_{3400}-bacteriorhodopsin (bR) conjugates and use them to anchor lipid bilayer membranes to streptavidin-coated microspheres. Motivation for our approach to use bR comes from the point of view of the enhancement of the stability of tether-supported membranes. In the lipid-based tethers mentioned above, single lipid molecule is inserted into the supported membrane. On the contrary, if we have a molecule, which spans the entire membrane and has much larger contact area with the hydrophobic parts of the bi-

layer, it could act as a "molecular rivet" and provide the supported membrane with much higher stability.

This chapter describes the construction of biotin-PEG_{3400}-bacteriorhodopsin conjugates for the formation of solid-supported membranes on particles. We have used amine-based coupling to conjugate biotin-PEG_{3400} to bR. The conjugates were characterized using sodium dodecyl sulfate polyacrylamide gel electrophoresis (SDS-PAGE) and Matrix-Assisted Laser Desorption Ionization Mass Spectrometry (MALDI-MS) after purification. The biotin-PEG_{3400}-bR conjugate was further labeled with Texas Red to facilitate localization via fluorescence imaging.

2.2 Background

Supported lipid membranes have gained a lot of importance over the past decade due to their potential applicability in various areas. They serve as a model of biological cell membranes and hence a very attractive candidate for the design of biomimetic interfaces [43, 51]. The fact that in vivo, lipid membranes house a variety of transmembrane proteins makes the supported membranes an ideal candidate to be used for ex vivo reconstitution of these biomolecules upon isolation from native cell. Potential applications for such systems range from understanding the functional role of a membrane protein to building biosensing devices. The basic building block of these supported membranes being a lipid molecule makes these a natural method of biofunctionalization of surfaces. Furthermore, supported lipid bilayers have also recently been suggested for use as a passivating background for attaching intact liposomes to an interface [52, 53, 54]. This was accomplished by incorporation of a lipid-DNA (or cholesterol-DNA) conjugate into the liposome and the display of the complementary DNA strand on the upper leaflet of the supported lipid bilayer.

A lot of effort has been put in the direction of forming tether-supported lipid membranes. As mentioned above, one of the primary reasons is to be able to space

the bilayer farther from the substrate surface. From the point of view of our research objectives, there is an additional reason, mainly concerned with the stability aspects of these systems. A tethering molecule can impart more stability to the bilayer if it is spanning the entire membrane instead of being inserted into one of the leaflets. Bacteriorhodopsin, which is a transmembrane protein, is one good candidate.

Bacteriorhodopsin is a protein found in the cell membranes of Halobacteria, which grow in hypersaline aquatic lakes. Due to presence of high salt concentration, oxygen solubility in these habitats is drastically low — a condition that drives these organisms to resort to anaerobic means of growth — one of which is solar energy. bR is the key element, which helps in harvesting solar energy for life support of these organisms. This is an alternative route to photosynthesis, as it doesn't use a chlorophyll-based reaction center as in the case of plants and bacteria. bR is a light driven proton pump. It drives a gradient of protons across the cell membrane, which is coupled with the synthesis of ATP — a chemical energy source for cell growth. bR is a member of the retinal protein family, of which rhodopsin — the protein found in visual pigments — is also a member. These proteins have a retinal molecule bound in the intrahelical region which imparts them the essential functionality of being a proton transporter. bR is the most extensively studied archaeal retinal protein and is the paradigm of light-driven proton pump and seven-transmembrane helical proteins [55].

By comparing a single phosphatidylcholine with bR one can verify that the total hydrophobic surface area of bR is at least an order of magnitude higher than that of the lipid (Figure 2.1). Also, It has been recently reported that the magnitude of free energy difference for bR for the two states — membrane inserted vs. water solvated — is 88 kcal/mol, whereas for a lipid molecule it is 10–20 kcal/mol [56]. As our ultimate goal is to construct robust, supported membrane particles for immobilization of membrane proteins for applications such as biocatalysis, the

potential benefits of bacteriorhodopsin anchoring are multifold and linked to greater control over the stability of supported bilayers. Shown schematically in Figure 2.2, the use of bR (26.5 kDa without retinal) as a building block provides a means for more extensive anchor-membrane interactions relative to lipid-mediated tethering. Supported membrane assemblies on surfaces and particles fabricated in this fashion should exhibit greater stability under shear or processing flows. In addition, due to the increase in anchoring efficiency that could be obtained from the bR anchor, it is conceivable that fewer tethering points would be needed for a given supported membrane area. This would allow for greater native lipid areas for the introduction of membrane proteins into supramolecular assemblies of this type. A further benefit of bR anchoring is that reactive sites on the outer surface of the bR opposite the tether can be exploited to further stabilize the assemblies via crosslinking or by ligating large hydrophilic polymers such as glycans.

In order to use bR as a structural element to form tether supported membranes, it had to be anchored to a hydrophilic polymer, which could serve as a spacer moiety between the membrane and the supporting surface. One obvious choice was polyethylene-based polymer as it has been widely utilized in lipid-based tether molecules. In addition, bR also needed to be labeled by a fluorescent dye in order to localize it with confocal microscopy technique. PEG is a highly versatile polymer and a number of features, which make it one of the extensively used molecules in biotechnology. Its biocompatibility and non-toxicity make it ideal for in vivo applications. Due to its highly hydrophilic characteristic, it has been used to modify surfaces to minimize protein adsorption [57, 58]. When conjugated to a protein, PEG can drastically modify its properties. PEG modification shields the protein surface and can make it more water-soluble [59, 60, 61]. In the case of therapeutic proteins, PEG can reduce immunogenicity, thus increasing the circulation time and efficacy of the drug [62, 63].

In current study we utilized amine based coupling of PEG to lysine residues on bR. There are a few precedents related to the present study that have involved bacteriorhodopsin or rhodopsin conjugation that warrant mention here. In one such study, Sirokman and Fasman explored the amine-based PEGylation of bR in conferring water solubility to the protein, providing an analysis of likely conjugation sites [59]. In addition, their studies indicated that PEG_{5000}-bR retained similar proton pumping activity relative to that of unlabeled bR when the conjugate was reconstituted into lipid bilayers. In more recent work, Puu et al. utilized biotinylation of bR to allow for the localization of the protein in surface deposited proteoliposomes, which was verified via AFM imaging of streptavidin-colloidal gold probes [42]. Also related to the present study is the work of Bieri et al. in which rhodopsin that was biotinylated at the extracellular glycan moiety was used to tether the protein in a specific orientation in a biosensor microarray [64]. While these studies demonstrate feasibility of conjugation of bR and tethering via closely related rhodopsin, our work explores the first use of bR as a building block for a potentially improved means to anchor supported membranes.

2.3 Experimental

Abbreviations

bR, Bacteriorhodopsin; PEG, Polyethylene Glycol; mPEG, methoxy-Polyethylene Glycol; NHS, N-hydroxylsuccinimide; SPA, succinimidyl propionate; DMSO, Dimethyl Sulfoxide; TR, Texas Red; OG, Octyl β-Glucoside; MALDI-TOF-MS, Matrix-Assisted Laser Desorption/Ionization Time of Flight Mass Spectrometry.

Materials

Bacteriorhodopsin was obtained as lyophilized powder of the Purple Membrane from Halobacterium salinarum strain S9 (Munich Innovative Biomaterials (MIB)

GmbH, Germany). Biotin-PEG_{3400}-SPA (MW 3400) was obtained from Nektar Therapeutics, Huntsville, AL. OG was obtained from Pierce Biotechnology Inc., Rockford, IL. Texas Red-X, succinimidyl ester was obtained from Molecular Probes, Eugene, OR. Sephadex G-50 was obtained from Amersham Biosciences Inc, Piscataway, NJ. Sequencing grade Trypsin (Bovine Pancreatic) was obtained from Roche Allied Science, Indianapolis, IN. RapiGestTM was purchased from Waters Corp, Waltham, Mass.

Labeling of bR with biotin-PEG_{3400} and Texas Red

Purple membrane (3.45 mg bR) and biotin-PEG_{3400}-SPA (38.2 mg) were each dissolved in 200 μl, 50 mM Na_2HPO_4 buffer stocks, pH 9.0 with 100 mM OG. The two solutions were mixed together and incubated at room temperature with gentle shaking for two hours. Texas Red-X succinimidyl ester stock (16.7 mg/ml) was prepared in DMSO and 30 μl was added to 200 μl of reaction mixture. The remaining reaction mixture was saved for SDS-PAGE and MALDI-TOF-MS analysis after the addition of 15 μl of hydroxylamine (1.5 M) stop reagent. Texas Red-X containing reaction mixture was further incubated in the dark at room temperature for 2 hours before the addition of 15 μl of hydroxylamine (1.5 M) stop reagent. Excess reactants were separated over a Sephadex G-50 column (1 cm X 50 cm) equilibrated with 50 mM Na_2HPO_4 buffer without any OG. bR fractions (labeled and unlabeled) collected from the first peak were pooled together and concentrated using Amicon Ultra 15 filters (30 kDa cutoff, 2800 X g; 30min). bR aggregates formed on filter membrane were resolubilized using 100 mM OG. To achieve greater purification, traces of excess fluorescent probe TR and unattached biotin-PEG_{3400} were further removed by another G-50 column. bR fractions from the first peak were pooled together again and exchanged with Hepes Buffer A (Hepes 20 mM, EDTA 1 mM, NaCl 100 mM, pH 7.5) using Amicon Ultra-15 filters (2800 X g; 30 min) in

three rinse-spin cycles. The final retentate containing both labeled and unlabeled bR was redissolved in 100 mM OG (25 μM protein, 600 μl total volume) and was stored at -4°C until required.

Other methods

MALDI-TOF mass spectrometry analysis was conducted at the Columbia University Protein Core Facility on a Perceptive Biosystems delayed-extraction reflector instrument. Trypsin digestion was carried out overnight at 37°C in 0.5% RapiGest SF, at concentrations of bR and sequencing grade trypsin of 0.5 mg/ml and 0.05 mg/ml, respectively. The detergent was removed via ultrafiltration and a 10 minute, 100°C. denaturing step preceded the digestion. SDS-PAGE was done on Bio-Rad Mini PROTEAN II apparatus using 4–15% Linear Gradient Ready Gel Tris-HCl Gels. Bio-Safe Coomassie stain from Bio-Rad Laboratories was used to detect protein bands. Gel densitomograms were obtained using a 16-bit Umax flatbed scanner, with image processing carried out using Igor Pro 4.0 (Wavemetrics, Inc). UV-Vis analysis was done on Hitachi U-3010 Spectrophotometer. Extent of fluorophore labeling was determined by comparison of Texas Red absorbance relative to protein concentration. Presence of Texas Red was also evident from a corresponding shift of peaks in MALDI-MS study [65].

2.4 Results and Discussion

Our strategy to conjugate bacteriorhodopsin for anchoring membranes was adapted from earlier work of Sirokman and Fasman [59]. In their study, the main objectives were to analyze the effect of mPEG conjugation on the water solubility, refolding characteristics and proton pumping activity of bR. We have utilized PEG conjugation of bR with distinctly different objective. Our aim was to utilize bR-PEG_{3400} conjugates as structural elements in the design of supported membranes. In our

application, predominantly single site labeling is desired. Furthermore, low yield is tolerable because only the biotinylated bR conjugates will be assembled into the supramolecular complexes. Therefore, in contrast to the earlier bR PEGylation study in which moderate double labeling was obtained, we did not employ two reaction cycles nor include non-reactive PEG to increase reactivity of the protein [59]. The first step of the conjugation was carried out at pH 9 at a ninety-fold molar excess of biotin-PEG_{3400}-SPA. To enable fluorescence imaging of the biotin-PEG_{3400}-bR conjugates, an amine-based labeling (at 5-fold molar excess) with Texas Red-X succinimidyl ester was conducted after PEGylation, also at pH 9. Separation of the excess reactants was carried out using gel filtration followed by ultrafiltration to remove all traces of Texas Red dye not covalently linked to the protein. Figure 2.3 displays MALDI-TOF-MS traces of the bacteriorhodopsin (bR) starting material (trace A), the bR-PEG_{3400}-biotin conjugate (trace B), and the biotin-PEG_{3400}-bR-Texas Red conjugate (trace C). The inset of Figure 2.3 displays SDS-PAGE densitomograms that correspond to the MALDI-TOF-MS traces; bacteriorhodopsin starting material (trace A'), the bR-PEG_{3400} conjugate (trace B'), and the molecular weight markers (trace M). Traces B (MALDI-TOF-MS) and B' (SDS-PAGE) each contain two peaks — a lower molecular weight peak from the unreacted bR and an additional peak of higher molecular weight that we assign to the conjugate. In trace B, we assign the conjugate peak (denoted by an asterisk (*)) to the broad band located approximately 3400 Daltons higher in molecular weight. A very weak band that appears to correspond to bR-$(PEG_{3400}\text{-biotin})_2$ is evidenced near 34100 Da in trace B, We assign this feature to a small amount of double labeling of bR. As MALDI-TOF characterization does not provide direct quantitative information about conjugate yield due to differences in desorption of various species [62], SDS-PAGE studies were also employed. SDS-PAGE densitomograms were obtained for separate bioconjugation trials. Multipeak fitting gave estimated yields of the bR-PEG_{3400}-biotin

conjugates that ranged from 13 to 25%. Also, comparison of the bR band with the marker bands in SDS-PAGE data (Figure 2.3) reveals that it is located in between the two bands for 20 kDa and 25 kDa protein markers. This apparently is the effect of higher degree of interactions of SDS surfactant with a membrane protein, which results in higher charge/mass ratio and enhanced electrophoretic mobility.

Figure 2.4 shows a schematic of the amino acid sequence of bR, with reference to the secondary structures of bR as determined by X-ray crystallography in recent work by Belrhali et al. (1999; 1qhj) [66]. The seven lysine residues are indicated by the circles, the residues that comprise the transmembrane helices are located inside the rectangles. We note that the N-terminus is post-translationally modified and does not contain a primary amine [67]. The most likely polymer conjugation sites are Lys 129 and Lys 159 (indicated by arrows), as these are found on loops interconnecting the transmembrane helices and are solvent accessible to bulky reactants such as the biotin-PEG_{3400}-SPA employed here [59]. Furthermore, in aforementioned studies carried out by Sirokman and Fasman with amine-reactive PEG_{5000}, chymotrypsin digestion studies were consistent with loop lysine labeling [59]. Their findings were further bolstered by cogent arguments also based on the structure of bR. Early work with small molecule labeling indicated that Lys 129 was the most likely site [68, 69].

Analysis of bR structure using a molecular modeling program (e.g., Rasmol) reveals further information about the two likely conjugation sites, Lys 129 and Lys 159. Lysine residue at position 129 seems to be freely accessible to the solvent while the neighboring residues comparatively restrict the access to Lys 159 (Figure 2.5-A). Moreover, it is in the vicinity of two aspartic acid residues (Asp 102, Asp 104) (Figure 2.5-B). Side chain carboxylic (COOH) groups of these Asp residues are within 5 Å distance from the side chain amine (NH_2) of Lys 159. Presence of acidic residues in this close proximity is likely to protonate the amine, rendering it inactive

to amine labelling agents such as biotin-PEG_{3400}-SPA. This implies that we might have only one lysine residue in the entire amino-acid sequence of the bR (Lys 129), which is likely to be conjugated by biotin-PEG_{3400}-SPA.

To address this issue directly, we have performed a trypsin digestion of the bR-PEG_{3400}-biotin conjugate, followed by MALDI-TOF-MS characterization of the resulting fragments. The degree of difficulty of trypsin fragmentation is especially high for membrane proteins such bR, as most cleavage sites are buried. In addition, digestion of the protein gives rise to highly hydrophobic peptides [67]. Furthermore, the addition of detergents to achieve protein solubiliation dramatically reduces trypsin activity towards exposed cleavage sites as well. To obtain greater digestion yields we employed a new, acid-cleavable denaturant (RapiGestTM SF; Waters Corp) that does not greatly inhibit proteases and allows for higher trypsin reaction yields. In our experiments, run over a wide set of conditions including ranges of RapiGestTM SF concentration and Trypsin:bR ratio, we obtained peptides with missed cleavages almost exclusively. Table 2.1 lists the tryptic digest fragments detected that contain either K129 or K159. The corresponding MALDI-TOF-MS traces are shown in Figure 2.6. Trace A is from bR (control) and traces B and B' (= 3 X B) are from the bR-PEG_{3400}-biotin conjugate. Prominent in Trace A are the peaks at 17,578 and 24,856 m/z, assigned to 1–159 and 1–227, respectively, formed from loop site cleavage. Inspection of the bR-PEG_{3400}-biotin conjugate trace magnified 3X shows broad peaks shifted over by approximately 3400 Da from peaks assigned to sequences 1–159 and 1–227. These peaks are assigned to 1–159-PEG_{3400}-biotin and 1–227-PEG_{3400}-biotin conjugated fragments. The doubly-charged 1–159-PEG_{3400}-biotin species was also detected as a broad peak centered at 10,826 m/z. We were unable to detect any other PEGylated species, including conjugates of 83–159 and 41–159, a consequence, presumably, of lower yields of intrahelical-site cleavage that precluded detection. Due to the high yield of 1–159-PEG_{3400}-biotin species in the

trypsin digest, we infer that the predominant PEG_{3400}-biotin conjugation site is K129, as PEG_{3400}-biotin labeling at K159 would be expected to inhibit trypsin due to steric hindrance.

The other 5 lysines are thought to be less solvent accessible and are the likely sites of conjugation of the hydrophobic Texas Red fluorophore. Evidence for successful fluorophore labeling was first seen in the SDS-PAGE gels, as the bands from bR labeled with Texas Red generated a different hue due to the colorimetric properties of this chromophore combined with the bromophenol blue protein stain. MALDI-TOF-MS of the biotin-PEG_{3400}-bR-Texas Red conjugate is shown in trace C of Figure 2.3. Two broad peaks with complex lineshapes were evidenced, centered at approximately 27,700 and 31,500 Daltons. These features are shifted by over 600 Daltons from the corresponding peaks arising from bR and the bR-PEG_{3400}-biotin conjugate (found in trace B). These shifts are consistent with the successful conjugation of Texas Red (ligated molecular weight 702 Da) to a fraction of both the unreacted bR starting material and the bR-PEG_{3400}-biotin conjugate, giving rise to broad composite peaks comprised of fluorophore-labeled and unlabeled molecules.

UV-Vis analysis was performed to determine the degree of protein labeling with Texas Red. Figure 2.7 shows the absorption spectra for bR starting material, bR-PEG_{3400}, bR-PEG_{3400}-TR conjugate. Analysis of the absorption data revealed that approximately 1–2 Texas Red fluorophores were conjugated to each protein molecule. An interesting observation that came up from the absorption analysis of the conjugates was that retinal was found to be missing from TR labeled bR-PEG_{3400}-biotin. This could be a manifestation that retinal linkage to Lys 216 residue through the Schiff's base is relatively weak. As the retinal was present in bR-PEG_{3400}-biotin conjugates, it is likely that presence of lysine reactive Texas Red NHS reagent could have enhanced the detachment of retinal from bR.

2.5 Conclusions

We have demonstrated successful conjugation of bacteriorhodopsin with biotin-PEG_{3400} to synthesize bR-PEG_{3400}-biotin molecule. Conjugates were purified using gel chromatography combined with ultrafiltration. Characterization of the conjugates was done by MALDI-MS, SDS-PAGE and UV-Vis absorption spectroscopy. Reaction yields were determined from SDS-PAGE densitomograms and were estimated to be 13–25% for different bioconjugation runs. We have predominantly observed single site labeling with a small amount of double labeling as seen in MALDI-MS analysis. Trypsin digest was performed in order to determine the conjugation site for biotin-PEG_{3400}. Acid cleavable denaturant, Rapigest was utilized to maximize the digestion yields. Based on the MALDI-MS analysis of trypsin digested fragments of the bR conjugates, we have assigned Lys 129 as the conjugation site. This result is in agreement with previous bioconjugation studies on bR [59, 68, 69]. Further analysis of the conjugates with UV-Vis technique revealed 1–2 Texas Red dye molecules per protein molecule in the conjugated mixture.

A membrane tethering molecule should have the following characteristics: (i) a hydrophobic part which will insert into the lipid bilayer; (ii) a hydrophilic polymer (PEG) which can act like a spacer molecule; and (iii) a terminal functionality which will be useful in terms of anchoring the tether onto a suitable supporting bead surface. bR-TR-PEG_{3400}-biotin conjugates synthesized here qualify these criteria. Predominant single site labeling with biotin-PEG_{3400} ensures that there will be no crosslinking with the supporting bead surface and fluorescent labeling of bR will facilitate the characterization of tether assemblies on the bead surface using confocal microscopy.

Table 2.1: Trypsin fragments of bacteriorhodopsin detected by MALDI-MS that contain potentially accessible lysines

Trypsin Fragment number	bR Observed $(m/z)^a$	bR-PEG_{3400}-biotin Observed $(m/z)^a$	Assigned Sequence or Conjugate (Expected MW:Species)
T6-7	3566	3600	130-159 ($3645:[M+H]^{+1}$)
T5-7	8479	8481	83-159 ($8470:[M+H]^{+1}$)
T1-7	9025	9017	1-159 ($9034:[M+H]^{+2}$)
T1-7 PEG_{3400}-biotin	-	10826	1-159-PEG_{3400}-biotin ($9034:[M+H]^{+2}$)
T1-12	12355	12432	1-227 ($24882:[M+H]^{+2}$)
T3-7	13262	13307	41-159 ($13198:[M+H]^{+1}$)
T1-7	17578	17662	1-159 ($17487:[M+H]^{+1}$)
T1-7-PEG_{3400}-biotin	-	21200	1-159-PEG_{3400}-biotin ($20870:[M+H]^{+1}$)
T1-12	24856	24885	1-227 ($24882:M^{+1}$)
T1-12-PEG_{3400}-biotin	-	28551	1-227-PEG_{3400}-biotin ($28282:[M+H]^{+1}$)

[a]the moderate errors in m/z relative to the expected MWs are attributed to external calibration of the spectra and some degree of amino acid side reactions such as methionine oxidation.

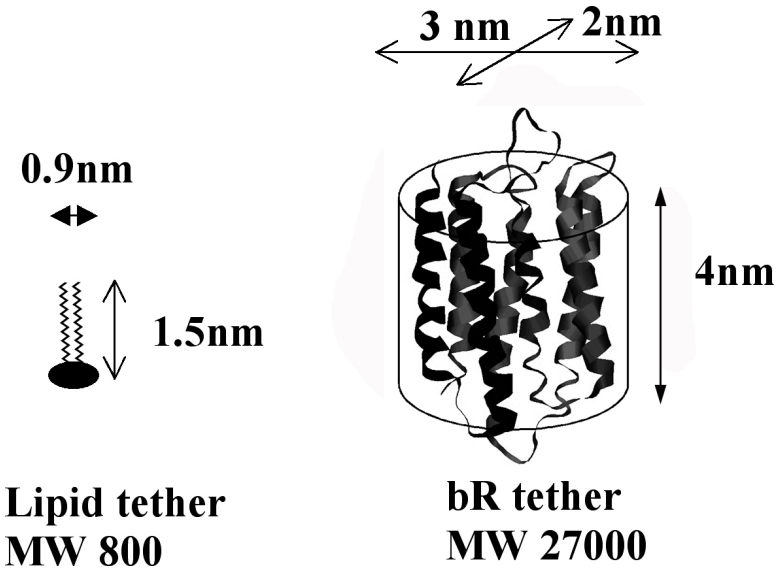

Figure 2.1: Side by side comparison of a lipid molecule and bacteriorhodopsin (bR). Lateral area of the protein is shown in an elliptical envelop for comparison. The dimensions are not exact and have been roughly estimated by using Chem3D.

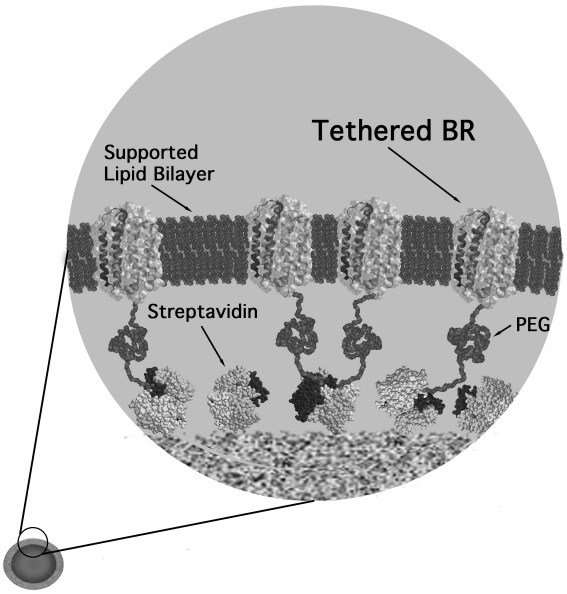

Figure 2.2: Schematic diagram of solid supported vesicles that integrate bacteriorhodopsin conjugates as lipid bilayer membrane anchors.

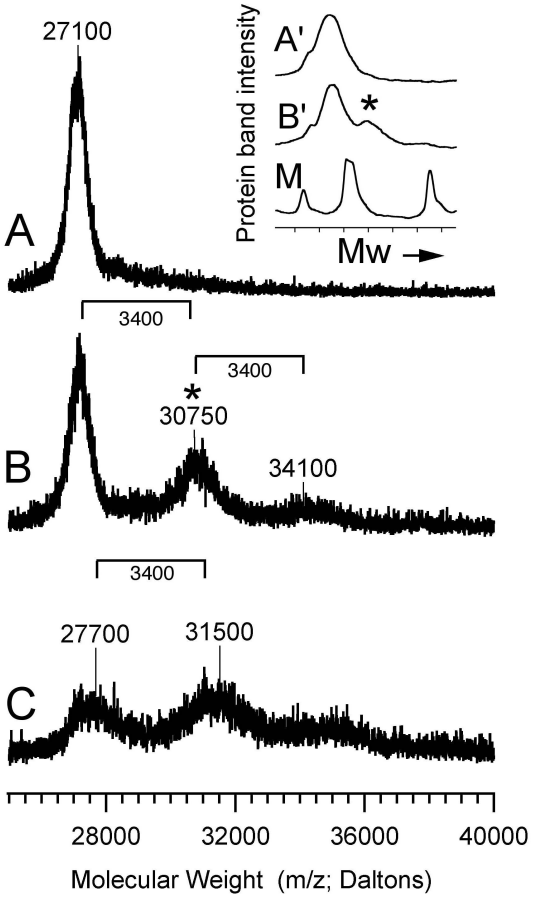

Figure 2.3: MALDI-TOF-MS and SDS-PAGE gel densitometry results for the biotin-PEG_{3400}-bacteriorhodopsin conjugate. Trace A was obtained from the Bacteriorhodopsin (bR) starting material. Trace B was obtained from the biotin-PEG_{3400}-bR conjugate. The peak denoted by the asterisk (*) in the main figure and inset is assigned to the biotin-PEG_{3400}-bacteriorhodopsin conjugate. Trace C was obtained from the biotin-PEG_{3400}-bR-Texas Red conjugate. In the inset SDS-PAGE gel densitometry results are shown for samples corresponding to traces A and B of the MALDI-TOF-MS results. Trace A' was obtained from the bR starting material. Trace B' was obtained from the biotin-PEG_{3400}-bR conjugate. Trace M was from the molecular weight markers (20, 25 and 37 kDa; left to right).

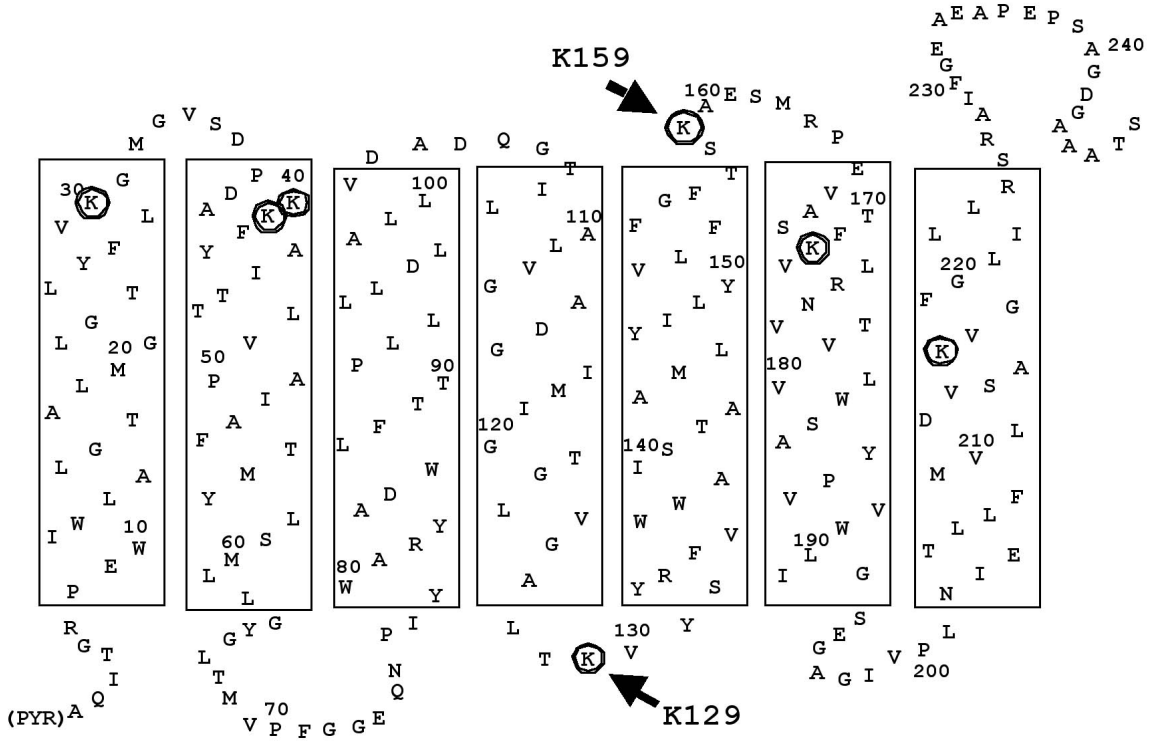

Figure 2.4: Schematic Diagram of the Structure of bacteriorhodopsin. The amino acid residues located in transmembrane helices are indicated by the rectangular boxes.

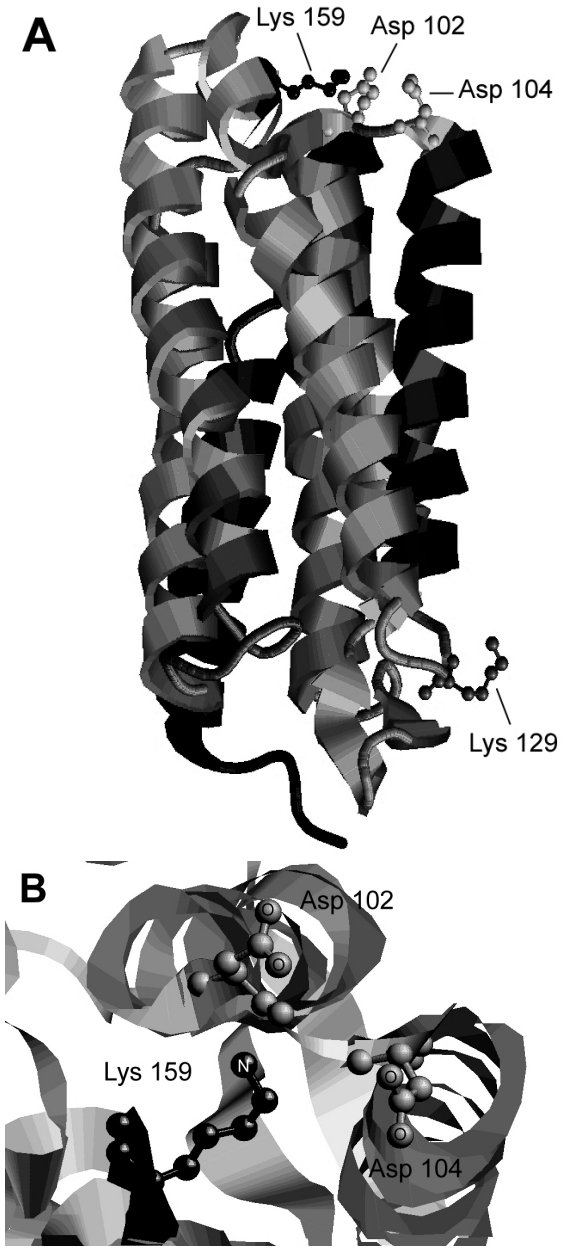

Figure 2.5: Analysis of Lys 129 and Lys 159 residues using Rasmol program. A) Lys 129 residue is freely accessible to the solvent whereas Lys 159 is in close proximity to Asp 102 and Asp 104 residues. B) A zoomed in view of the vicinity of Lys 159 from top showing the proximity of side chain carboxyl groups (COO-) of Asp 102 and Asp 104 to the side chain amine (NH_2) group of Lys 159. Hydrogen atoms are not shown for clarity.

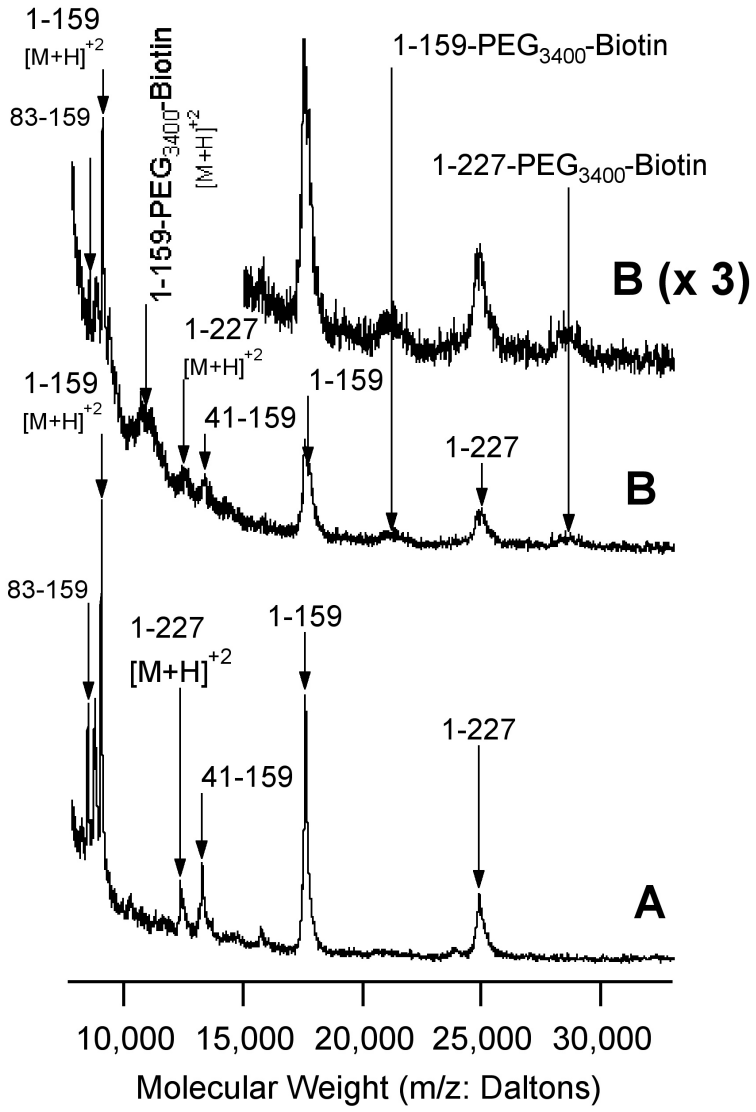

Figure 2.6: MALDI-TOF-MS results for the tryptic digest reaction products of the biotin-PEG_{3400}-bacteriorhodopsin conjugate. Trace A was obtained from a tryptic digest of the bacteriorhodopsin (bR) starting material. Trace B was obtained from a tryptic digest of biotin-PEG_{3400}-bR conjugate, conducted at the same conditions as in trace A. For closer examination, the region from 15,000 to 32,000 of trace B is shown magnified three times in the top trace.

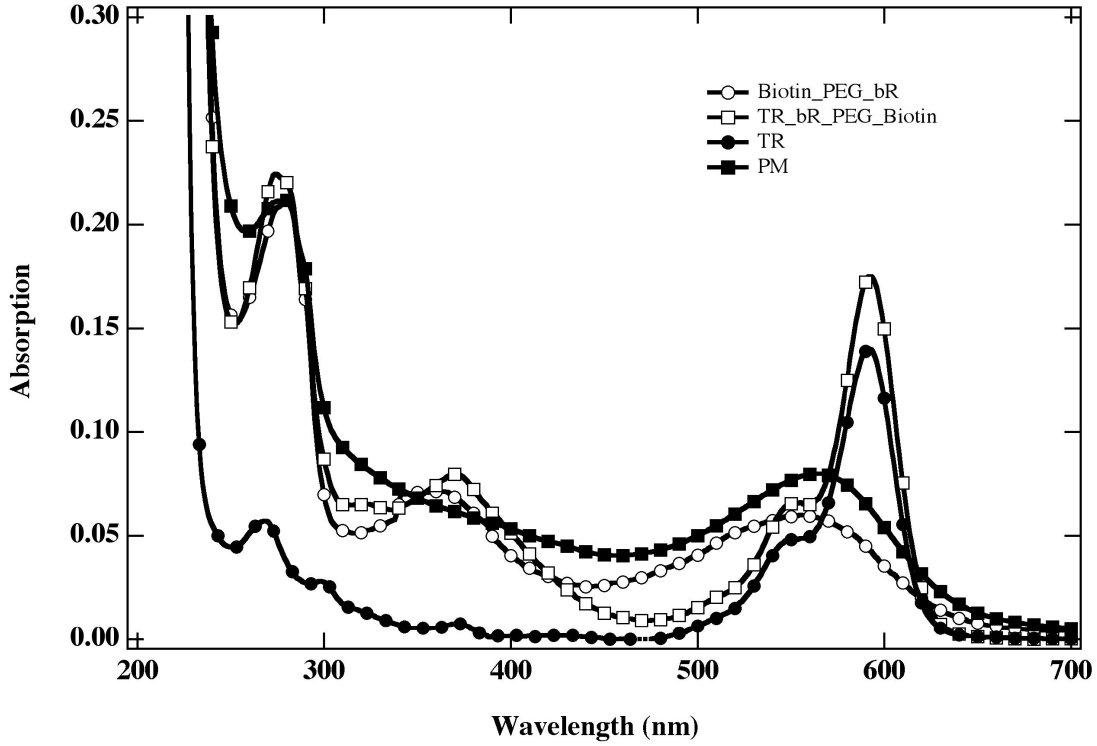

Figure 2.7: UV-Vis absorption spectra for bR starting material, biotin-PEG_{3400}-bR, TR-bR-PEG_{3400}-biotin and TR alone. Data points have been shown sparsely distributed for clarity. Absorption pattern of bR shows the characteristic peak at 570nm which is originated from retinal bound to Lys 216 of bR structure. Protein concentration in bR-PEG_{3400}-biotin was calculated by using an extinction coefficient at 570 nm (ϵ_{570} = 63,000). In TR-bR-PEG_{3400}-biotin sample the 570 nm peak is missing indicating that the chromophore retinal has been lost. Instead we have the characteristic absorption pattern of Texas Red (Compare with the absorption spectrum of free TR). Using an extinction coefficient of Texas Red at 594 nm (ϵ_{594} = 80,000) concentration of TR was estimated. Protein concentration in TR-bR-PEG_{3400}-biotin was indirectly estimated by comparison with the absorption (A_{280}) of bR-PEG_{3400}-biotin. Biotin-PEG_{3400} gives no detectable interfering signals at these concentration levels.

Chapter 3

Functionalization of Silica Bead Surface with Streptavidin

3.1 Motivation

In the previous chapter we described the synthesis of bR-PEG conjugates and characterized them for use as a suitable tethering alternative for supported bilayers. As discussed in the research outline given in the introduction chapter, our next goal was to functionalize a suitable surface to be used as a support for tethered membrane formation. We have synthesized the bR tethers with terminal biotin functionality in order to be able to use streptavidin–biotin interactions to anchor the tethers on a suitable surface. Our goal is to immobilize these tethers on spherical microparticles and subsequently fabricate supported lipid membrane on them. Desirable properties of the particles include a specific biofunctionality (biotin binding ability in this case), homogeneous and smooth surface to facilitate the uniform display of tether molecules, and satisfactory control over non-specific interactions of various molecules with the surface. Commercially available streptavidin (SA) coated beads were not very satisfactory in this regard. There could be non-uniform distribution of SA on these beads. In the case of polystyrene based beads, occasional cracks were evident on the surface. These can be potential sites for lipid aggregation. Another issue was the presence of unfolded SA on commercially available beads due to the shelf-life issue. To this end, we set out to functionalize silica beads in-house with fresh SA according to our requirements and further passivate them to minimize any non-specific interactions with hydrophobic molecules or fluorescent probes. Silica was chosen as the starting material for the microparticles as it is hydrophilic and will reduce non-specific hydrophobic interactions with the bare surface.

3.2 Introduction

Silica chemistry has been extensively studied and reported in the literature. A number of approaches can be used to modify the silica surface. Silanization has been

the most widely used method to derivatize silica surfaces. It was originally used to modify silica bead surface for the design of liquid chromatography supports [70, 71]. In general, this method involves covalent linking of organic molecules to surface siloxy groups by silylation with methoxy – or chlorosilanes [72]. Silanization of a silica surface despite its apparent simplicity is an enormously complex process. The reaction is very sensitive to a number of factors including the nature of silica surface, presence of surface impurities, and most important of all, presence of water traces on the surface. In general, it required extensive pretreatment of silica surface to completely dehydrate the surface followed by treatment with excess reactive silanes without a solvent or dissolved in anhydrous benzene or toluene [72, 73, 74, 75]. Modified silica surface achieved in this manner contains molecules covalently linked to it. However, they are sparsely distributed, which leaves a considerable fraction of silanol groups exposed on the surface [74, 76].

More compact density of these surface modifiers can be achieved by the formation of self-assembled monolayers (SAMs) on silica substrates. Basic building blocks of SAMs are amphipathic molecules, which spontaneously adsorb onto a solid surface from a solution to form a densely packed, two-dimensional structure. Silane based SAMs were first studied on planar substrates by Sagiv et al. [77, 78, 79, 80] and since then they have become a subject of great interest due to their potential applications, which require design of tailor made surfaces for biosensors, optoelectronic devices [81], liquid chromatography [76], nanopatterning of surface [82, 83, 84] etc. The details of the process of SAM formation on a substrate are not entirely understood but it is generally accepted that the traces of water molecules present on the substrate surface play a crucial role. Silica surface is highly hydrophilic and spontaneously adsorbs atmospheric humidity leading to the formation of a thin water layer [85, 86, 87]. It is believed [88] that the first step in the SAM formation is the physisorption of the polar head groups on the surface. Surface bound water

layer then hydrolyzes them into silanols. It is assumed here that the organic phase used to deposit the silanes on the surface contains small or no traces of water and hence the silanes cannot be completely hydrolyzed in the bulk solvent. If the surface adsorbed silane molecule contains more than one active group (e.g., Si-X_2 or Si-X_3 where X = chloride or methoxy group), there is a possibility of lateral polymerization through intermolecular Si-O-Si bond formation to give strongly bound monolayers. Figure 3.1 shows the sequence of events discussed above for the case of the surfactant used in the present case. Under uncontrolled conditions vertical polymerization can also take place, which can lead to the formation of aggregates on the substrate surface. Also, it is expected that curing the surfaces (heating the sample in air at 100–200°C.) can eliminate surface adsorbed water and can lead to covalent linking of adsorbed silanes with surface silanol groups [89]. However, there are contradicting views on this hypothesis. In one such study, the use of ^{29}Si-NMR analysis on mixed-C_3/C_{18}-alkyltrichlorosilanes horizontally polymerized monolayers on silica gel revealed that about 30% of the head groups were covalently attached to the silica substrate [90].

We decided to derivatize the silica bead surface by the formation of self-assembled monolayers as it can give quite compact and uniform distribution of the desired functionality on silica bead surface. p-Aminophenyltrimethoxysilane (APhMS) was used as the building block of the SAMs. This gives rise to amine terminal functionality on the bead surface, which can be exploited further to attach molecules of our choice to further derivatize the silica surface. The presence of a terminal amine functionality presents a possibility for the use of N-hydroxysuccinimide (NHS) based reagents. NHS based reagents are highly reactive towards nucleophilic amine groups. The reaction links the molecule of interest to the amines and liberates hydrolyzed NHS ester molecule. Another advantage of derivatizing the surface with amine terminated SAMs is that the further chemistry can be carried out in aqueous phase. This is

crucial for our system as we aim to functionalize our beads with streptavidin, which can potentially unfold and remove its ability to bind biotin in an organic solvent. We have used biotin-PEG-NHS linkers to attach to the top of APhMS SAMs. This was followed by treatment with excess PEG-NHS to block any unreacted sites and also to make the surface completely passive to non-specific adsorption. The biotin-derivatized surface was then coated with fresh streptavidin when it was required.

3.3 Experimental

Abbreviations

APhMS, p-Aminophenyltrimethoxysilane; PEG, Polyethylene Glycol; mPEG, methoxy-Polyethylene Glycol; NHS, N-hydroxylsuccinimide; SPA, succinimidyl propionate; TR, Texas Red; SAM, Self-assembled monolayer; DMSO, Dimethyl Sulfoxide; HABA, 2-(4-Hydroxyazobenzene) Benzoic Acid; POPC, L-α- Phosphatidylcholine; DOPG, 1, 2-Dioleoyl-sn-Glycero-3-[Phospho-rac-(1-glycerol)] (Sodium Salt); SA, Streptavidin.

Materials

APhMS was obtained from Gelest, Inc., Morrisville, PA. Texas Red-X, succinimidyl ester was obtained from Molecular Probes, Eugene, OR. Biotin-PEG_{3400}-SPA and $mPEG_{2000}$-SPA were obtained from Nektar Therapeutics, Huntsville, AL. SA and SA-FITC were obtained from Sigma-Aldrich Corp., St. Louis, MO. POPC (egg, chicken) and DOPG were purchased from Avanti Polar Lipids, Inc. Alabaster, AL. Green fluorescent lipid probe β-BODIPY 500/510 C_{12}-HPC was purchased from Molecular Probes, Eugene, OR.

Modification of silica microsphere surface with p-aminophenyltrimethoxy silane (APhMS)

Surface of silica beads was cleaned by treating them with sulfuric acid contain-

ing nochromix (4.8% w/v) for 40 min. This was followed by 3 cycles of deionized water wash and centrifugation. Finally, the beads were washed once with anhydrous toluene and centrifuged again. A 200 mM stock solution of APhMS was prepared by dissolving it in toluene just before using it and a controlled amount of deionized water was put in it (0.54% v/v corresponding to water concentration of 300 mM). This was done to facilitate controlled hydrolysis of silane in solution phase. APhMS stock in toluene was used to suspend the silica palette obtained after centrifugation. The suspension was gently shaken after regular interval to keep the beads from settling due to gravity. After 30 min of incubation, excess unreacted APhMS solution was decanted and APhMS coated beads were washed with pure toluene and centrifuged. Traces of toluene were removed by putting the beads in vacuum overnight. After 24 hours of curing at room temperature, beads were washed thrice with acetone to further remove any clumps of APhMS from bead surface. Beads were then dried under vacuum and stored at room temperature.

In order to test the uniformity of APhMS distribution on the bead surface it was tagged with Texas Red-NHS. A 2-mg/ml stock of the reactive dye was prepared in anhydrous DMSO and a 10 μl aliquot of the reactive dye stock was added to the slurry of beads in phosphate buffer pH 9.0 (9 mg beads in 250 μl). After 1 hour of reaction time 10 μl of stop reagent (Hydroxylamine 1.5 M, pH 8.5) was added to terminate the reaction and beads were washed with fresh buffer. In order to wash last traces of surface adsorbed dye, beads were washed with DMSO in 10 rinse-spin cycles. Beads were finally re-suspended in phosphate buffer pH 9.0 and were analyzed using epi-fluorescence and confocal microscopy.

Functionalization of modified silica surface with biotin

APhMS-coated silica beads were treated with biotin-PEG_{3400}-NHS to attach biotin-PEG_{3400} to the bead surface. NHS end of the molecule is highly reactive

towards nucleophilic amine groups on the bead surface. The reaction leads to binding of biotin-PEG_{3400} to surface amines and liberation of hydrolyzed NHS ester molecule. In a typical PEGylation run, 40 mg APhMS coated silica beads were pre-washed twice with 1 mM NaOH to deprotonate most of the amine groups on the surface. Beads were then suspended in 500 μl of biotin-PEG_{3400}-NHS solution. Biotin-PEG_{3400}-NHS solution was made by dissolving 18.4 mg reagent in 500 μl phosphate pH 9.0 and immediately added to the bead palette, as it hydrolyzes very rapidly in aqueous phase (Nektar Therapeutics) Mixture was incubated at room temperature with frequent gentle mixing to redisperse settled beads. After 30 minutes a freshly made 500 μl solution of biotin-PEG_{3400}-NHS (10.3 mg/500 μl) was added to the reaction mixture. This was followed by another addition of 300 μl of third biotin-PEG_{3400}-NHS stock (9.8 mg/300 μl) after 30 min. Subsequent additions of fresh biotin-PEG_{3400}-NHS stocks were done to maintain a high concentration of reactive biotin-PEG_{3400}-NHS as it hydrolyzes very fast in aqueous phase and becomes unreactive. After another 60 min of incubation a freshly made 300 μl stock of $mPEG_{2000}$-SPA (26.3 mg/ml) was added. This was done to tag unlabeled amine groups and completely passivate any bare surface on the beads. For making PEG-passivated control microspheres, APhMS coated beads were directly treated with $mPEG_{2000}$-SPA at similar concentration levels as described above. After overnight incubation to maximize PEGylation of the surface, beads were subjected to 10 spin-rinse cycles with phosphate buffer (pH 9.0) to remove excess PEG reagents.

Streptavidin tagging to biotinylated bead surface

Streptavidin was attached to biotin-PEG_{3400} tethered beads by incubating the beads with a solution of streptavidin in phosphate buffer (pH 9.0). In a typical run, a 10 mg beads were dispersed in 200 μl streptavidin stock (0.5 mg/ml) and incubated for 2 hours at room temperature with gentle mixing. Beads were then

washed 4 times with phosphate buffer to remove excess unbound protein. Similar protocol was followed to tag the beads with fluorescent streptavidin (SA-FITC) in order to verify the labeling using confocal microscopy. As a test for specific biotin labeling by SA-FITC, a set of PEG passivated control beads was also treated with SA-FITC under similar conditions.

2-(4-Hydroxyazobenzene) Benzoic Acid (HABA) displacement assay to determine biotin surface density

HABA assay was performed to determine surface density of biotin on biotin-PEG_{3400} tethered silica beads. As a negative control, $mPEG_{2000}$ passivated beads were used. Four milligram beads from each set were washed 3 times in HABA assay buffer (Phosphate 100 mM, NaCl 150 mM, pH 7.2). HABA-avidin mother stock was prepared in HABA assay buffer by dissolving the HABA-avidin premix in 100 μl DI water and adding 900 μl of HABA assay buffer. This was further diluted 10 times to prepare HABA-avidin mother stock. Both bead sets after 3X washing in HABA assay buffer were resuspended in 250 μl each of HABA-avidin working stock. After 3 hours of incubation with gentle mixing, beads were spinned out of the reaction mixtures and absorption of the supernatant solutions was measured using Beckman DU-640 spectrophotometer. Comparison was done with the absorption of HABA-avidin working stock.

Test of nonspecific binding of lipids to the functionalized beads at different stages of surface modification

One of the important goals was to minimize non-specific interactions of the lipids with silica surface. To this end we passivated the beads with $mPEG_{2000}$ as described earlier. In order to verify that we had achieved control over non-specific interactions with the surface, silica beads at different stages of surface modification were incubated with lipid formulation (POPC/DOPG/β-Bodipy-HPC). Different surfaces

that were tested were: (i) bare silica, (ii) APhMS coated, (iii) biotin-PEG_{3400} functionalized without $mPEG_{2000}$ passivation, (iv) biotin-PEG_{3400} functionalized and $mPEG_{2000}$ passivated, and (v,vi) SA tagged beads of sets (iii) and (iv) respectively. In a typical run, 4 mg of beads were mixed with 20 μl of fluorescently doped liposomes solution (lipid concentration 4 mg/ml) and incubated for 1 hour. Fluorescent lipid β-Bodipy 500/510 C_{12}-HPC was present in the liposome formulations at a ratio of 1:100 (probe:lipid). Excess liposomes were removed by centrifugation. Beads were analyzed by confocal microscopy.

Confocal microscopy

Confocal microscopy was used to image the fluorescently tagged bead surface. This is a very powerful fluorescence imaging technique as it gives advanced capabilities compared to fluorescence microscopy. These include control over the illuminated spot size and depth of field, ability to reject out of focus fluorescence and ability to image thin sections of a sample, and a number of more advanced features not available in regular fluorescence microscopes. A confocal imaging system achieves out-of-focus rejection by the combination of two strategies: (a) by illuminating a single point of the specimen with a laser beam attenuated through source pinhole, so that illumination intensity drops off rapidly above and below the plane of focus; and (b) by the use of a pinhole aperture in a conjugate focal plane to the specimen, so that light emitted from the out-of-focus point in the specimen is blocked from reaching the detector.

Samples were imaged using Leica TCS SP2 AOBS Spectral Confocal Microscope System equipped with Argon ion and HeNe lasers. Texas Red was excited by 594 nm excitation line and 63X/1.4 oil immersion objective was used. FITC was excited using 488 nm line of Argon laser and images were taken with the detection window set between 502–614 nm. Pinhole aperture was set at airy value of 1, which was

equivalent to ≈ 500 nm vertical slice of the bead.

3.4 Results and Discussion

3.4.1 APhMS coating of silica bead surface

In order to use hydrophilic silica beads we needed to modify the surface to provide it with a suitable functionality. Silane based chemistry has been widely used to modify planar silica surfaces as discussed earlier. We employed the APhMS molecule, which has been shown to coat the silica surface through the formation of SAMs [83]. A potential advantage of using APhMS is that there is a possibility of hydrogen bonding at the terminal group further stabilizing the assemblies. As we were using spherical silica beads, we had much larger surface area to volume ratio and we needed to optimize the APhMS concentration accordingly. Another issue was that it was harder to control the amount of water on sulfuric acid cleaned beads as we were processing milligram quantities of beads. Amount of surface adsorbed water has been shown to be critical in silane chemistry [70]. To address this issue, beads were washed with toluene once to remove any excess water from the system. Toluene does not completely dehydrate the bead surface, as water is not completely miscible in toluene. Also, hydrolysis of methoxy silanes was facilitated in the stock solution by adding controlled amount of water. This has been shown to be an effective strategy to optimize surface coverage of silane SAMS [83]. In a parallel batch, as-received silica beads were directly exposed to APhMS stock solution in toluene containing trace amounts of water. No significant difference was observed in the APhMS coverage for the H_2SO_4-pretreated beads as analyzed by Texas Red staining explained below. The results shown in Figure 3.2 are for the set of beads, which was directly exposed to APhMS without any sulfuric acid pretreatment.

APhMS coverage of the bead surface was analyzed by staining it with Texas Red-NHS. Analysis of Texas Red distribution on the bead surface was done with

confocal microscopy. Figure 3.2 shows the different sections of Texas Red stained bead surface. Each section corresponds to ≈ 500 nm thickness of the imaged bead as shown in the schematic in the figure. A three dimensional reconstruction of the images shows perfectly homogeneous labeling of the bead surface with Texas Red indicating that APhMS was uniformly coating the bead surface. Analysis of the control beads (bare silica) incubated with Texas Red-NHS showed no detectable fluorescence on the bead surface indicating that Texas Red-NHS was specifically labeling surface amines.

3.4.2 Verification of homogeneous biotin distribution using streptavidin-FITC labeling

As mentioned earlier, it was very crucial to achieve a uniform density of the functional groups on the silica bead surface. Distribution of biotin on the biotin-PEG_{3400} derivatized, $mPEG_{2000}$ passivated beads was analyzed by tagging the surface with FITC labeled streptavidin (SA-FITC). Confocal imaging (Figure 3.3) clearly indicates that streptavidin was uniformly tagging the biotinylated surface showing uniformity of biotin distribution. Also shown in the figure is the confocal image for one representative control bead ($mPEG_{2000}$ derivatized), which shows minimal staining by SA-FITC. This confirms that streptavidin was specifically attaching on to surface biotin groups on the on the biotin-PEG_{3400} derivatized, $mPEG_{2000}$ passivated beads.

3.4.3 Determination of surface density of biotin on modified silica surface

In order to determine the surface density of biotin on the silica beads, HABA binding assay was performed. HABA-avidin complex was added to a known amount of biotinylated silica beads. Biotin, due to its high affinity for avidin displaces HABA from the complex. This is accompanied by a decrease in the absorption at 500

nm, which is a spectral signature of the HABA-avidin complex. By monitoring the decrease in 500 nm absorption and using an extinction coefficient of 34,000 $M^{-1}cm^{-1}$ for the HABA-avidin complex, the total number of HABA molecules displaced from the complex can be calculated. To get accurate estimation of biotin sites on the bead surface, HABA-avidin concentration was required above saturation level. This was verified by the experimental observation that the absorption at 500 nm did not drop to zero, indicating that there was still excess HABA-avidin complex in the solution.

Figure 3.4 has the UV-Vis absorption spectra for the HABA assay, which shows decrease in the HABA-avidin complex absorption at 500 nm upon incubation with biotinylated beads. As a negative control, HABA-avidin complex was incubated with silica beads that had been passivated with $mPEG_{2000}$. Control showed no decrease in the absorption at 500 nm indicating specificity of the biotin-avidin interaction. Based on the absorption difference of 0.01, biotin surface density was calculated to be 0.0185 molecules/nm^2. This corresponds to 1 molecule per 54 nm^2. Assuming that we can tag all the surface biotins with streptavidin molecules, this translates into a biotin binding capacity of 0.038 μg/mg beads. This number is comparable to the biotin-FITC binding capacity of commercially available beads of similar sizes (Polysciences Inc.). Also, assuming streptavidin cross-section to be approximately 5 nm X 5 nm, biotin functionalization at this level can lead to coverage of $\approx$ 46% of the bead surface with streptavidin.

3.4.4 Test of nonspecific binding of lipids to the functionalized beads at different stages of surface modification

As the final goal was to fabricate lipid bilayers on these modified silica surfaces, it was imperative to test for the non-specific interactions of lipids with these beads. To achieve this, a fixed quantity of silica beads at different processing steps were

incubated with identical concentrations of liposomes containing fluorescently tagged lipid probes. Figure 3.5 shows the confocal images for different sets. It was apparent from this study that lipids strongly interact with bare silica as well as APhMS coated silica beads. Whereas, there was minimal adsorption of lipids to all the remaining sets. As there was no apparent difference between beads containing biotin-PEG_{3400} with or without $mPEG_{2000}$, it appears that biotin-PEG_{3400} alone was sufficiently packed to keep the lipids from interacting with the surface. Also, streptavidin functionalized surfaces showed no lipid staining, indicating that streptavidin was not acting as a seeding site for the non-specific adsorption of lipids.

3.5 Conclusions

The main conclusions for this chapter are the following:

1. We have successfully coated the silica bead surface with APhMS. Conditions for APhMS self-assembly on silica beads were optimized in terms of (i) concentration, (ii) solvent, (iii) and bead treatment after APhMS exposure.

2. APhMS coated silica beads were functionalized with biotin-PEG_{3400}. Homogeneity of biotin distribution was verified by specific labeling with fluorescent streptavidin (SA-FITC) followed confocal analysis. Biotin density on the surface was estimated by HABA displacement assay and was found to be approximately one biotin-PEG_{3400} molecule per 54 nm^2.

3. Passivating properties of the beads were assessed for lipids at different stages of the surface modification. Lipid were observed to be highly attracted towards bare silica surface and APhMS coated surface. Bare silica surface is expected to be covered by a lipid bilayer when exposed to lipid vesicles, therefore current result is not a surprise. APhMS coated surface can have a high charge density due to terminal amine groups, which can lead to favorable interactions with

polar head groups of the lipids. Biotin-PEG_{3400} and $mPEG_{2000}$ passivated surfaces showed good control over non-specific interactions with lipids. This indicates that the surface was completely derivatized with biotin-PEG_{3400} and $mPEG_{2000}$ and there were no spots where bare silica or bare APhMS surface was exposed.

4. Silica surface was successfully derivatized with streptavidin. Streptavidin tagging was verified by the use of fluorescently tagged streptavidin (SA-FITC). The specificity of streptavidin towards biotin was verified by using a negative control surface, which was derivatized only with $mPEG_{2000}$. This surface showed minimal staining by fluorescent streptavidin as verified by confocal imaging.

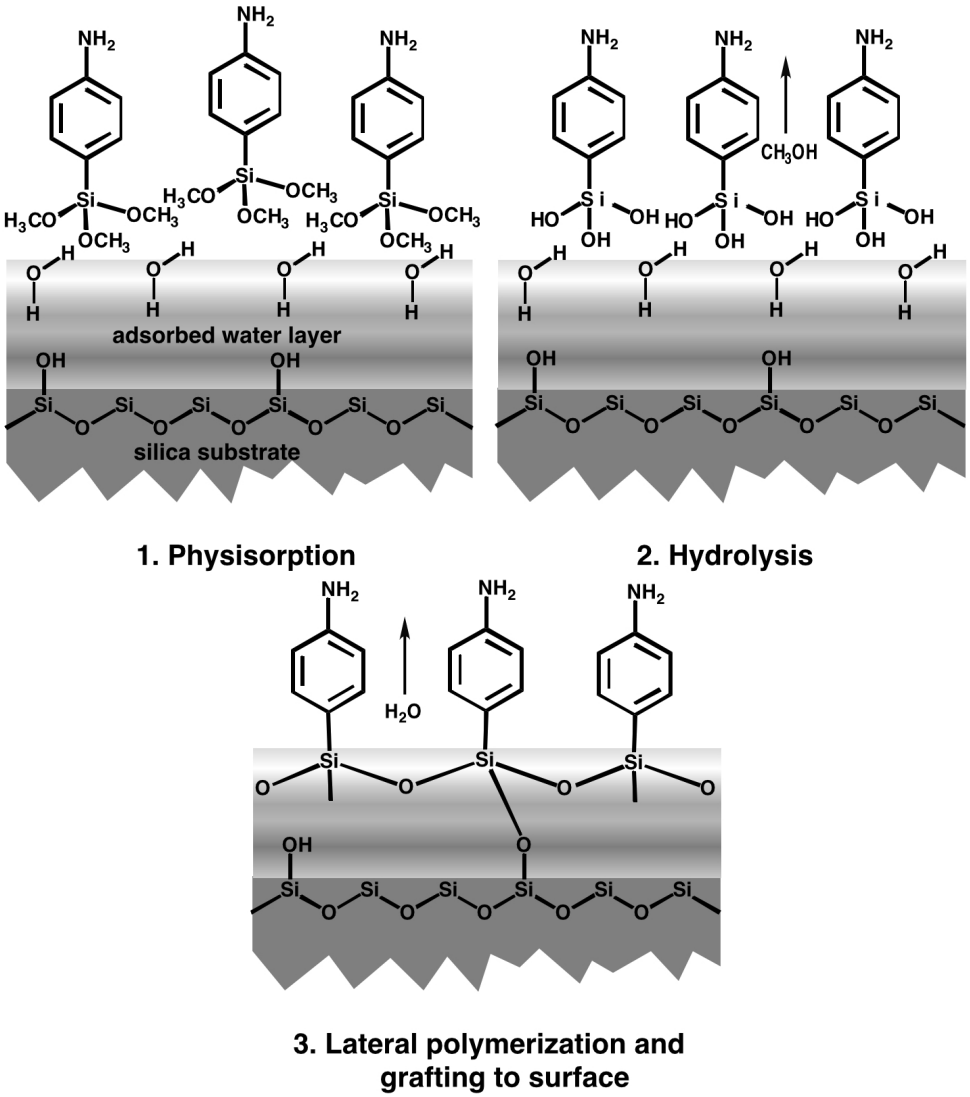

Figure 3.1: Schematic representation of APhMS self-assembly on silica surface showing major changes occurring in the process. First step of self-assembly is the physisorption of the surfactant on the thin water layer present of the substrate. This is followed by the hydrolysis of the methoxy-silanes into silanols. Further curing of the samples can lead to lateral polymerization and may also result in covalent linking with the substrate.

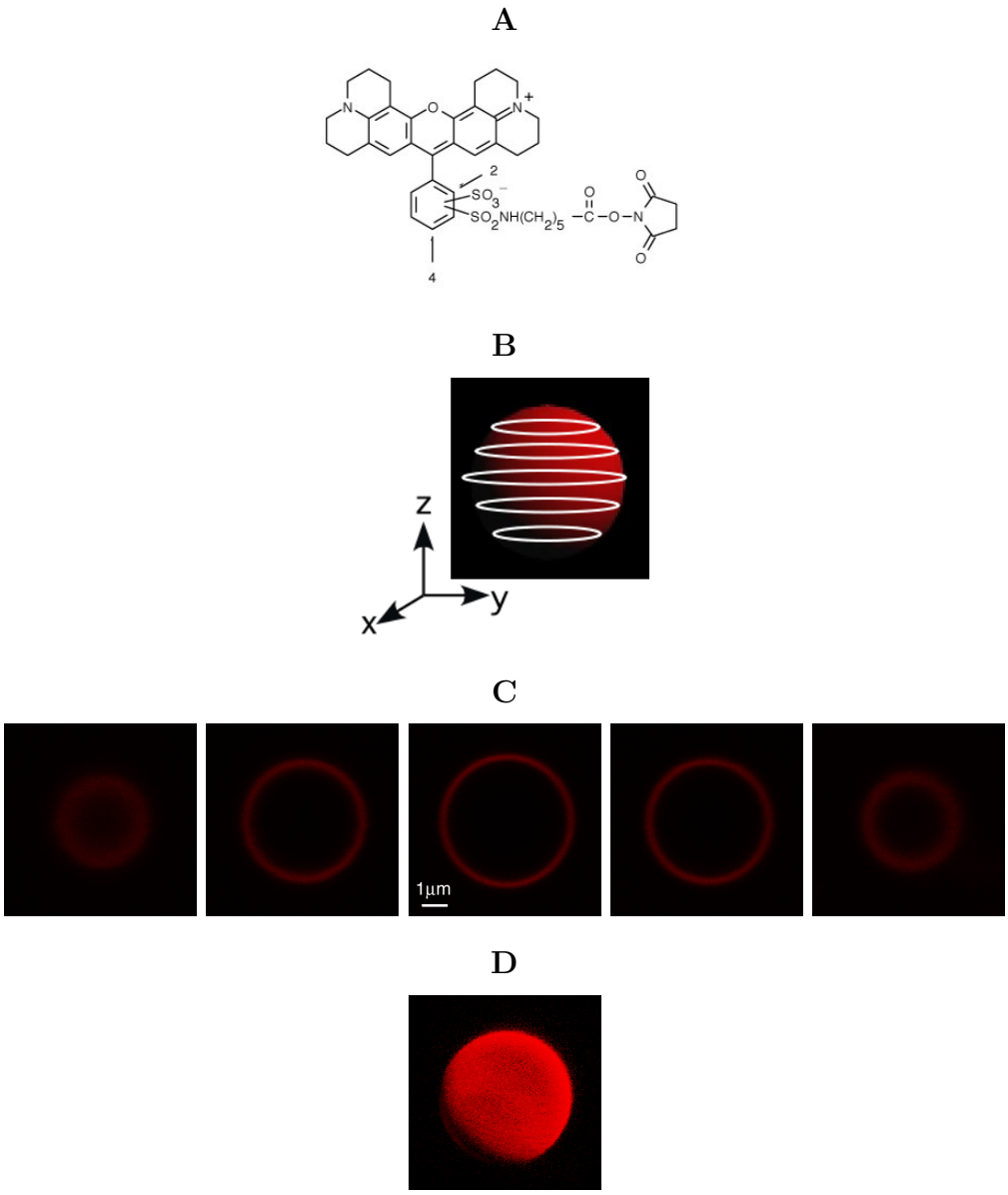

Figure 3.2: Analysis of APhMS distribution on silica bead surface through Texas Red staining. A) Structure of Texas Red-X Succinimidyl Ester (Texas Red-NHS). B) Schematic representation of 5 slices of Texas Red labeled bead surface. C) Five representative slices of bead showing uniformity of Texas Red distribution along the perimeter of the bead. Each image corresponds to $\approx$ 500 nm thick section of the bead. D) A reconstruction of the bead made by the Simulated Fluorescence Process (SFP) algorithm.

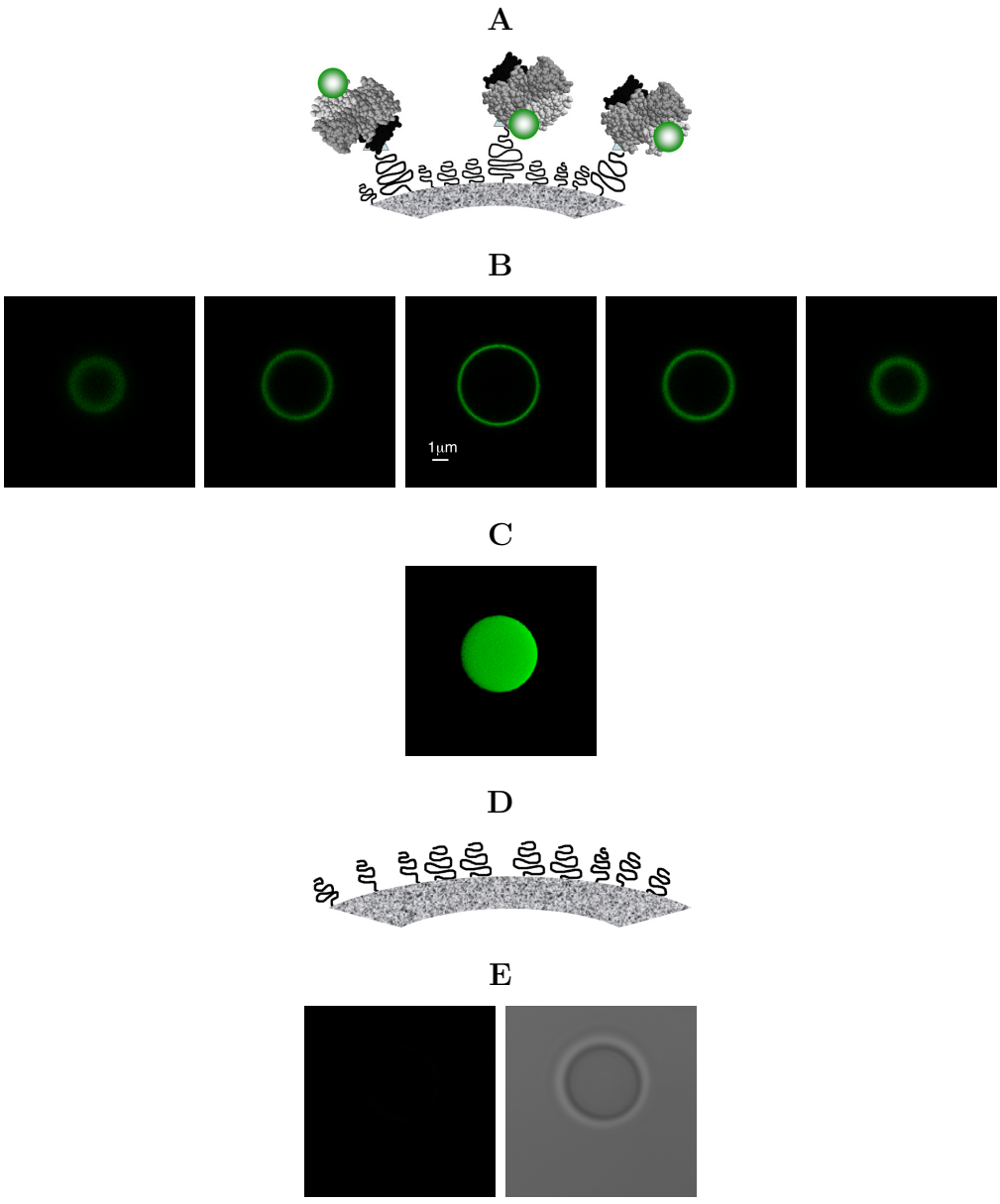

Figure 3.3: Analysis of streptavidin distribution on biotinylated beads. A) Schematic representation of SA-FITC bound to biotin functionalized bead surface. B) Optical sections of SA-FITC stained bead surface. C) A reconstruction of the SA-FITC stained bead made by the Simulated Fluorescence Process (SFP) algorithm. D) Schematic representation of control surface, which is negative in biotin but is $mPEG_{2000}$ derivatized. E) Confocal images of control surface incubated with SA-FITC at the equator of the bead. Transmission channel image has been included to indicate the presence of the bead.

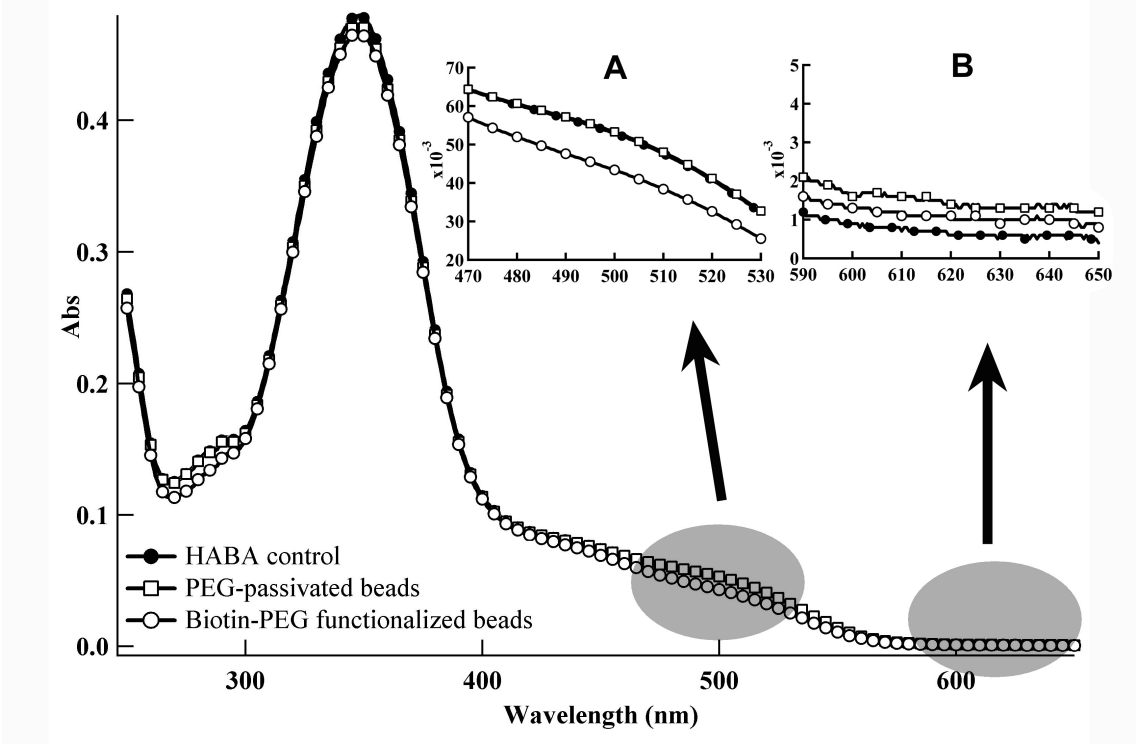

Figure 3.4: UV-Vis absorption curves for HABA-avidin control reagent, $mPEG_{2000}$-passivated beads incubated with HABA-avidin mixture and biotin-PEG_{3400} functionalized beads incubated with HABA-avidin complex. Spectra were collected after beads had been centrifuged out of the reaction mixture. Inset figures show two regions of the spectra, 470 nm–530 nm and 590 nm–650 nm. Inset A shows the reduction of Abs_{500} for the biotin-PEG_{3400} functionalized bead set. Inset B shows that at wavelengths considerably far from 500 nm the absorption spectra for the three sets are close to each other. Notice the change of y-axis scale from inset A to inset B.

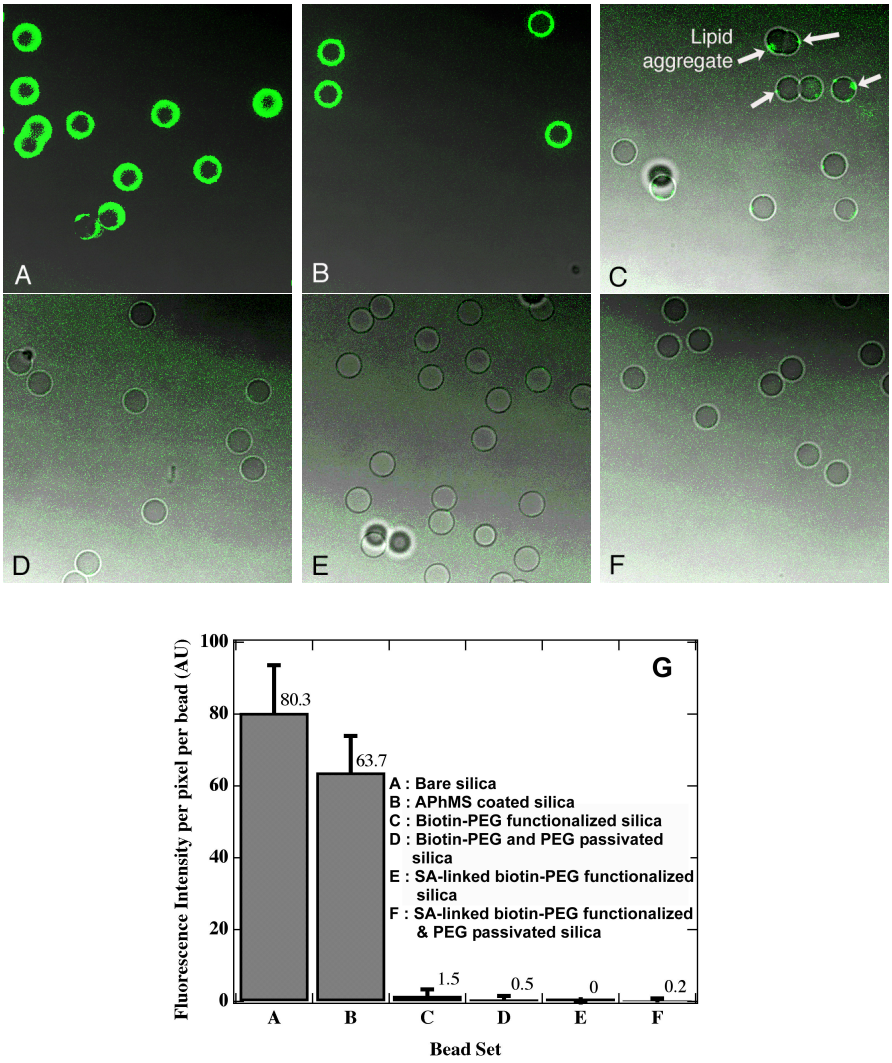

Figure 3.5: Study of non-specific interaction of fluorescent lipid molecules to silica surface at different stages of surface modification. Each image shows an overlay of green channel (excitation 488 nm, detection 502–614 nm, AOTF 24%, Gain 772) with transmission channel for one particular set. A) Bare silica surface, B) APhMS coated silica surface, C) biotin-PEG_{3400} functionalized surface; D) biotin-PEG_{3400} functionalized and $mPEG_{2000}$ passivated surface; E) SA linked surfaces with biotin-PEG_{3400} but no $mPEG_{2000}$; F) SA linked surfaces with biotin-PEG_{3400} and $mPEG_{2000}$ passivating layer. G) Comparison of average fluorescence intensity per pixel on a per bead basis showing minimal signal for the bead sets which have been functionalized with biotin-PEG_{3400}. Images A–F have been enhanced for contrast after acquisition. Arrows in image C point out towards the lipid aggregates identified on the bead surface.

Chapter 4

Fabrication of Solid-Supported Membranes on Silica Beads using Bacteriorhodopsin Conjugates as Integrated Anchors

4.1 Introduction

Supported membranes have gained a lot of importance due to their potential applicability in various areas. These systems serve as a model of biological cell membranes and hence are a very attractive candidate for the design of biomimetic interfaces. The fact that the cellular lipid membranes house a variety of transmembrane proteins makes supported membranes an ideal candidate to be used for ex-vivo reconstitution of these biomolecules upon isolation from native cellular sources. Potential applications for such systems range from understanding the functional role of a membrane protein to building biosensing devices. The fact that the basic building block of a supported membrane is a phospholipid molecule makes these assemblies a natural method for the biofunctionalization of surfaces.

Supported membranes are generally fabricated by unrolling lipid vesicles onto a suitable surface. The Langmuir-Blodgett deposition technique is also used to transfer a monolayer, or a bilayer, on to a suitable substrate. The supporting surface could be modified or unmodified silica, quartz, glass, and it can either be planar or spherical. The characteristics and long-range order of supported membranes are determined by the underlying support. For example, in the case of a planar glass or silica surface, the supported bilayer will be continuous and have long-range order. Whereas, in the case of modified surface — which consists of domains of hydrophilic and hydrophobic regions — there will be domains of lipid monolayer and lipid bilayer respectively.

Fabrication of supported membranes on spherical particles has various advantages compared with flat geometry. These include increases in the surface to volume ratio, and ease of purification and processing, and in general more versatility with regards to applications. Various groups have shown that lipid membranes spontaneously form on spherical silica beads when these are exposed to lipid vesicles.

Thus, unrolling of lipid vesicles onto a hydrophilic glass or silica surface is a standard method to fabricate supported membranes on planar surfaces as well as spherical particles. The Supported membrane is separated from the supporting hydrophilic surface (planar or spherical) by a thin water layer (10–30 Å). Lipid bilayer can be simply adsorbed onto the surface or tethered through intermediate molecules ranging from polymers to peptides.

Here we are reporting on fabrication of supported membranes on silica surface using bacteriorhodopsin (bR) as an anchoring moiety. There are many reasons that make bR as an appropriate anchoring moiety. First, bR is a highly robust membrane protein and has the natural affinity for the lipid membrane. Compared with a relatively widely used tethering molecule, lipid phosphatidylethanolamine (PE), which only spans half of the lipid membrane, bR spans the entire bilayer. Moreover it possesses a much larger surface area of interaction with the lipid bilayer making it a much stronger "molecular rivet" for holding the supported membrane on the supporting structure. Presence of amino acid Lys on the bR backbone provides possibility of fluorescence labeling and/or tagging other molecules of interest on the surface of the molecule external to the lipid bilayer.

To our knowledge, so far, the use of tethers to fabricate supported membranes has been limited to flat geometries. Sodrosky and coworkers [91] reported the only related study where lipid bilayers were fabricated on paramagnetic particles by detergent dialysis of biotin-DOPE doped lipid formulations. In their work, paramagnetic beads were coated with 1D4 monoclonal antibody and streptavidin. Streptavidin allowed for the membrane reconstitution around beads while the 1D4 antibody allowed for the immobilization of CCR5 heptahelical protein (β-chemokine receptor)in the supported membranes. Our work differs from their work in the sense that we have used a totally different surface as the substrate. From our experience with polystyrene and paramagnetic Dynal beads (similar to the ones used in above

study), we have seen that nonspecific adsorption of the lipids to the surface is a very crucial issue and it makes it impossible to confirm the formation of supported membranes around such particles. Silica particles that we used have hydrophilic surface and therefore any non-specific interactions with hydrophobic molecules (lipids, lipid probes) will be at a minimum level. However, it is very well known that silica surface can easily be coated by a lipid bilayer separated from the surface by a few layers of water molecules. We have eliminated this spontaneous formation of bilayers on bare silica surface by completely passivating it with a layer of polyethyleneglycol (PEG) of molecular weight 2000. In order to attach tethering molecules to the silica surface, we have functionalized it with streptavidin. Biotin-PEG_{3400}-bR conjugates were synthesized and employed as the tethering molecules in present study.

This chapter describes the fabrication of new tether-supported lipid bilayer on silica particles of 5 μm diameter. Synthesis of bacteriorhodopsin tethers and functionalization of silica beads with streptavidin has been described earlier in chapters two and three respectively (Also see [65]). We attached bacteriorhodopsin tethers on streptavidin-conjugated beads and subsequently attempted to form fluid lipid-bilayer assemblies on these structures. We explored various approaches and found that detergent-based method results in the desired assemblies. Confocal microscopy was utilized to colocalize Texas Red labeled bacteriorhodopsin and β-Bodipy 500/510 C_{12}-HPC (green) doped lipid probe in the assemblies. Fluidity of the lipids in the tether-supported lipid bilayer assemblies was characterized by using fluorescence recovery after photobleaching (FRAP) measurements.

4.2 Background

4.2.1 Supported lipid membranes on planar surfaces

Researchers have long been interested in studying membrane-membrane interactions for understanding cellular surface processes. A number of studies utilized liposomes

as model for biological cell membranes. About two decades back, researchers started to explore the use of planar supported membranes for such studies. One of the first reasons for utilizing supported membranes was to have a geometrically well-defined planar surface. This was motivated from two underlying issues related to studying cell-cell interactions using lipid vesicles as model for cell membranes. First issue was the effect of finite radius of curvature (focusing effect) of vesicles and second issue was the difficulty in observing membrane-membrane contacts using optical microscopy for both cell-cell interactions and cell-vesicle interactions.

Initial efforts towards the design of planar membranes included the formation of lipid monolayers on hydrophobic alkylated surfaces using a Langmuir-Blodgett transfer mechanism [92]. This system was essentially a monolayer of lipid on alkylated glass, and was not suitable for incorporation of membrane protein due to steric issues and the lack of fluidity of the lipids. The shortcomings of this approach led to the design of supported lipid bilayer membrane system [44]. In this study, the Langmuir-Blodgett deposition technique was utilized to sequentially transfer two monolayers of phospholipids (DPPC, DMPC and DOPC) from the air-water interface to solid substrates viz. glass, quartz and silicon. These constructs not only were useful from the point of view of studying membrane-membrane interactions but also from the standpoint of studying the lateral diffusion of lipids as well as other macromolecules associated with the membranes. This was accomplished using fluorescence recovery after photobleaching (FRAP) and total internal reflection fluorescence microscopy (TIRF-M) to probe lipid dynamics ([41] and references therein).

Supported lipid bilayers have since become increasingly important as a model for cellular membranes. Various other methods have been utilized to construct supported membranes on suitable surfaces. One of the most widely utilized methods involves the fusion of lipid vesicles on a suitable hydrophilic glass or silica surface

to coat it with the lipid bilayer. This method was originally developed [93] to reconstitute membrane proteins into supported lipid bilayers using vesicles containing membrane proteins (proteoliposomes). This method was further modified to spreading the lipid vesicle [41] membrane on a surface already containing one leaflet of lipids deposited by the Langmuir-Blodgett transfer mechanism. The motivation was to minimize unwanted interactions of the membrane protein with supporting surface in the technique involving direct exposure of proteoliposomes to the surface.

Other methods of forming supported lipid bilayers on surfaces essentially modify the underlying surface to get different patterns. These techniques have been discussed in details by Cheng et. al. [35]. These methods include making patterned surfaces using self-assembled monolayers of two different kinds of functionalities. In one such study, a supported membrane was constructed on gold surface micropatterned with micrometer-sized hydroxyl and cholesterol terminated thiol regions (Figure 4.1-D) [94, 95]. Lithographic techniques have also been used to modify the underlying supporting surface. Groves et al. used lithographically patterned grids of photoresist, aluminum oxide, or gold on oxidized silicon substrates to partition supported lipid bilayers into micrometer-scale arrays of isolated fluid membrane corrals [40]. In a similar study, Heyse et al. used selective photo-oxidation (by masking) of thiol derivatized surfaces to create patterned structures of anchoring units on gold surfaces [96]. Supported membranes were formed by the self-assembly of the lipids and rhodopsin from detergent solution onto functionalized gold surfaces.

Although supported membranes are widely used to study various membrane-associated proteins (peripheral and integral), there has been a serious limitation to their applicability. Lipid bilayers fabricated on hydrophilic surfaces are separated from the substrate by an ultra-thin (1–3 nm) layer of water (Figure 4.1-A). This ultra-thin water layer is sufficient to impart the essential fluidity to the lipids in both the leaflets of the bilayer. However, it presents issues when membrane proteins

are incorporated into these structures. Extraneous parts of the membrane proteins can interact with the supporting surface and get immobilized, thus loosing their mobility [97, 98, 99]. Lateral mobility plays an important role in the activity of certain membrane proteins and immobilization of these molecules to the supporting surface is undesirable. There have been several attempts to address this problem with a general approach to separate the bilayer from the supporting surface by a polymer cushion (Figure 4.1-B) [43]. Bilayers formed on such polymer cushions were not very successful as they were patchy and displayed a lot of defects. ([47] and references therein, [100, 101, 102].) This strategy of forming supported membranes was further modified by the use of a tethering molecule at the end of polymer spacer. In this approach, in general, a part of the polymer tether is integrated into the lower leaflet of the supported bilayer and other end is covalently linked to the surface (Figure 4.1-C). So far primarily single lipid [47, 50, 96, 103] or a cholesterol [39, 104, 105] linked to a hydrophilic polymer or a hydrophilic oligomer molecule have been used as the part of the tether that gets integrated into the supported bilayer. Most commonly used polymer spacer is polyethylene glycol (PEG) polymer or oligomer.

4.2.2 Supported lipid membranes on spherical particles

So far tether-supported membranes have only been fabricated on planar surfaces. There are only few examples of supported membranes on other kind of geometry, e.g. spherical beads. The first reported study concerning the formation of bilayers on spherical silica beads was given by Bayerl et. al. [46]. These structures were formed by spreading sonicated liposomes on ultraclean glass beads of 0.5 μm and 1.5 μm diameter and characterized by ^{2}H-NMR. Primary motivation behind the work was to recreate the unilamellar model membrane systems of well-defined shape (preferably spherical in order to understand the role of membrane curvature)

and a size range comparable to that of biological cells. Since then, these systems have become increasingly attractive for experimental studies. Subsequent reports by various researchers described the studies on the effect of curvature on the phase transition behavior of a DSPC/DMPC mixed bilayers on spherical glass beads [106] and comparisons between the physical properties of lipid monolayers and bilayers on spherical surfaces [107]. These systems have since been studied for various bioseparation [108], biosensing [109, 110], high throughput screening [111, 112, 113] and other biotechnological applications [114]. In order to address the issues related to the close proximity of the bilayer to the supporting surface, these structures have been modified with a polymeric cushion, which separates the supported bilayer from the glass surface [115]. This approach is similar to that proposed by Sackmann [43] for planar surfaces.

So far, the use of membrane integrated tethers to fabricate supported bilayers has been limited to flat geometries. Sodrosky and coworkers [91] reported the closest study where lipid bilayer was fabricated on paramagnetic particles by detergent dialysis of biotin-DOPE doped lipid formulations. In their work, paramagnetic beads were coated with 1D4 antibody and streptavidin. Streptavidin allowed for the membrane reconstitution around beads through immobilization of biotin-DOPE while the 1D4 antibody allowed for the immobilization of CCR5 heptahelical protein in supported membranes. Supported membranes were formed using biotin-DOPE and CCR5 heptahelical protein as membrane spanning parts of the tether, but no spacer molecules were utilized to separate the membranes from the bead surface. Moreover no direct evidence was provided to support the fact that membranes were actually spaced apart from the surface instead of directly resting on it. This can be an important issue because in later case the membranes are likely to have significant loss of fluidity, and, due to the lack of separation they will not be ideal for incorporation of any membrane proteins.

4.2.3 Bacteriorhodopsin as a membrane tether

As mentioned earlier, the use of membrane-spanning molecule to tether the bilayers has been limited to a lipid or cholesterol molecule. Our approach is to utilize bacteriorhodopsin, a transmembrane protein, as a tethering molecule. Motivation for our strategy comes from the cytoskeleton structure of the cells, which consists of an array of protein filaments (Actins and Spectrins) forming a polymeric network (Figure 4.2-A). This polymeric network is covalently linked to various membrane proteins, which span the lipid bilayer. Thus, a membrane protein linked cytoskeleton is the key structural feature, which provides the cells with their shape, strength and locomotive abilities. Our strategy is to recreate this membrane protein tethered polymeric network to support the lipid bilayers formed on spherical particles (Figure 4.2-B). We have chosen bacteriorhodopsin as the anchoring protein as it is very well characterized and highly robust membrane protein. Side by side comparison of bacteriorhodopsin with a representative lipid tether shows that it has an order of magnitude higher surface area or interaction with the membrane lipids (Figure 2.1). Hence, it is expected to impart much higher stability to the supported lipid membrane. Furthermore, recent theoretical calculations to predict the insertion energies of different molecules have shown that bR has more than four fold higher membrane insertion energy than that of a typical phospholipid [56].

4.3 Experimental

Abbreviations

bR, Bacteriorhodopsin; PEG, Polyethylene Glycol; TR, Texas Red; POPC, L-α-Phosphatidylcholine; DOPG, 1, 2-Dioleoyl-sn-Glycero-3-[Phospho-rac-(1-glycerol)] (Sodium Salt); DMPC, dimyristoyl-sn-glycero-3-phosphatidylcholine; DPPC, 1,2-Dipalmitoyl-sn-Glycero-3-Phosphatidylcholine; DOPC, 1,2-dioleoyl-sn-glycero-3-ph-

osphatidylcholine; DMPC, 1,2-Dimyristoyl-sn-Glycero-3-Phosphatidylcholine; DSPC, distearoyl-sn-glycero-3-Phosphatidylcholine; biotin-DOPE, 2-dioleyl-sn-glycero- 3-phosphoethanolamine-n-(biotinyl); TRITC-DHPE, N-(6-tetramethylrhodaminethiocarbamoyl)-1,2-dihexadecanoyl- sn-glycero-3-phosphoethanolamine, triethylammonium salt; DSPE-PEG_{2000}-biotin, 1,2-Distearoyl-sn-Glycero- 3-Phosphoethanolamine-N-[Biotinyl(Polyethylene Glycol)2000] (Ammonium Salt); APhMS, p-Aminophenyltrimethoxysilane; SA, Streptavidin. Hepes A buffer, Hepes 20 mM, NaCl 100 mM, EDTA 1 mM, pH 7.5.

Bacteriorhodopsin was obtained as lyophilized powder of Purple Membrane from Munich Innovative Biomaterials (MIB) GmbH, Germany. Cy5 Mono SPA Ester dye was obtained from Amersham Biosciences Inc, Piscataway, NJ. POPC (egg, chicken), DOPG and DSPE-PEG_{2000}-biotin were purchased from Avanti Polar Lipids, Inc. Alabaster, AL. Lipid probes β-BODIPY 500/510 C_{12}-HPC and TRITC-DHPE were purchased from Molecular Probes, Eugene, OR. Bio-Beads SM-2 adsorbents were obtained from Bio-Rad Laboratories, Hercules, CA. Detergent OG and Slide-A-Lyzer Dialysis Cassettes, 10 kDa MWCO membranes, 0.5–3 ml capacity were purchased from Pierce Biotechnology, Inc. Rockford, IL.

Attaching bR-PEG_{3400} tethers to SA functionalized Silica Surface

Synthesis of bR-PEG_{3400}-biotin tethers has been described in details in chapter three. For long-term storage, bR tether stock (50 μM, Hepes A, OG 100 mM) was stored in 200 μl aliquots at –20°C. Functionalization of silica beads with SA has been described in chapter four in details. Prior to bR tether addition, SA coated beads were exchanged from Phosphate pH 9.0 buffer to Hepes A buffer by four spin-rinse cycles. In a typical tethering run 20 μl of tether stock was diluted to 500 μl using Hepes Buffer A (containing 100 mM OG). Diluted tether stock was then

used to re-suspend 1 mg SA coated beads. Reaction mixture was incubated at room temperature for 2–3 hours with gentle mixing to re-disperse the beads settled due to gravity. Excess unbound tethering molecules were separated by multiple washing with Hepes A containing OG. Surface density of bacteriorhodopsin was estimated by analyzing the absorption spectrum (Abs_{594} from Texas Red) of bR-tether displaying beads. Prior to the analysis, the absorption data was corrected for the scattering signal due to silica beads.

Formation of lipid vesicles

Lipid constituents (Figure 4.3) were first dissolved in chloroform at 10 mg/ml total lipid concentration. POPC was the main constituent and was present in all the lipid formulations used. In some cases DOPG (negative head group) was present in a molar ratio of 9:1 (POPC:DOPG). Fluorescent lipid β-BODIPY 500/510 C_{12}-HPC was also added to the chloroform solution at a ratio of 1:100 (probe:lipid). The lipid solution was then subdivided into parts containing 2 mg of total lipid stock and transferred into 4 ml glass vials. Chloroform solvent was evaporated using vacuum overnight or by a stream of N_2. Vials containing lipid films were stored under argon at $-20°C$ until required. To form multilamellar vesicles (MLVs), 2 mg lipid formulation was hydrated using Hepes buffer A at 2 mg/ml and the suspension was subjected to 5 freeze-thaw cycles with vortexing in between cycles. Small unilamellar vesicles (SUVs) were formed by extruding MLVs through polycarbonate membranes (Avanti Mini-Extruder) or by sonicating the MLV suspension to optical clarity using tip sonicator (Biologics Inc. Ultrasonic Homogenizer, 150 W model, microtip, 40% Power, 15 min). Size of the vesicles was verified using Malvern Zetasizer Nano ZS.

Fusion studies on lipid vesicles

In order to study the fusion of vesicles at room temperature samples were incubated at room temperature for 24 hours and particle size was measured before and

after incubation. Later this solution was incubated in 750 mM sucrose to monitor the effect of sucrose on vesicle fusion. Effect of PEG on vesicle fusion was studied on a microscope slide by adding a drop of 60% PEG to vesicles sample.

Formation of non-tethered lipid bilayer on silica beads

As a reference set, supported bilayer was formed on silica particles without any tethering molecules. This was achieved by incubating silica microspheres (1 mg beads) with 100 μl of sonicated liposomes solution (2 mg/ml lipid). Liposomes spontaneously coated the clean silica surface with a lipid bilayer. Excess liposomes were separated by centrifugation and successive washing with fresh Hepes A buffer. These samples were stored at 5°C until required.

Formation of supported membrane using bR-PEG$_{3400}$-biotin tethers

As mentioned above, lipid bilayer around silica particles were formed by fusion of intact lipid vesicles which coat silica surface with lipid bilayer separated by a thin water layer. In the first pass we tried to fabricate lipid bilayers around bR-PEG$_{3400}$-biotin tethered beads using similar approach. Lipid vesicles of the desired size were obtained by either sonication or extrusion through polycarbonate membranes as explained above. 100 μl vesicle solution (2 mg/ml total lipid) was used to resuspend a 1 mg pellet of bR-tethered beads. Mixture was incubated at room temperature for 1–2 hours with gentle mixing in between to ensure proper dispersion of the beads. Excess liposomes were separated by centrifugation (1000 X g; 1 min) and beads were washed with fresh Hepes A buffer in 4–5 spin-rinse cycles.

Fusogenic PEG treatment was performed on the beads as follows: A small quantity of beads (0.5 mg, $\approx$ 50 μl suspension) was made up in fusogenic PEG solution at 20% (w/v) concentration in the presence of excess sonicated liposomes (50 μl, 1 mg/ml lipid). Beads were recovered by centrifugation and successive rinsing with Hepes A buffer. Sucrose (750 mM) was also used as a fusogenic agent using the

protocol similar to the one described for fusogenic PEG

In order to test if the liposomes were immobilized to the beads in intact manner we encapsulated Cy5 dye in the liposomes by incorporating it in the hydration buffer (10 μM). Liposomes loaded with Cy5 were used for incubation with bR tethered beads or plain silica beads using the protocol mentioned above.

In the detergent method lipid formulation was solubilized in 1.6% (w/v) Octyl-Glucoside (OG). 1 mg bR tethered beads were incubated with 300 μl of solubilized lipids (1 mg/ml total lipid) and the detergent was dialyzed using Pierce Slide-A-Lyzer Dialysis Cassettes (10 kDa MWCO) in a 4 liter buffer container. Cassettes were gently shaken every 30 min to redisperse the settled silica beads. Total incubation time was 24 hours. Samples were subsequently washed with fresh Hepes A buffer three times before any further analysis.

If desired, the samples were subjected to heat treatment for short period of time. This was done by suspending a small amount of bead sample (5–10 μl) in 500 μl vial containing Hepes A which was already equilibrated at 50°C. Beads were allowed to remain at 50°C for a period of 10 min after which the samples were allowed to cool down to room temperature. Heat-treated beads were recovered by centrifugation.

Confocal microscopy

Confocal microscopy was used to image the formation of fluorescently-tagged supramolecular structures on the bead surface. Samples were imaged using Leica TCS SP2 Confocal Microscope System equipped with argon ion and HeNe lasers. Bodipy lipid was excited using 494 nm line of argon laser and images were taken with a 63X oil immersion objective with the detection window set between 500–580 nm. Texas Red was excited using 594 nm line of HeNe laser and images were acquired using a detection window of 610–700 nm. Pinhole aperture was set at Airy value of 1.0, which was equivalent to $\approx$ 500 nm vertical slice of the bead.

Photobleaching studies were done using built-in protocol of Leica SP2 system. Image plane was set at the equator of the bead and a 512 X 32 pixel format was used (zoom value 16; scan speed 400 Hz, 488 nm AOTF 2%). This enabled the fast imaging (0.4 sec/scan) of two equatorially opposite ends of the bead. After 10 pre-scans a region of 1μm X 1μm on the bead was subjected to 25X laser intensity (AOTF 50%) for the duration of one scan. This resulted in bleaching of the selected region on the sample. Recovery of fluorescence was monitored for 12 sec at normal laser intensity (AOTF 2%). Data was collected for the normalized fluorescence intensity of the bleached region throughout and analyzed using *Mathematica* to estimate the value of time constant τ_D.

4.4 Discussion

4.4.1 Particle size analysis of liposomes

Liposome size distributions were analyzed using Malvern Zetasizer Nano ZS. Sonicated vesicles were found to have narrow size distribution around 50 nm (Figure 4.4-A). On the contrary, extruded liposomes had a broad size distribution (Figure 4.4-A, 4-B). In this case the results were interesting as only 200 nm-extruded vesicles showed the size distribution centered on 200 nm. Vesicles formed through 50 nm and 100 nm filters showed the peak at a value larger than the respective pore size (125 nm and 150 nm respectively). This presents an interesting issue to the applicability of extrusion technique to form vesicles smaller than 100 nm as we have repeatedly observed this phenomenon. We believe that formation of ultra-small liposomes (<100 nm) requires much higher energy input and is therefore achievable only by using a tip type sonicator. Vesicles formed by extrusion through 1000 nm pores were centered on 800 nm.

The vesicle fusion (POPC/bodipy) was monitored for a period of 24 hrs by recording the vesicle sizes. Figure 4.4-C shows the size distribution at two time

steps indicating no significant difference. This indicates that sonicated POPC/β-Bodipy liposomes do not fuse together in the time frame that we are interested in studying them and hence we need to use fusogenic reagents to drive vesicle fusion on the bead surface. Addition of sucrose to the above samples led to the shift of the average size distribution from 50 nm to around 100 nm. Although this result seems promising, addition of sucrose when the vesicles are immobilized on a surface may not be able to yield such results due to the limited mobility or other effects.

4.4.2 Estimation of surface density of bR tethers

Absorption spectrum of the beads displaying bR-tethers on the surface was analyzed for 594 nm absorption peak to get an estimate of the tether density. This analysis was made complicated by two limitations – presence of scattering due to the silica beads, and sparse coverage of the beads leading to minimal signal. The later issue required us to use concentrated suspension, but this led to higher scattering signals from the silica beads. The surface density of bR was found to be approximately 4 x 10^{-3} molecules/nm^2, which corresponds to 1 bR molecule per 250 nm^2 area. This translates into a surface coverage of $\approx 2\%$. (Cross sectional area of one bR molecule assuming it has an elliptical cross section as shown in Figure 2.1 = $\frac{\pi.a.b}{4}$ = 3.14 x 2 x 3 / 4 = 4.7 nm^2)

4.4.3 Fabrication of bR-tether supported membranes on SA modified silica beads

Bacteriorhodopsin tether synthesis and functionalization of silica bead surface with streptavidin has been described in earlier chapters. The focus of this chapter is to describe the reconstitution of lipid membranes around functionalized silica surface by using bacteriorhodopsin tethering. There were two possible strategies to achieve this goal. First strategy was to incubate bacteriorhodopsin tethered silica beads with intact liposomes. Bacteriorhodopsin due to its inherent hydrophobic

nature is expected to insert into the lipid bilayer of the vesicle. This would lead to a distribution of surface immobilized liposomes on the bR-tethered beads. Surface immobilized liposomes, upon subsequent fusion would lead to the formation of supported bilayer on the modified silica surface. A number of variables are involved in this problem (viz. lipid composition, vesicle size, temperature, tether density etc.) which make the study highly complex in nature.

Second strategy to form supported membranes would be to introduce the lipids in the system of bR-tethered beads in detergent solubilized form. Removal of the detergent from the system will drive the lipids to self-assemble, and a fraction of the lipids will assemble around hydrophobic surface of bacteriorhodopsin as well. This, under the right set of conditions can lead to formation of a continuous supported bilayer around the silica beads; tethered to the surface through the bacteriorhodopsin tethers. Variables that are involved in the detergent approach, apart from the above-mentioned variables, are detergent type, method of detergent removal, etc.

4.4.4 Intact liposomes based approach

First pass at making supported membranes was to mix bR-tethered beads with liposomes obtained by simple vortexing of hydrated lipid formulation (POPC/β-Bodipy). Confocal analysis of this set suggested the presence of individual liposomes immobilized on the bead surface instead of a supported membrane (Figure 4.5). In the next iteration, vesicles formed by sonication were utilized. The rationale was that sonicated vesicles of ultrasmall size have high surface curvature and would conceivably be more prone to fusion compared to large vesicles obtained by simple vortexing. This gave a considerable improvement of homogeneity of green probe on the bead surface as shown in Figure 4.6. Unfortunately these beads exhibited minimal signs of fluidity of lipids on the surface of the beads (Figure 4.6-C), indicating the lack of continuity of supported membranes. Fluorescence recovery

behavior of 24 beads was documented and was found to be qualitatively similar to the one shown in Figure 4.6-C. Since the distribution of lipid probe as seen in confocal images (Figure 4.6-A) was fairly homogeneous, this led us to consider the scenario that bead surface had small fragments of lipid bilayers not interconnected to form continuous bilayer. In order to verify this, we used two different populations of lipid vesicles (β-Bodipy doped and TRITC-DHPE doped). This set showed perfect co-localization of two probes on the bead surface instead of patches of green and red. However, no fluidity was observed for either one of the lipid probe. This could be an indication that the surface immobilized vesicles are not fusing together and remain in intact form. This cannot be directly observed by confocal microscopy, as the vesicle size ($\approx$ 50 nm) is below the resolution limit of a confocal laser scanning microscope. This basically means that a single layer of intact liposomes on the bead surface can show a distribution of green probe around the bead as shown in Figure 4.7. Particle size analysis performed on the sonicated vesicles had also suggested that these are not prone to fusion (Figure. 4.4–C)

In order to test the presence of intact, non-fusing liposomes on the bead surface, they were loaded with Cy5 dye. Analysis of the complexes indicated the presence of Cy5 containing liposomes immobilized on the beads (Figure 4.8) but the data was not very convincing, as the signal detected in the Cy5 window could just be a bleed through from Texas Red channel. Spectral dye separation analysis indicated the presence of Cy5 to some degree (Figure 4.8-E). Fluidity analysis on these membranes also gave negative results (Data not shown). Even though detection of Cy5 is not absolutely reliable, but there are only few ways to explain the non-fluidity of supported membranes — first, these indeed are non-fusing vesicles on the surface, and second, these are patches of lipid membranes not interconnected together to give continuous structure. It has been shown earlier on planar supports that fusogenic PEG can promote the fusion of surface immobilized vesicles and lead to formation

of continuous bilayer [116, 117]. Sucrose can also be used as an agent that promotes vesicle fusion. Unfortunately, use of both the fusogens on current samples in the presence of excess vesicles did not show any apparent improvement in the fluidity. Use of fusogenic PEG lead to immobilization of much larger liposomes on the bead surface which could be identified with confocal imaging. (Figure 4.9)

So far the use of vesicles of large size (obtained by vortexing, size $\geq$ few microns) and ultra-small size (obtained by sonication, size $\approx$ 50 nm) led to non-fluidic membrane on bead surface. Use of vesicles of intermediate size (200 nm and 1000 nm, made by extrusion) also gave negative results. Instead of using a fusogenic agent, these sets were subjected to heat treatment in the presence of excess vesicles of respective size (200 nm or 1000 nm). Sample corresponding to 200 nm vesicles showed significant improvement in the lipid fluorescence signal upon heat treatment, but did not show any fluidity. Beads incubated with 1000 nm showed no improvement upon heat treatment indicating that larger liposomes are less prone to fusion upon heating compared to their smaller counterparts. (Data not shown)

Repeated failure in getting fluidic membranes using intact liposome approach motivated us to use additional factors, which might aid in the interaction of liposomes with the bR-tethered bead surface. In order to achieve this, commercially available DSPE-PEG_{2000}-biotin tether was used in addition to bR-PEG_{3400}-biotin tethers. Lipid formulations were doped with DSPE-PEG_{2000}-biotin molecules (2.8 mole %) and sonicated vesicles were added to bR-tethered beads. Motivation behind this approach was to utilize any unoccupied streptavidin sites left on the bead surface — after bR-PEG_{3400}-biotin addition — to drive DSPE-PEG_{2000}-biotin doped (2.8 mole %) liposomes to bind more tightly with the bead surface. Unfortunately, this turned out to be very high doping level of DSPE-PEG_{2000}-biotin as the liposomes showed much lower affinity for the bR tethered beads as compared with the set which had liposomes containing no DSPE-PEG_{2000}-biotin molecules added to the

beads. In another run DSPE-PEG_{2000}-biotin was used instead of bR-PEG_{3400}-biotin tethers to streptavidin-coated beads prior to the liposome addition. These beads were then incubated with sonicated liposomes (without any DSPE-PEG_{2000}-biotin) to immobilize them on the bead surface, driven by the expected tendency of lipid DSPE to insert into the bilayer of the liposomes. This set also showed much lower signal for lipid fluorescence on the bead surface, indicating that lipid based tethers were not able to provide sufficient driving force for the immobilization of the liposomes on the bead surface under these conditions. (Data not shown; low levels of fluorescence)

Further experiments utilized the negatively charged (POPC/DOPG/β-Bodipy, molar ratio 9:1:0.01) and DSPE-PEG_{2000}-biotin doped liposomes (0.1% by moles). Addition of this set of liposomes to streptavidin-functionalized beads also led to immobilization of intact liposomes on the bead surface, as there was no fluidity in these structures. Positively charged liposomes (POPC/Sterylamine/TRITC-DHPE, 9:1:0.01) were added to this system in order to promote vesicle fusion on the bead surface. Unfortunately, this led to the formation of aggregates on the surface, which could be identified even by epi-fluorescence microscopy. In another trial we added streptavidin coated beads in the buffer and used it to hydrate DSPE-PEG_{2000}-biotin doped lipid formulations. We hoped to get formation of supported lipid bilayers through anchoring of biotin present in the lipid films to streptavidin molecules on the bead surface during the process of lipid hydration. Unfortunately, these samples showed patches of lipid aggregates as well as intact liposomes immobilized on the bead surface instead of a continuous distribution. (Data not shown)

4.4.5 Detergent based method

Use of intact liposomes based approach repeatedly failed to yield continuous membrane on the bead surface. This led us to explore the detergent approach to assemble

lipid bilayer around bR tethers on silica surface. In the first pass we used bio-beads adsorbents to remove detergent from the system. This led to a homogenous, but non-fluidic lipid probe distribution on the bead surface (data not shown). One of the potential issues with bio-beads is that the use of stoichiometrically required amount of these to remove the detergent can lead to significant amount of lipid losses. This led us to use detergent dialysis approach to remove detergent from the system. In the first trial, detergent was dialyzed against plain deionized water. This again led to formation of homogenous but non-fluidic membranes. In the next pass we dialyzed the detergent against Hepes A buffer. Supported membranes obtained in this set were not perfectly homogenous but they displayed fluidity. A moderate heat treatment (50°C for 10 min) of these samples improved the homogeneity of lipid distribution as well as the fluidity of the membrane. Figure 4.11 shows the distribution of green lipid probe and Texas Red probe along horizontal sections of a representative bead fabricated with bR-tethered membrane. A preliminary analysis was done to get quantitative results for colocalization of the green lipid probe with Texas Red dye. Colocalization indices of 0.30 and 0.23 were found for green and red channel respectively. Figure 4.12 shows qualitative results of this analysis. A detailed analysis (described below) was performed to estimate the diffusion coefficient of these membranes and to compare it with the membranes formed on plain silica particles. In order to test the reproducibility of this approach we repeated the entire procedure with a new batch of streptavidin-coated beads. This batch was also found to have the essential fluidity in the membranes assembled on the surface.

4.4.6 Analysis of membrane fluidity using FRAP

Fluidity of the supported membranes was studied by performing fluorescence recovery after photobleaching (FRAP) measurements. This was accomplished by bleaching a small region on one side of the bead (See Figure 4.13) and monitor-

ing the recovery thereafter. A typical recovery curve for the bleached region has been shown in Figure 4.14. In order to estimate the diffusion coefficient of the fluorescent lipid (Bodipy) a simple formulation proposed by Axelrod et. al. [32] was used. Klonis et al. [37] have reported this in a simple mathematical formulation for fluorescence recovery with time as:

$$F(t) = \alpha F_p \sum_{n=0}^{\infty} [(\frac{(-K)^n}{n!}) \frac{1}{(1 + n(1 + \frac{2t}{\tau_D}))}] + (1 - \alpha) F_o \tag{4.1}$$

Where

$F(t)$ = Fluorescence intensity of the bleached spot at time t after bleaching

F_p = Prebleach intensity

F_o = Intensity immediately after bleaching

$$\alpha = \frac{F_\infty - F_o}{F_p - F_o} \tag{4.2}$$

K = Parameter related to the degree of bleaching

$$\frac{F_o}{F_p} = \frac{(1 - e^{-K})}{K} \tag{4.3}$$

The τ_D parameter is related to the diffusion coefficient as:

$$D = \frac{\omega^2}{4\tau_D} \tag{4.4}$$

Where ω is $\frac{1}{e^2}$ of the Gaussian radius of the bleached spot

As $F(t)$, F_o, F_p and F_∞ were known from the raw data (Figure 4.14, compare with Figure 1.8), parameters K and α could be calculated from the above relationships (Equations 4.2 and 4.3). These values were used in the above formulation (Equation 4.1) to get a best fit for the experimental data (Figure 4.14) by using different values of τ_D by a trial-and-error method. The best-fit value of τ_D was then used to estimate

D as represented above. As our bleached spot was 1 μm X 1 μm, we used a value of 1 μm as an approximation of ω.

Results for the calculations of fluidity measurements have been tabulated for bR-tethered bilayer (Table 4.1). Results for silica-supported membranes have also been tabulated as a reference. We can see that the diffusion coefficient for bR-tether supported membrane is comparable to the value obtained for silica-supported membrane within the standard deviation limits. This indicates that the differences in the lateral fluidity of the two systems are not statistically significant in our analysis. Estimates of the mobile fractions for the two cases are also comparable to each other within the standard deviation limits. Also, the fraction of the beads showing successful FRAP was found to be 0.45 based on a total of approximately 100 beads that were analyzed. A small percentage of beads (approximately 2%) exhibited the desired fluidity on one location and no or minimal fluidity on another location. This indicated that there could be local regions of fluidic membrane coexisting with other lipid aggregate structures on the surface of a single bead.

4.5 Conclusions

We have demonstrated here the fabrication of new tether-supported lipid bilayer on silica particles of 5 μm diameter. To the best of our knowledge, this is the first study on the use of PEG tethered bilayer on spherical particles. Earlier studies on spherical particles have reported on the use of PEG only as a cushion separating the supported bilayer from the particle surface [115]. In another study, tethered bilayer was fabricated on streptavidin and CCR5 coated paramagnetic particles using self-assembly of biotin-DOPE doped lipid formulations [91]. However, no spacer molecule was used to separate the bilayer from the supporting surface. Also, the lateral fluidity of the supported membranes was not characterized. We have demonstrated in the present study that it is imperative to characterize the lateral

fluidity in order to establish the formation of a true lipid bilayer.

Our study is the first report on the use of membrane protein based anchors to tether the lipid bilayer to spherical particles. We have successfully used biotin-PEG_{3400}-bR molecules as tethering agents, where biotin end was attached to streptavidin functionalized silica beads and bacteriorhodopsin was incorporated in the tether supported lipid bilayer separated from the surface by PEG spacer.

We have observed that the approach that is generally taken to form supported bilayer on flat surfaces — exposure of the hydrophilic surface to a solution of lipid vesicles — does not work in the present case. We used lipid vesicles of various sizes (50 nm to 1000 nm) on beads displaying bR-PEG_{3400}-biotin on their surface. Confocal microscopy analysis of the complexes showed homogenous distribution of the lipid probe in the case of sonicated vesicles (Figure 4.6) and not so homogeneous distribution in the case of 200 nm (Figure 4.10). Use of larger liposomes (e.g. vortexed liposomes, Figure 4.5-A) indicated the presence of surface immobilized liposomes. We believe that even in the case of sonicated vesicles, where the lipid distribution appears to be homogenous (Figure 4.6), we have surface immobilized liposomes. This was indicated by apparent zero lateral fluidity of the lipids. In previous studies involving PEG-lipid tethered bilayer formation on flat surfaces, fusogenic PEG has been shown to promote the fusion of surface immobilize vesicles [116, 117]. Unfortunately, this approach did not lead to formation of continuous bilayer around spherical particles of the present case. Instead we observed the immobilization of large clumps on the bead surface, which could possibly be individual lipid vesicles ($\approx 1\ \mu$m, see Figure 4.9). Even these assemblies did not show any signs of lateral fluidity of lipids. Use of fusogenic sucrose was unsuccessful as well. In a parallel study, the use of lipid-based tether (DSPE-PEG_{2000}-biotin) instead of bR-PEG_{3400}-biotin tether on the surface of the streptavidin coated beads did not even lead to sufficient immobilization of vesicles on the surface (data not shown).

We succeeded in fabricating the tethered membrane with essential fluidity using the detergent based approach. Silica beads displaying bR on the surface were mixed with detergent solubilized lipids and the removal of the detergent using dialysis technique resulted in self-assembly of the lipid bilayer around the bR tethered beads. A moderate heat treatment of these samples resulted in improved fluidity of the membranes. Diffusion coefficient and mobile fraction of the fluorescent lipid were estimated using FRAP analysis and were comparable to the reference case of lipid bilayer (non-tethered) supported on silica beads. We believe that the bR-PEG tether-supported membranes will be more stable compared to the non-tethered membranes on silica. More work needs to be done in order to establish optimal conditions for the formation of these structures, and also for the stability comparison with conventional case of non-tethered membrane. These constructs can then be used to reconstitute various membrane proteins in the tether-supported lipid bilayer for enhanced stability and functionality under a wider range of processing conditions required for applications of interest.

Table 4.1: Lateral mobility of lipid (β-BODIPY 500/510 C_{12}-HPC) in silica-supported membranes and bR-PEG_{3400}-biotin tethered solid supported membranes.

Type of support	Number of data sets	Diffusion coefficient ($\mu m^2/sec$)	Mobile fraction (%)
Silica-supported	20	0.264 ± 0.039	63.9 ± 6.2
bR-tethered	14	0.330 ± 0.095	50.2 ± 10.4

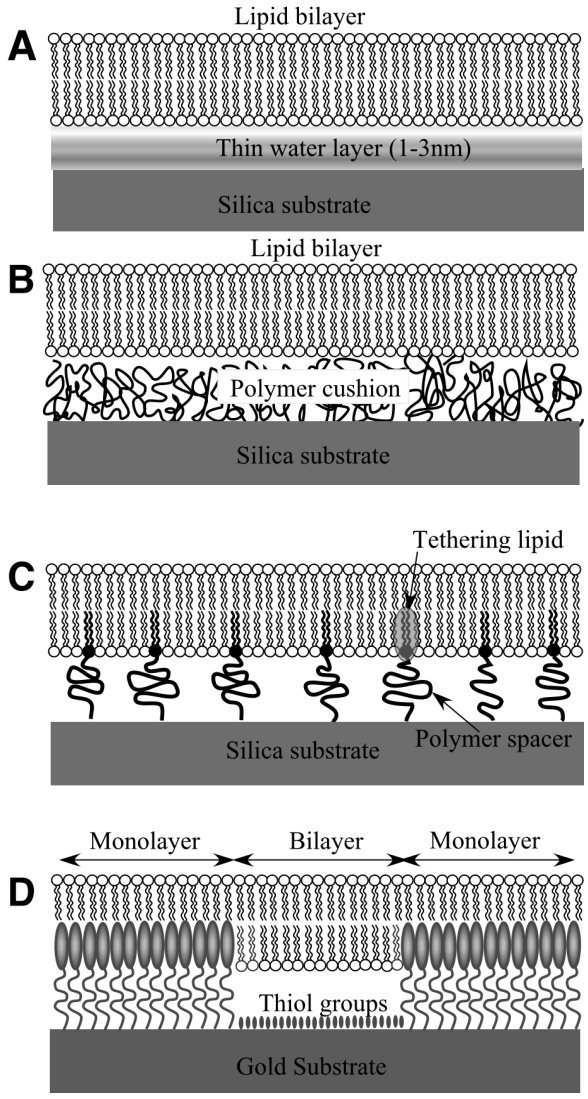

Figure 4.1: Various examples of supported lipid bilayers, A) freely floating on a support, B) cushioned by a polymer, C) tethered to the support through a polymer, D) patterned bilayers.

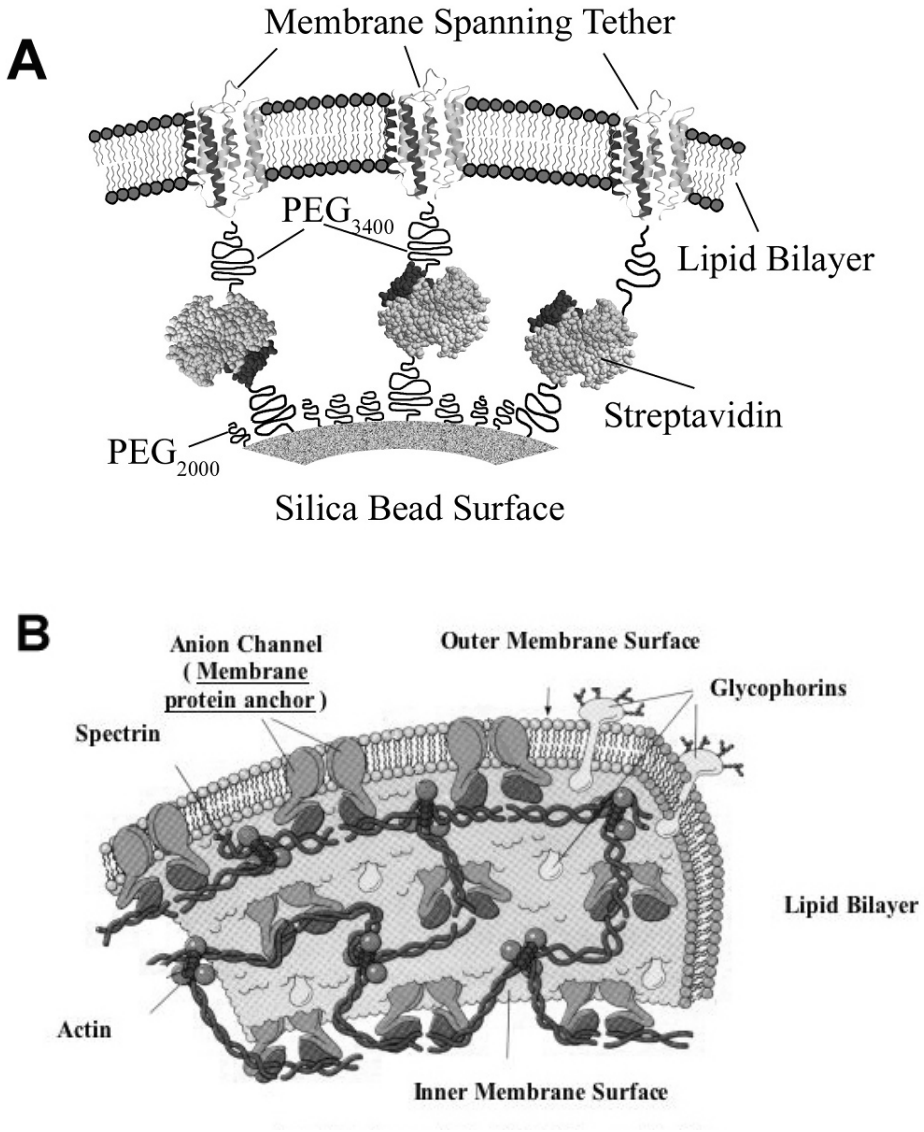

Figure 4.2: Proposed methodology to stabilize lipid-bilayer membrane and comparison with the cytoskeleton structure of the cell. A) Schematic representation of the bR-tethered supported lipid membrane. B) Cytoskeleton structure of the cell showing the cytoskeleton network integrated into the bilayer through linkages with integral membrane proteins (Anion channels).

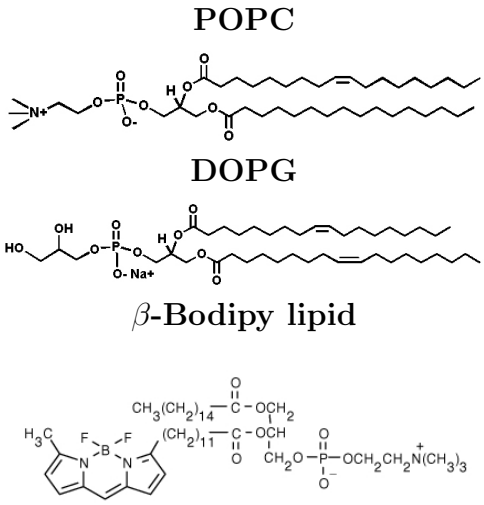

Figure 4.3: Structures of the lipid components used to make liposome formulations.

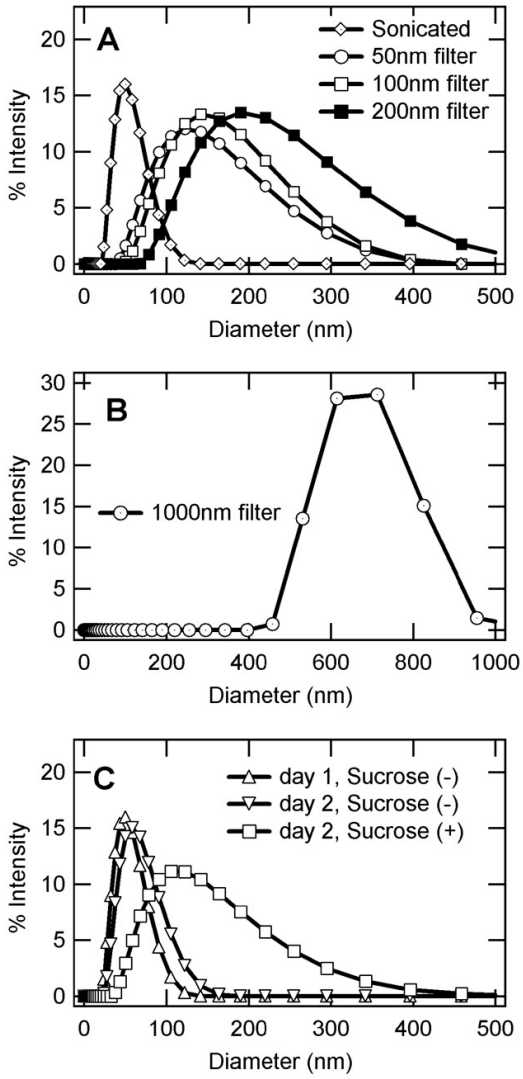

Figure 4.4: Particle size characterization of lipid vesicles. A, B) Liposomes (POPC/β-Bodipy 1%) formed by sonication or extrusion through polycarbonate filters of different pore sizes. C) Fusion assay of sonicated liposomes. There was no significant change in the size distribution upon incubation at room temperature for 24 hours. Sucrose addition (750 mM) shifted the vesicle size distribution and made it broader.

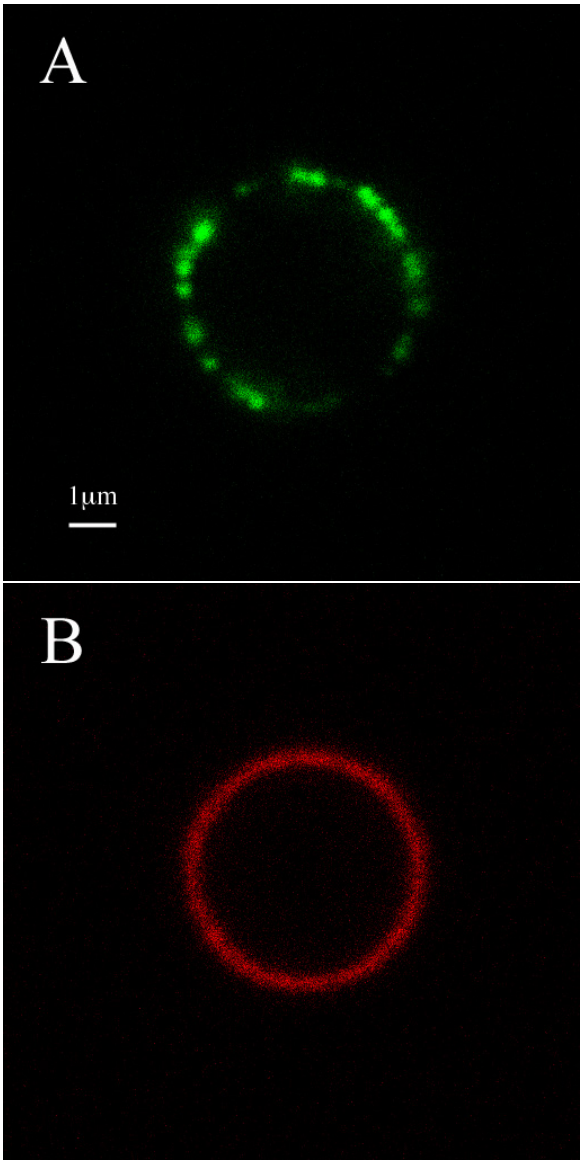

Figure 4.5: Confocal images of a bR tethered bead incubated with vortexed liposomes. A) Green channel (excitation 488 nm, detection 500–583 nm, AOTF 5%, Gain 650) showing immobilized liposomes on the bead surface. B) Red channel (excitation 594 nm, detection 610–706 nm, AOTF 10%, Gain 737) showing the distribution of Texas Red labeled bR tethers.

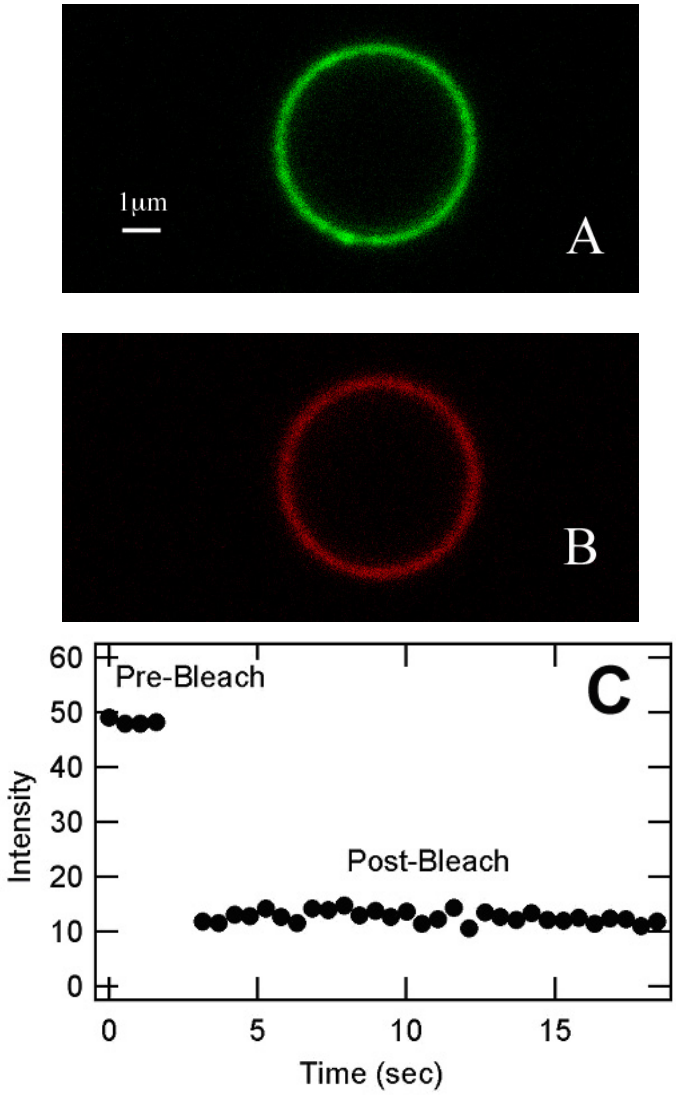

Figure 4.6: Confocal images of a bR tethered bead incubated with sonicated liposomes. A) Green channel (excitation 488 nm, detection 500–583 nm, AOTF 3%, Gain 820) showing the distribution of green lipid probe (β-Bodipy) on the bead surface. B) Red channel (excitation 594 nm, detection 610–706 nm, AOTF 5%, Gain 900) showing the distribution of Texas Red labeled bR tethers. C) FRAP data on green lipid probe for this bead showing no recovery in fluorescence. This clearly indicates that there was no fluidity in the supported lipid assemblies on the bead surface.

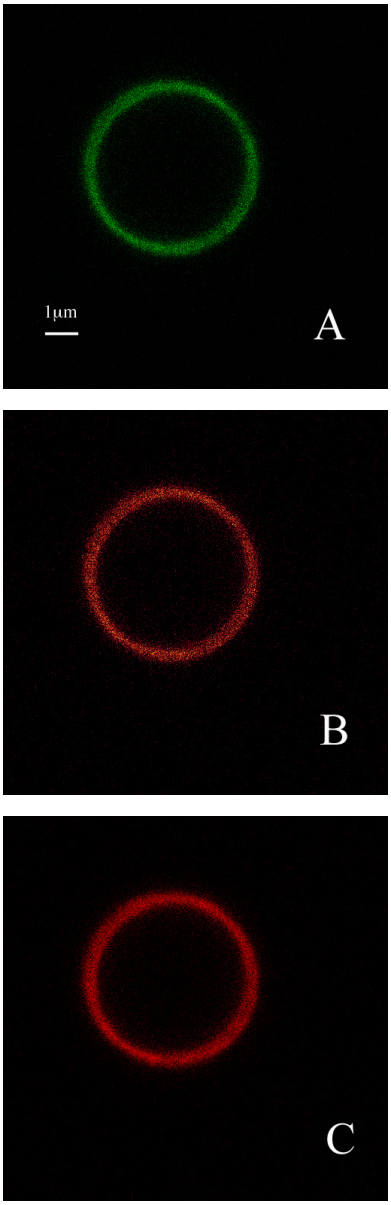

Figure 4.7: Confocal images of a bR tethered bead incubated with two different populations of fluorescently doped vesicles. A) Green channel (excitation 488 nm, detection 500–535 nm, AOTF 5%, Gain 853) showing the distribution of green lipid probe (β-Bodipy) on the bead surface. B) TRITC channel (excitation 543 nm, detection 550–590 nm, AOTF 7%, Gain 868) showing the distribution of TRITC-DHPE lipid probe. C) Red channel (excitation 594 nm, detection 618–713 nm, AOTF 10%, Gain 922) showing the distribution of Texas Red labled bR tethers on the bead surface. This set of beads also did not show any signs of fluidity (Data not shown).

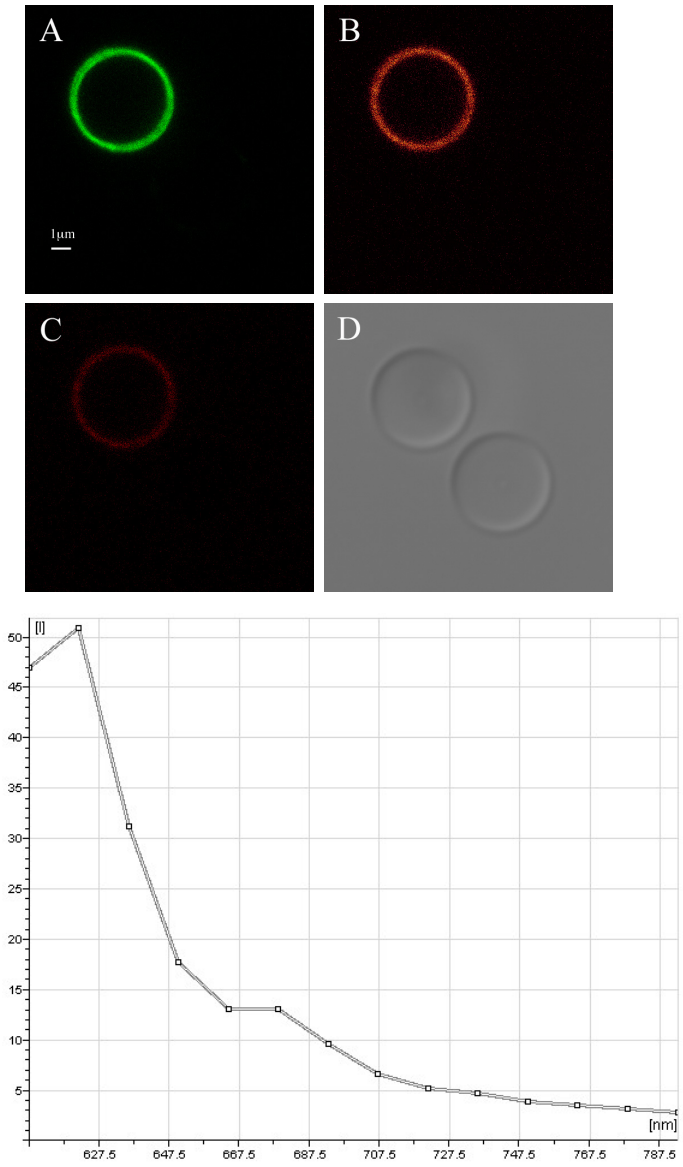

Figure 4.8: Confocal images of a bR tethered bead incubated with Cy5 loaded liposomes. A) Green channel (excitation 488 nm, detection 500–570 nm, AOTF 5%, Gain 678) showing the immobilized liposomes on the bead surface. B) Red channel (excitation 594 nm, detection 602–630 nm, AOTF 5%, Gain 809) showing the distribution of Texas Red labeled bR tethers. C) Cy5 channel (excitation 633 nm, detection 658–734 nm, AOTF 5%, Gain 963) indicating the presence of Cy5. D) Transmission image showing the bR tethered bead (top, left) and a control bead (bottom, right) without any bR tethers. E) Spectral analysis of the fluorescent bead showing a small shoulder peak near 670 nm. This indicates the presence of Cy5.

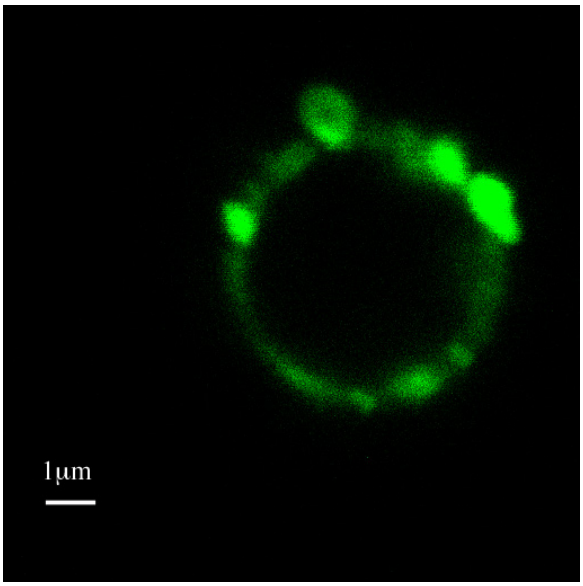

Figure 4.9: Distribution of lipids on a bead after treatment with fusogenic PEG (M_r 8000, 15%), in the presence of excess sonicated liposomes. Individual clumps on the bead indicate immobilized liposomes

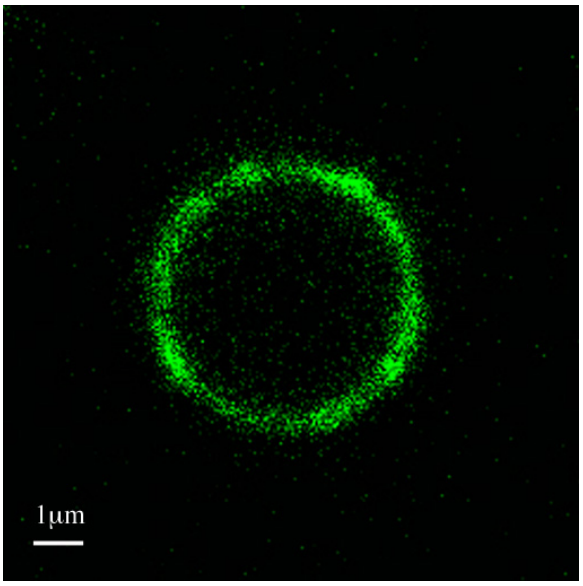

Figure 4.10: Lipid distribution on bead surface after heat treatment of the beads in the presence of 200 nm extruded liposome.

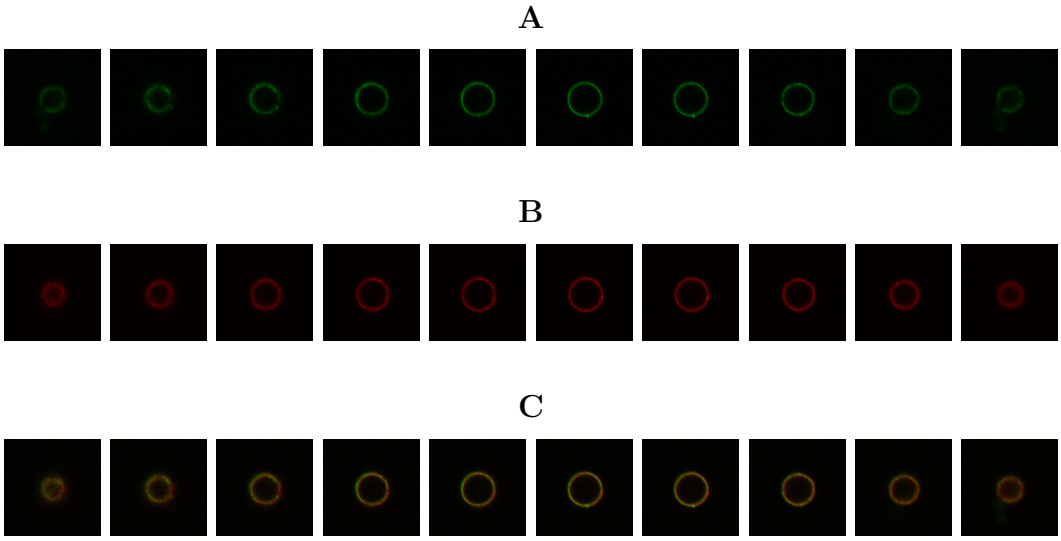

Figure 4.11: Optical sections of a bead containing bR tether supported membrane. A) Green channel (excitaion 488 nm, detection 500–576 nm, AOTF 3%, Gain 750) showing the lipid distribution on the bead surface. B) Red channel (excitation 594 nm, detection 610–712 nm, AOTF 20%, Gain 710) showing the distribution of Texas Red labeled bR tethers. C) Overlay of green and red shows colocalization of two probes on the bead surface.

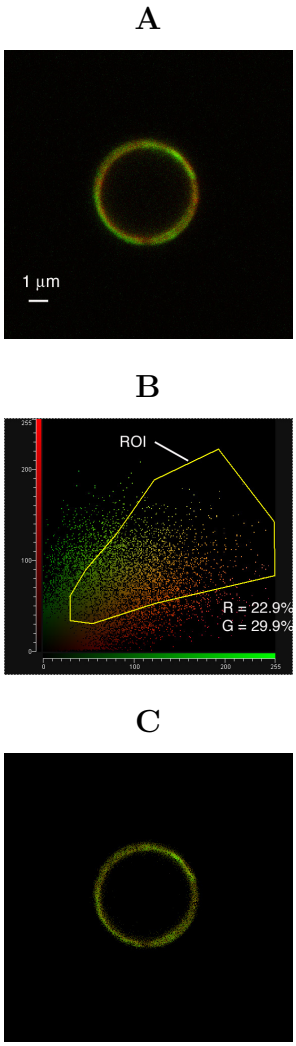

Figure 4.12: Colocalization analysis for β-Bodipy lipid and Texas Red in tether supported lipid bilayer assemblies on silica bead surface. A) Original overlay image of green and red channel. B) Intensity scatterplot showing the intensity of red channel (y-axis) versus green channel (x-axis). Each pixel in image A is characterized by a pair of intensity values for the two channels, which are plotted along the two axes in the scatterplot. Points close to the abscissa are shown in red. These represent the pixels lacking the signal from green probe, indicating the absence of green probe. Similarly points shown near ordinate are shown in green as they are lacking signal from red channel. Points along a y = x line represent the pixels where red and green probes are colocalized. Such pixels are represented in orange color. The region of interest (ROI) shown with yellow boundary represents such pixels where both red and green probes can be expected. Colocalization indices listed in the figure are calculated for this region using the protocol on Leica Confocal program. C) Overlay image showing the pixels, which are bounded by the ROI.

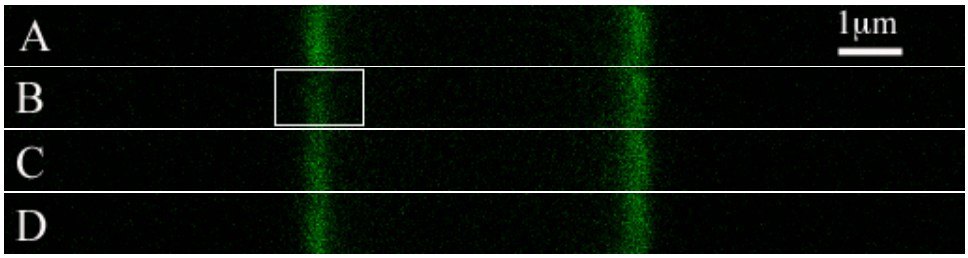

Figure 4.13: Snapshots of the equatorially opposite ends of a bead studied for fluorescence recovery after photobleaching. Images were acquired in a *512 pixel X 32 pixel* format to be able to scan at a fast enough speed to monitor fluorescence recovery. A) Prebleach image. B) Immediately after bleach event. Bleached region on the left side of the bead is shown with a rectangle. C) 2 seconds after bleach event. D) 12 seconds after bleach event.

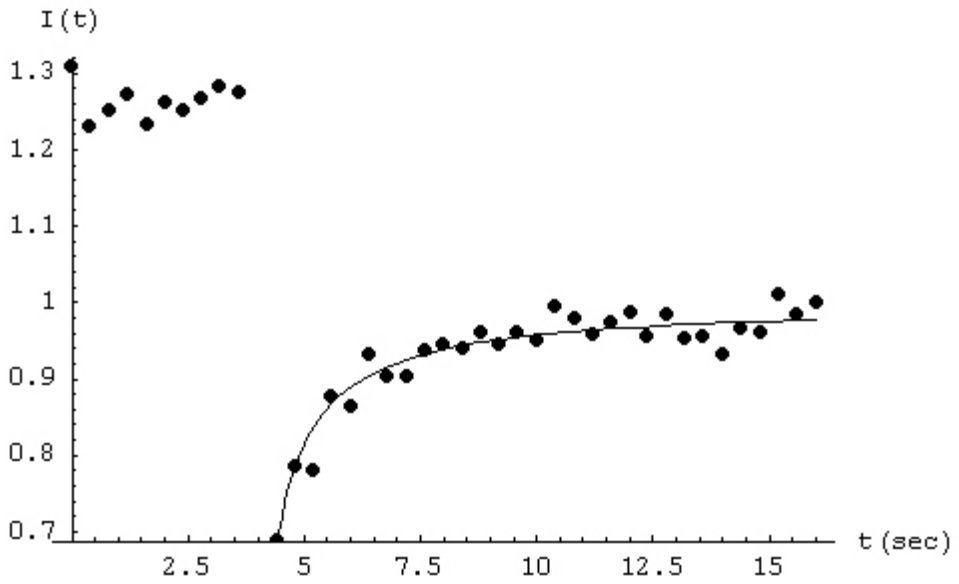

Figure 4.14: Time variation of the normalized fluorescence intensity of the bleached spot. Experimental data has been shown by discrete points whereas the line is a plot of the power series fit on the data. Intensity was normalized to the final steady level at large values of time ($t \geq 15$ sec). (Compare the overall variation of fluorescence in this figure to Figure 1.8)

Chapter 5

Conclusions and Future Work

5.1 Conclusions

Biological systems are becoming an important source of both inspiration and motivation for the design and construction of novel materials. Interfacing biological molecules that exhibit unique functional capabilities, with materials having desired physical properties can lead to the development of miniature electronic and optical devices including sensing and probing devices. The current thesis serves as a primer for a new method that can be used to interface lipid bilayer membranes on microparticles with integrated anchoring to enhance the stability. Our ultimate goal is to construct similar assemblies on nanoparticles (e.g. quantum dots) and structures of arbitrary topology. Major conclusions of this thesis project are summarized below:

1. We have successfully conjugated bacteriorhodopsin with biotin-PEG_{3400} and Texas Red (TR) to synthesize fluorescently labeled TR-bR-PEG_{3400}-biotin molecules. Characterization of the conjugates revealed predominantly single site labeling with biotin-PEG_{3400} as required for their use as an anchoring agent. The tether conjugation site was identified using a trypsin digestion assay and was found to be in agreement with the conclusions of the previous studies.

2. Surface of the silica beads was successfully biofunctionalized with streptavidin in order to immobilize the bR tethers . This was achieved in three steps—(i) self-assembly of APhMS on the bead surface imparting amine functionality to it; (ii) attachment of biotin-PEG_{3400} to amine functionalized surface using NHS based chemistry, and passivation of the remaining surface with PEG of smaller molecular weight ($mPEG_{2000}$); and (iii) attachment of streptavidin to biotin functionalized bead surface. Confocal microscopy was utilized to analyze the bead surface at different stages of surface modification by employing fluorescent staining techniques.

3. Tether supported lipid bilayer membranes were constructed successfully on streptavidin functionalized silica particles (5 μm). This is the first study on the use of membrane protein based anchors to tether lipid bilayer on spherical particles. We tried different routes to form supported lipid bilayers around the particles and found that detergent approach led to the desired assemblies. The fluidity of the supported membranes was analyzed using the FRAP technique. Furthermore, the mobility of the lipids was found to be comparable to the case of un-tethered bilayer on plain silica particles, as well as value reported in literature for the lipid membranes supported on planar surfaces.

5.2 Future Work

Overall objectives of this project are the following: (1) Formation of tether supported lipid bilayer membranes on spherical particles, (2) characterization of the stability and comparison with the regular un-tethered structures, (3) incorporation of membrane proteins of interest into the stabilized structures, and (4) immobilization of these assemblies on a functionalized surface to display an array of microparticles for sensing applications.

Motivation behind the project is to build stable lipid microenvironment for membrane proteins for the development of novel surfaces for biosensing applications. So far we have successfully fabricated lipid bilayer assemblies on modified silica microparticles. We have integrated bacteriorhodopsin-based tethers to anchor the supported bilayer structures onto the bead surface to impart it with enhanced stability. Next steps in the light of above discussion will be the following:

- Stability assays
- Incorporation of functional membrane proteins
- Formation of sensor arrays on the functionalized surface

5.2.1 Stability assays

We adopted the approach of fabricating tether supported lipid membrane from the point of view of stability enhancement. This is essential as the un-tethered lipid bilayer structures can potentially fall apart in various processing and shear conditions that we might need to expose them in the desired applications. Hence it is imperative to assess the stability of the constructs and compare them with the membranes without any tether supports.

One of the ways to assess the stability is to subject the assemblies to elevated temperatures for certain time duration. They can also be subjected to controlled shear stress in a viscometer or to ultrasonic waves in a micro-tip homogenizer. At certain level of these conditions (temperature, shear stress, or ultrasonic power) the lipid assemblies will start to fall apart. The damage to the lipid bilayer can be assessed using confocal microscopy and comparison can be done with untethered structures.

5.2.2 Incorporation of functional membrane proteins

As mentioned earlier, the motivation behind construction of tether supported bilayer assemblies is to build stronger supports for membrane proteins. Two of the potential candidates as prototypical proteins for this purpose are: the photosynthetic reaction center and G-protein coupled receptors. We have done some preliminary work with the photosynthetic reaction center, which is briefly described below. This will serve as an experimental protocol, which can be suitably modified for future trials.

Reaction center is the cardinal element in the photosynthetic pathway. It converts the solar energy into electron transfer reaction, which is further coupled to ATP synthesis. There were two reasons behind using reaction center as the prototype for membrane protein. Presence of the cofactor chlorophyll provides an in-built mechanism to assess the structural integrity of the protein, and, electron separation

ability of the reaction center can be studied in-vitro to assess its functional state. In our experiments, we conjugated reaction center with a fluorescent probe Cy5-NHS (excitation 549 nm, emission 670 nm) using a protocol similar to the one described earlier for Texas Red-NHS labeling of bR conjugates. Fluorescently tagged reaction center was incorporated into lipid bilayer assemblies on 6 μm sized beads. These beads were precoated by streptavidin and biotin-PEG_{3400}-bR based tethers were utilized to anchor the lipid membranes on their surface. Bacteriorhodopsin in the biotin-PEG_{3400}-bR tethers had been conjugated with Texas Red dye as described in earlier chapter. Detergent-based lipid reconstitution was used to assemble lipid bilayer on biotin-PEG_{3400}-bR tethered bead surface. Detergent solubilized RC-Cy5 complex was added prior to the detergent removal. Detergent was removed using bio-beads adsorbents. Figure 5.1 shows confocal micrographs of the resulting structures. This confirms that reaction center was successfully reconstituted into the lipid assemblies built around the beads. However, in these preliminary experiments no mobility measurements were done to test the fluidity of the lipids or proteins in the resulting structures.

5.2.3 Formation of sensor arrays on the functionalized surface

Once we have the membrane protein in the functional form in stabilized lipid assemblies on microparticles, we can pursue the ultimate goal, which is to immobilize these particles onto a functionalized surface. Such a surface will have a specific display of functionality in an inert matrix. Microparticles carrying membrane proteins will be immobilized onto these surfaces on the basis of specific tags that identify the surface (Figure 5.2). Such a surface can then be developed into a specific recognition or screening device based on the functionality of the reconstituted membrane protein. Preliminary work in this regard has been the arraying of intact liposomes (with-

out any supporting microspheres) of 1 μm diameter onto chemically functionalized microwell surfaces using streptavidin-biotin interactions [118].

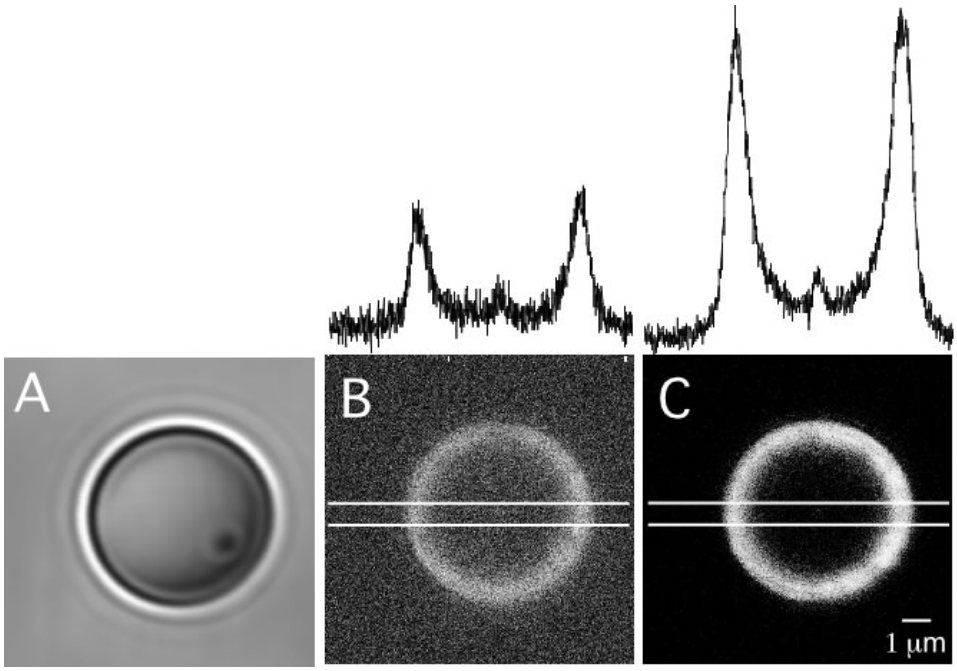

Figure 5.1: Confocal images along the equator of a 6 μm sized bead displaying reaction center containing lipid assemblies. A) Transmission image showing the bead. B) Red channel (excitation 568 nm, detection 580–615 nm) showing the presence of bacteriorhodopsin tagged with Texas Red. C) Cy5 channel (excitation 633 nm, detection 653–783 nm) showing the presence of Cy5 tagged reaction center. Two dyes are co-localized as evident above. The intensity distribution of two dyes along a horizontal section (shown by two parallel lines) has been shown to demonstrate the individual spikes on both ends of the equatorial plane of the bead. Images have been edited in order to get better representation and contrast when printed on paper.

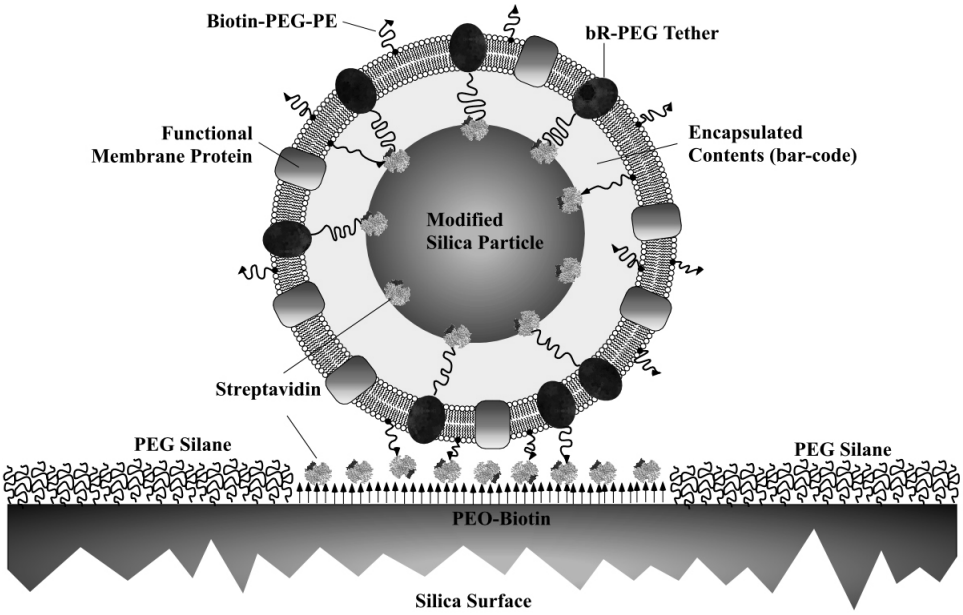

Figure 5.2: Immobilization of membrane protein displaying microparticles on a micropatterned surface for biosensing application. Streptavidin-biotin interaction can be used to rest the particles on the functionalized surface. Particles will have biotin display (through biotin-PEG-PE lipid, or biotin-PEG-bR) whereas the surface will have islands of streptavidin in an inert matrix of PEG-silane.

Bibliography

[1] L. K. Srivastava, S. M. Kazmi, A. J. Blume, and R. K. Mishra. Reconstitution of affinity-purified dopamine d2 receptor binding activities by specific lipids. *Biochim Biophys Acta*, 900(2):175–82, 1987.

[2] A. Chattopadhyay, M. Jafurulla, S. Kalipatnapu, T. J. Pucadyil, and K. G. Harikumar. Role of cholesterol in ligand binding and g-protein coupling of serotonin1a receptors solubilized from bovine hippocampus. *Biochem Biophys Res Commun*, 327(4):1036–41, 2005.

[3] T. J. Pucadyil and A. Chattopadhyay. Cholesterol modulates ligand binding and g-protein coupling to serotonin(1a) receptors from bovine hippocampus. *Biochim Biophys Acta*, 1663(1-2):188–200, 2004.

[4] D. H. Nguyen and D. Taub. Cxcr4 function requires membrane cholesterol: implications for hiv infection. *J Immunol*, 168(8):4121–6, 2002.

[5] A. D. Bangham. Liposomes: realizing their promise. *Hosp Pract (Off Ed)*, 27(12):51–6, 61–2, 1992.

[6] G. Gregoriadis and A. T. Florence. Liposomes in drug delivery. clinical, diagnostic and ophthalmic potential. *Drugs*, 45(1):15–28, 1993.

[7] D.D. Lasic. *Liposomes: From Physics to Applications*. Elsevier Science, Amsterdam, 1993.

[8] M. Ollivon, S. Lesieur, C. Grabielle-Madelmont, and M. Paternostre. Vesicle reconstitution from lipid-detergent mixed micelles. *Biochim Biophys Acta*, 1508(1-2):34–50, 2000.

[9] D. Papahadjopoulos, editor. *Liposomes and Their Uses in Biology and Medicine. Ann. N.Y. Acad. Sci., 308*. 1978.

[10] Jr. Szoka, F. and D. Papahadjopoulos. Comparative properties and methods of preparation of lipid vesicles (liposomes). *Annu Rev Biophys Bioeng*, 9:467–508, 1980.

[11] M. C. Woodle and D. D. Lasic. Sterically stabilized liposomes. *Biochim Biophys Acta*, 1113(2):171–99, 1992.

[12] T. Sato and J. Sunamoto. Recent aspects in the use of liposomes in biotechnology and medicine. *Prog Lipid Res*, 31(4):345–72, 1992.

[13] Jr. Szoka, F. and D. Papahadjopoulos. Procedure for preparation of liposomes with large internal aqueous space and high capture by reverse-phase evaporation. *Proc Natl Acad Sci U S A*, 75(9):4194–8, 1978.

[14] N. K. Subbarao, R. I. MacDonald, K. Takeshita, and R. C. MacDonald. Characteristics of spectrin-induced leakage of extruded, phosphatidylserine vesicles. *Biochim Biophys Acta*, 1063(1):147–54, 1991.

[15] R. C. MacDonald, R. I. MacDonald, B. P. Menco, K. Takeshita, N. K. Subbarao, and L. R. Hu. Small-volume extrusion apparatus for preparation of large, unilamellar vesicles. *Biochim Biophys Acta*, 1061(2):297–303, 1991.

[16] J. H. Ipsen, O. G. Mouritsen, and M. Bloom. Relationships between lipid membrane area, hydrophobic thickness, and acyl-chain orientational order. the effects of cholesterol. *Biophys J*, 57(3):405–12, 1990.

[17] S. Lesieur, C. Grabielle-Madelmont, M. T. Paternostre, and M. Ollivon. Size analysis and stability study of lipid vesicles by high-performance gel exclusion chromatography, turbidity, and dynamic light scattering. *Anal Biochem*, 192(2):334–43, 1991.

[18] D. Papahadjopoulos, W. J. Vail, C. Newton, S. Nir, K. Jacobson, G. Poste, and R. Lazo. Studies on membrane fusion. iii. the role of calcium-induced phase changes. *Biochim Biophys Acta*, 465(3):579–98, 1977.

[19] R. Welti and M. Glaser. Lipid domains in model and biological membranes. *Chem Phys Lipids*, 73(1-2):121–37, 1994.

[20] F. Olson, C. A. Hunt, F. C. Szoka, W. J. Vail, and D. Papahadjopoulos. Preparation of liposomes of defined size distribution by extrusion through polycarbonate membranes. *Biochim Biophys Acta*, 557(1):9–23, 1979.

[21] L. D. Mayer, M. J. Hope, and P. R. Cullis. Vesicles of variable sizes produced by a rapid extrusion procedure. *Biochim Biophys Acta*, 858(1):161–8.

[22] M. Paternostre, M. Viard, O. Meyer, M. Ghanam, M. Ollivon, and R. Blumenthal. Solubilization and reconstitution of vesicular stomatitis virus envelope using octylglucoside. *Biophys J*, 72(4):1683–94, 1997.

[23] J. M. Salvador, G. Inesi, J. L. Rigaud, and A. M. Mata. Ca^{2+} transport by reconstituted synaptosomal ATPase is associated with H^+ countertransport and net charge displacement. *J Biol Chem*, 273(29):18230–4, 1998.

[24] J. J. Lacapere, D. L. Stokes, A. Olofsson, and J. L. Rigaud. Two-dimensional crystallization of ca-atpase by detergent removal. *Biophys J*, 75(3):1319–29, 1998.

[25] C. W. Heegaard, M. le Maire, T. Gulik-Krzywicki, and J. V. Moller. Monomeric state and Ca^{2+} transport by sarcoplasmic reticulum $Ca^{2+/-}$ ATPase, reconstituted with an excess of phospholipid. *J Biol Chem*, 265(20):12020–8, 1990.

[26] H. Ringsdorf, B. Schlarb, and J. Venzmer. Molecular architecture and function of polymeric oriented systems: Models for the study of organization, surface recognition, and dynamics of biomembranes. *J. Angew. Chem.*, 27(1):113–148, 1988.

[27] S. Liu and D. F. O'Brien. Stable polymeric nanoballoons: lyophilization and rehydration of cross-linked liposomes. *J Am Chem Soc*, 124(21):6037–42, 2002.

[28] A. Graff, M. Winterhalter, and W. Meier. Nanoreactors from polymer-stabilized liposomes. *Langmuir*, 17(3):919–923, 2001.

[29] C. Nardin, T. Hirt, J. Leukel, and W. Meier. Polymerized aba triblock copolymer vesicles. *Langmuir*, 16(3):1035–1041, 2000.

[30] T. M. Allen. The use of glycolipids and hydrophilic polymers in avoiding rapid uptake of liposomes by the mononuclear phagocyte system. *Adv. Drug Delivery Rev.*, 13(3):285–309, 1994.

[31] K. Braeckmans, L. Peeters, N. N. Sanders, S. C. De Smedt, and J. Demeester. Three-dimensional fluorescence recovery after photobleaching with the confocal scanning laser microscope. *Biophys J*, 85(4):2240–52, 2003.

[32] D. Axelrod, D. E. Koppel, J. Schlessinger, E. Elson, and W. W. Webb. Mobility measurement by analysis of fluorescence photobleaching recovery kinetics. *Biophys J*, 16(9):1055–69, 1976.

[33] D. Axelrod, P. Ravdin, D. E. Koppel, J. Schlessinger, W. W. Webb, E. L. Elson, and T. R. Podleski. Lateral motion of fluorescently labeled acetylcholine receptors in membranes of developing muscle fibers. *Proc Natl Acad Sci U S A*, 73(12):4594–8, 1976.

[34] W. Denk, J. H. Strickler, and W. W. Webb. Two-photon laser scanning fluorescence microscopy. *Science*, 248(4951):73–6, 1990.

[35] T. S. Chen, S. Q. Zeng, Q. M. Luo, Z. H. Zhang, and W. Zhou. High-order photobleaching of green fluorescent protein inside live cells in two-photon excitation microscopy. *Biochem Biophys Res Commun*, 291(5):1272–5, 2002.

[36] G. H. Patterson and D. W. Piston. Photobleaching in two-photon excitation microscopy. *Biophys J*, 78(4):2159–62, 2000.

[37] N. Klonis, M. Rug, I. Harper, M. Wickham, A. Cowman, and L. Tilley. Fluorescence photobleaching analysis for the study of cellular dynamics. *Eur Biophys J*, 31(1):36–51, 2002.

[38] G. Carrero, D. McDonald, E. Crawford, G. de Vries, and M. J. Hendzel. Using frap and mathematical modeling to determine the in vivo kinetics of nuclear proteins. *Methods*, 29(1):14–28, 2003.

[39] Y. Cheng, S. D. Ogier, R. J. Bushby, and S. D. Evans. Discrete membrane arrays. *J Biotechnol*, 74(3):159–74, 2000.

[40] J. T. Groves, N. Ulman, and S. G. Boxer. Micropatterning fluid lipid bilayers on solid supports. *Science*, 275(5300):651–3, 1997.

[41] E. Kalb, S. Frey, and L. K. Tamm. Formation of supported planar bilayers by fusion of vesicles to supported phospholipid monolayers. *Biochim Biophys Acta*, 1103(2):307–16, 1992.

[42] G. Puu, E. Artursson, I. Gustafson, M. Lundstrom, and J. Jass. Distribution and stability of membrane proteins in lipid membranes on solid supports. *Biosens Bioelectron*, 15(1-2):31–41, 2000.

[43] E. Sackmann. Supported membranes: scientific and practical applications. *Science*, 271(5245):43–8, 1996.

[44] L. K. Tamm and H. M. McConnell. Supported phospholipid bilayers. *Biophys J*, 47(1):105–13, 1985.

[45] J. Radler, H. Strey, and E. Sackmann. Phenomenology and kinetics of lipid bilayer spreading on hydrophilic surfaces. *Langmuir*, 11(11):4539–4548, 1995.

[46] T. M. Bayerl and M. Bloom. Physical properties of single phospholipid bilayers adsorbed to micro glass beads. a new vesicular model system studied by 2h-nuclear magnetic resonance. *Biophys J*, 58(2):357–62, 1990.

[47] M. L. Wagner and L. K. Tamm. Tethered polymer-supported planar lipid bilayers for reconstitution of integral membrane proteins: silane-polyethyleneglycol-lipid as a cushion and covalent linker. *Biophys J*, 79(3):1400–14, 2000.

[48] M. L. Wagner and L. K. Tamm. Reconstituted syntaxin1a/snap25 interacts with negatively charged lipids as measured by lateral diffusion in planar supported bilayers. *Biophysical Journal*, 81(1):266–275, 2001.

[49] W. W. Shen, S. G. Boxer, W. Knoll, and C. W. Frank. Polymer-supported lipid bilayers on benzophenone-modified substrates. *Biomacromolecules*, 2(1):70–9, 2001.

[50] V. Kiessling and L. K. Tamm. Measuring distances in supported bilayers by fluorescence interference-contrast microscopy: Polymer supports and snare proteins. *Biophysical Journal*, 84(1):408–418, 2003.

[51] H. M. McConnell, T. H. Watts, R. M. Weis, and A. A. Brian. Supported planar membranes in studies of cell-cell recognition in the immune system. *Biochim Biophys Acta*, 864(1):95–106, 1986.

[52] J. J. Benkoski and F. Hook. Lateral mobility of tethered vesicle-dna assemblies. *J. Phys. Chem. B*, 109:9773–9779, 2005.

[53] C. Yoshina-Ishii and S. G. Boxer. Arrays of mobile tethered vesicles on supported lipid bilayers. *J Am Chem Soc*, 125(13):3696–7, 2003.

[54] C. Yoshina-Ishii, G. P. Miller, M. L. Kraft, E. T. Kool, and S. G. Boxer. General method for modification of liposomes for encoded assembly on supported bilayers. *J Am Chem Soc*, 127(5):1356–7, 2005.

[55] C. M. Niemeyer and C. A. Mirkin. *Nanobiotechnology: Concepts, Applicatioins and Perspectives*. 2004.

[56] T. Lazaridis. Effective energy function for proteins in lipid membranes. *Proteins*, 52(2):176–92, 2003.

[57] M. Zhang, T. Desai, and M. Ferrari. Proteins and cells on peg immobilized silicon surfaces. *Biomaterials*, 19(10):953–60, 1998.

[58] M. Mrksich and G. M. Whitesides. Using self-assembled monolayers to understand the interactions of man-made surfaces with proteins and cells. *Annu Rev Biophys Biomol Struct*, 25:55–78, 1996.

[59] G. Sirokman and G. D. Fasman. Refolding and proton pumping activity of a polyethylene glycol-bacteriorhodopsin water-soluble conjugate. *Protein Sci*, 2(7):1161–70, 1993.

[60] F. Liu, S. C. Song, D. Mix, M. Baudys, and S. W. Kim. Glucose-induced release of glycosylpoly(ethylene glycol) insulin bound to a soluble conjugate of concanavalin a. *Bioconjug Chem*, 8(5):664–72, 1997.

[61] J. Wei and G. D. Fasman. A poly(ethylene glycol) water-soluble conjugate of porin: refolding to the native state. *Biochemistry*, 34(19):6408–15, 1995.

[62] F. M. Veronese. Peptide and protein pegylation: a review of problems and solutions. *Biomaterials*, 22(5):405–17, 2001.

[63] M. J. Roberts, M. D. Bentley, and J. M. Harris. Chemistry for peptide and protein pegylation. *Advanced Drug Delivery Reviews*, 54(4):459–476, 2002.

[64] C. Bieri, O. P. Ernst, S. Heyse, K. P. Hofmann, and H. Vogel. Micropatterned immobilization of a g protein-coupled receptor and direct detection of g protein activation. *Nat Biotechnol*, 17(11):1105–8, 1999.

[65] M. K. Sharma, H. Jattani, and M. L. Gilchrist. Bacteriorhodopsin conjugates as anchors for supported membranes. *Bioconjugate Chemistry*, 15(4):942–947, 2004.

[66] H. Belrhali, P. Nollert, A. Royant, C. Menzel, J. P. Rosenbusch, E. M. Landau, and E. Pebay-Peyroula. Protein, lipid and water organization in bacteriorhodopsin crystals: a molecular view of the purple membrane at 1.9 Å resolution. *Structure Fold Des*, 7(8):909–17, 1999.

[67] G. E. Gerber, C. P. Gray, D. Wildenauer, and H. G. Khorana. Orientation of bacteriorhodopsin in halobacterium halobium as studied by selective proteolysis. *Proc Natl Acad Sci U S A*, 74(12):5426–30, 1977.

[68] R. Henderson, J. S. Jubb, and S. Whytock. Specific labelling of the protein and lipid on the extracellular surface of purple membrane. *J Mol Biol*, 123(2):259–74, 1978.

[69] J. Heberle and N. A. Dencher. Surface-bound optical probes monitor protein translocation and surface potential changes during the bacteriorhodopsin photocycle. *Proc Natl Acad Sci U S A*, 89(13):5996–6000, 1992.

[70] J. B. Brzoska, I. Ben Azouz, and F. Rondelez. Silanization of solid substrates: A step toward reproducibility. *Langmuir*, 10(11):4367–4373, 1994.

[71] W. C. Bigelow, D. L. Pickett, and W. A. Zisman. Oleophobic monolayers : I. films adsorbed from solution in non-polar liquids. *Journal of Colloid Science*, 1(6):513–538, 1946.

[72] F. J. Feher and D. A. Newman. Enhanced silylation reactivity of a model for silica surfaces. *J. Am. Chem. Soc.*, 112(5):1931, 1990.

[73] J. N. Kinkel and K. K. Unger. Role of solvent and base in the silanization reaction of silicas for reversed-phase high-performance liquid chromatography. *J. Chromatogr.*, 316:193–200, 1984.

[74] L. C. Sander and S. A. Wise. Synthesis and characterization of polymeric phases for liquid chromatography. *J. Anal. Chem.*, 56:504–510, 1984.

[75] N. D. Danielson and J. J. Kirkland. Synthesis and characterization of 2-pm wide-pore silica microspheres as column packings for the reversed-phase liquid chromatography of peptides and proteins. *J. Anal. Chem.*, 59:2501–2506, 1987.

[76] M. J. Wirth, R. W. P. Fairbank, and H. O. Fatunmbi. Mixed self-assembled monolayers in chemical separations. *Science*, 275(5296):44–47, 1997.

[77] S. R. Cohen, R. Naaman, and J. Sagiv. Thermally i ndueed disorder in organized organic monolayers on solid substrates. *J. Phys. Chem.*, 90:3054–3056, 1986.

[78] J. Gun, J.and Sagiv. On the formation and structure of self-assembling monolayers iii. time of formation, solvent retention, and release. *J. Colloid Interface Sci.*, 112(2):457–472, 1986.

[79] J. Sagiv. Organized monolayers by adsorption, i . formation and structure of oleophobic mixed monolayers on solid surfaces. *J. Am. Chem. Soc.*, 102(1):92–98, 1980.

[80] J. Gun, R. Iscovici, and J. Sagiv. On the formation and structure of self-assembling monolayers ii. a comparative study of langmuir-blodgett and adsorbed films using ellipsometry and ir reflection-absorption spectroscopy. *J. Colloid Interface Sci.*, 101(1):201–213, 1984.

[81] R. A. Hatton, M. R. Willis, M. A. Chestersa, and D. Briggsb. A robust ultrathin, transparent gold electrode tailored for hole injection into organic light-emitting diodes. *J. Mater. Chem.*, 13:722–726, 2003.

[82] A. Couzis, C. Maldarelli, N. Kumar, and F. Q. Fan. Fabrication of surfaces with nano-islands of chemical functionality by controlling the phase behavior of self-assembling surfactants. *Abstracts of Papers of the American Chemical Society*, 225:U628–U628, 2003.

[83] F. Q. Fan, C. Maldarelli, and A. Couzis. Fabrication of surfaces with nanoislands of chemical functionality by the phase separation of self-assembling monolayers on silicon. *Langmuir*, 19(8):3254–3265, 2003.

[84] N. Kumar, C. Maldarelli, C. Steiner, and A. Couzis. Formation of nanometer domains of one chemical functionality in a continuous matrix of a second chemical functionality by sequential adsorption of silane self-assembled monolayers. *Langmuir*, 17(25):7789–7797, 2001.

[85] H. J. Muller. Extraordinarily thick water films on hydrophilic solids: A result of hydrophobic repulsion? *Langmuir*, 14(24):6789–6792, 1998.

[86] M. L. Hair and W. Hertl. Adsorption on hydroxylated silica surfaces. *J. Phys. Chem.*, 73(12):4269–4276, 1969.

[87] M. L. Gee, T. W. Healy, and L. R. White. Hydrophobicity effects in the condensation of water films on quartz. *J. Colloid Interface Sci.*, 140(2):450–465, 1990.

[88] P. Silberzan, L. Leger, D. Ausserre, and J. J. Benattar. Silanation of silica surfaces. a new method of constructing pure or mixed monolayers. *Langmuir*, 7(8):1647–1651, 1991.

[89] C. P. Tripp and M. L. Hair. Reaction of methylsilanols with hydrated silica surfaces - the hydrolysis of trichloromethylsilanes, dichloromethylsilanes, and monochloromethylsilanes and the effects of curing. *Langmuir*, 11(1):149–155, 1995.

[90] H. O. Fatunmbi, M. D. Bruch, and M. J. Wirth. ^{29}Si and ^{13}C NMR characterization of mixed horizontally polymerized monolayers on silica gel. *J. Anal. Chem.*, 65:2048–2054, 1993.

[91] T. Mirzabekov, H. Kontos, M. Farzan, W. Marasco, and J. Sodroski. Paramagnetic proteoliposomes containing a pure, native, and oriented seven-transmembrane segment protein, CCR5. *Nat Biotechnol*, 18(6):649–54, 2000.

[92] V. von Tscharner and H. M. McConnell. Physical properties of lipid monolayers on alkylated planar glass surfaces. *Biophys J*, 36:421–427, 1981.

[93] A. A. Brian and H. M. McConnell. Allogeneic stimulation of cytotoxic t cells by supported planar membranes. *Proc Natl Acad Sci U S A*, 81(19):6159–63, 1984.

[94] A. T. A. Jenkins, N. Boden, R. J. Bushby, S. D. Evans, P. F. Knowles, R. E. Miles, S. D. Ogier, H. Schonherr, and G. J. Vansco. Microcontact printing of lipophilic self-assembled monolayers for the attachment of biomimetic lipid bilayers to surfaces. *J Am Chem Soc*, 121(22):5274–5280, 1999.

[95] A. T. A. Jenkins, R. J. Bushby, N. Boden, S. D. Evans, P. F. Knowles, Q. Liu, R. E. Miles, and S. D. Ogier. Ion-selective lipid bilayers tethered to microcontact printed self-assembled monolayers containing cholesterol derivatives. *Langmuir*, 14(17):4675–4678, 1998.

[96] S. Heyse, O. P. Ernst, Z. Dienes, K. P. Hofmann, and H. Vogel. Incorporation of rhodopsin in laterally structured supported membranes: observation of transducin activation with spatially and time-resolved surface plasmon resonance. *Biochemistry*, 37(2):507–22, 1998.

[97] P. Hinterdorfer, G. Baber, and L. K. Tamm. Reconstitution of membrane fusion sites. a total internal reflection fluorescence microscopy study of influenza hemagglutinin-mediated membrane fusion. *J Biol Chem*, 269(32):20360–8, 1994.

[98] J. Salafsky, J. T. Groves, and S. G. Boxer. Architecture and function of membrane proteins in planar supported bilayers: a study with photosynthetic reaction centers. *Biochemistry*, 35(47):14773–81, 1996.

[99] C. L. Poglitsch, M. T. Sumner, and N. L. Thompson. Binding of igg to mofc gamma rii purified and reconstituted into supported planar membranes as measured by total internal reflection fluorescence microscopy. *Biochemistry*, 30(27):6662–71, 1991.

[100] J. Spinke, J. Yang, H. Wolf, M. Lily, H. Ringsdorf, and W. Knoll. Polymer-supported bilayer on a solid substrate. *Biophys J*, 63:1667–1671, 1992.

[101] M. Kuhner, R. Tampe, and E. Sackmann. Lipid mono- and bilayer supported on polymer films: composite polymer-lipid films on solid substrates. *Biophys J*, 67(1):217–26, 1994.

[102] D. Beyer, G. Elender, W. Knoll, M. Khner, S. Maus, H. Ringsdorf, and E. Sackmann. Influence of anchor lipids on the homogeneity and mobility of lipid bilayers on thin polymer films. *Angew. Chem. Int. Ed. Engl.*, 35:1682–1685, 1996.

[103] H. Lang, C. Duschl, and H. Vogel. A new class of thiolipids for the attachment of lipid bilayers on gold surfaces. *Langmuir*, 20:197–210, 1994.

[104] Y. L. Cheng, N. Boden, R. J. Bushby, S. Clarkson, S. D. Evans, P. F. Knowles, A. Marsh, and R. E. Miles. Attenuated total reflection fourier transform infrared spectroscopic characterization of fluid lipid bilayers tethered to solid supports. *Langmuir*, 14(4):839–844, 1998.

[105] L. M. Williams, S. D. Evans, T. M. Flynn, A. Marsh, P. F. Knowles, R. J. Bushby, and N. Boden. Kinetics of the unrolling of small unilamellar phospholipid vesicles onto self-assembled monolayers. *Langmuir*, 13(4):751–757, 1997.

[106] T. Brumm, K. Jorgensen, O. G. Mouritsen, and T. M. Bayerl. The effect of increasing membrane curvature on the phase transition and mixing behavior of a dimyristoyl-sn-glycero-3-phosphatidylcholine/ distearoyl-sn-glycero-3-phosphatidylcholine lipid mixture as studied by fourier transform infrared spectroscopy and differential scanning calorimetry. *Biophys J*, 70(3):1373–9, 1996.

[107] F. M. Linseisen, M. Hetzer, T. Brumm, and T. M. Bayerl. Differences in the physical properties of lipid monolayers and bilayers on a spherical solid support. *Biophys J*, 72(4):1659–67, 1997.

[108] A. Loidl-Stahlhofen, S. Kaufmann, T. Braunschweig, and T. M. Bayerl. The thermodynamic control of protein binding to lipid bilayers for protein chromatography. *Nat Biotechnol*, 14(8):999–1002, 1996.

[109] T. M. Bayerl. A glass bead game. *Nature*, 427(6970):105–6, 2004.

[110] M. M. Baksh, M. Jaros, and J. T. Groves. Detection of molecular interactions at membrane surfaces through colloid phase transitions. *Nature*, 427(6970):139–41, 2004.

[111] A. Loidl-Stahlhofen, A. Eckert, T. Hartmann, and M. Schottner. Solid-supported lipid membranes as a tool for determination of membrane affinity: high-throughput screening of a physicochemical parameter. *J Pharm Sci*, 90(5):599–606, 2001.

[112] A. Loidl-Stahlhofen, T. Hartmann, M. Schottner, C. Rohring, H. Brodowsky, J. Schmitt, and J. Keldenich. Multilamellar liposomes and solid-supported lipid membranes (transil): screening of lipid-water partitioning toward a high-throughput scale. *Pharm Res*, 18(12):1782–8, 2001.

[113] A. Loidl-Stahlhofen, Johannes Schmitt, J. Nller, T. Hartmann, H. Brodowsky, W. Schmitt, and J. Keldenich. Solid-supported biomolecules on modified silica surfaces - a tool for fast physicochemical characterization and high-throughput screening. *Adv. Materials*, 13(23):1829–1834, 2001.

[114] T. Buranda, J. Huang, G. V. Ramarao, L. K. Ista, R. S. Larson, T. L. Ward, L. A. Sklar, and G. P. Lopez. Biomimetic molecular assemblies on glass and mesoporous silica microbeads for biotechnology. *Langmuir*, 19(5):1654–1663, 2003.

[115] J. Schmitt, B. Danner, and T. M. Bayerl. Polymer cushions in supported phospholipid bilayers reduce significantly the frictional drag between bilayer and solid surface. *Langmuir*, 17(1):244–246, 2001.

[116] A. Berquand, P. E. Mazeran, J. Pantigny, V. Proux-Delrouyre, J. M. Laval, and C. Bourdillon. Two-step formation of streptavidin-supported lipid bilayers by peg-triggered vesicle fusion. fluorescence and atomic force microscopy characterization. *Langmuir*, 19(5):1700–1707, 2003.

[117] M. Seitz, E. Ter-Ovanesyan, M. Hausch, C. K. Park, J. A. Zasadzinski, R. Zentel, and J. N. Israelachvili. Formation of tethered supported bilayers by vesicle fusion onto lipopolymer monolayers promoted by osmotic stress. *Langmuir*, 16(14):6067–6070, 2000.

[118] N. D. Kalyankar, M. K. Sharma, C. Maldarelli, D. Calhound, A. Couzis, and L. Gilchrist. Arraying of intact liposomes into chemically functionalized microwell surfaces. *Submitted to Langmuir*, 2005.